Functional and expression analysis of heteromeric acetyl-CoA carboxylase subunit genes of Arabidopsis

by

Xu Li

A dissertation submitted to the graduate faculty

in partial fulfillment of the requirements for the degree of

DOCTOR OF PHILOSOPHY

Major: Biochemistry

Program of Study Committee:
Basil J. Nikolau, Major Professor
Stephen H. Howell
Alan M. Myers
Patrick S. Schnable
Eve S. Wurtele

Iowa State University

Ames, Iowa

2005

Graduate College

Iowa State University

This is to certify that the doctoral dissertation of

Xu Li

has met the dissertation requirements of Iowa State University

Signature was redacted for privacy.

Major Professor

Signature was redacted for privacy.

For the Major Program

TABLE OF CONTENTS

CHAPTER 1. GENERAL INTRODUCTION

FATTY ACID BIOSYNTHESIS

Fatty acid biosynthesis is an important metabolic pathway. As in almost all organisms, in plants biological membranes are composed of fatty acid-derived lipids. In addition, fatty acid-derived metabolites play a variety of important plant-specific roles in the physiology of these organisms. Very-long-chain fatty acids (VLCFAs; >18 carbons) are the precursors for cuticle waxes, the major component of a lipid layer that covers plant surfaces, and serves as the first line of defense against pathogens, phytophagous insects and environmental stresses (Post-Beittenmiller, 1996). Jasmonate, a derivative of linolenic acid, is essential for plant wound-signaling pathways, anther dehiscence and pollen development (Weber, 2002). Most importantly for human use, many plants use fatty acids to form triacylglycerols during seed development and thus accumulate oil in their seeds, which is an important source of fats for food and industrial uses.

De novo fatty acid synthesis in plants occurs in plastids. Acetyl-CoA carboxylase (ACCase) catalyzes the first reaction of this pathway converting acetyl-CoA into malonyl-CoA. Then malonyl transacylase transfers the malonyl moiety to acyl-carrier protein (ACP) to produce malonyl-ACP, which is the donor of 2-carbon units used for fatty acid biosynthesis. The carbon chains are extended by two carbons after a cycle of four-step reactions: (1) condensation of malonyl-ACP with an acyl acceptor (the initial acceptor is acetyl-CoA) catalyzed by 3-ketoacyl-ACP synthase; (2) reduction of the 3-ketoacyl-ACP to 3-hydroxyacyl-ACP by 3-ketoacyl-ACP reductase; (3) formation of an enoyl-ACP catalyzed by

3-hydroxyacyl-ACP dehydrase; and (4) reduction of the enoyl-ACP to the saturated acyl-ACP by enoyl-ACP reductase. This synthesis cycle is terminated by either acyl-ACP thioesterase or acyl transferase. Typically, the main products are 16:0 and 18:0.

While acyl transferases in plastids transesterify acyl chain from ACP to glycerol, acyl-ACP thioesterases hydrolyze the ACP and release the free fatty acids, which move out of the plastid and can be elongated to form VLCFAs or incorporated into lipid molecules. Fatty acid elongation is similar to *de novo* fatty acid synthesis, but instead, malonyl-CoA and acyl-CoA are used as C2 unit donor and acceptor, respectively.

ACETYL-COA CARBOXYLASE

General description

ACCase [EC 6.4.1.2] is a biotin-containing enzyme that catalyzes the ATP-dependent carboxylation of acetyl-CoA to form malonyl-CoA. This reaction occurs in two steps (Figure 1): (1) carboxylation of the biotin prosthetic group; (2) transfer of the carboxyl group from carboxyl-biotin to acetyl-CoA to form malonyl-CoA.

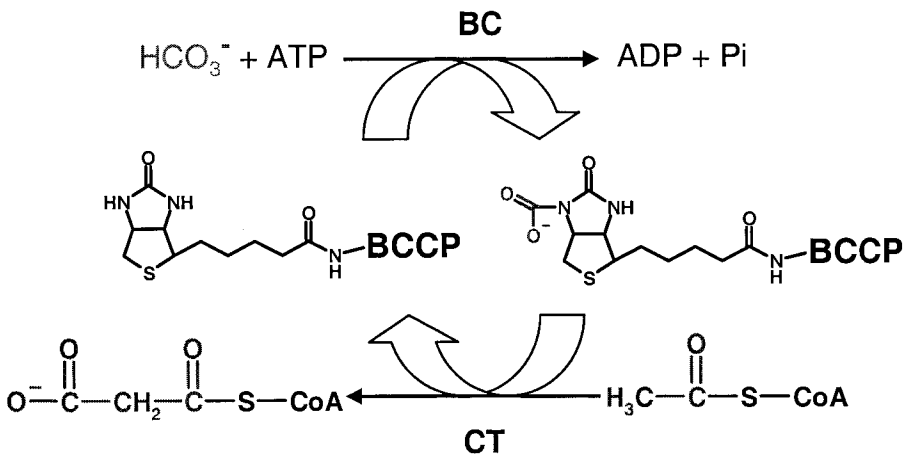

Figure 1. The two-step reaction of acetyl-CoA carboxylation catalyzed by ACCase.

ACCase has three conserved functional domains: biotin carboxyl-carrier protein (BCCP), biotin carboxylase (BC), and carboxyl transferase (CT). While BCCP acts as an intermediate carrier of the carboxyl group, BC and CT catalyze the two half reactions respectively.

Two forms of ACCase in plants

In most plants (excluding Graminae), there are two forms of ACCases: a homomeric ACCase in the cytosol and a heteromeric ACCase in plastids (Konishi and Sasaki, 1994; Konishi et al., 1996). While in the homomeric ACCase the three functional domains are on a single polypeptide, the heteromeric ACCase consists of separate dissociable subunits. Graminae plants, such as maize and wheat, don't have the heteromeric ACCase. Instead, they have two types of homomeric ACCases; one is cytosolic and the other is plastidic (Konishi and Sasaki, 1994; Konishi et al., 1996).

Homomeric ACCase

Plant homomeric ACCases are homologous to that of animals and yeasts. They are composed of two identical 250kD polypeptides, on which the BC, BCCP and CT domains are located sequentially from the N-terminus to the C-terminus. The homomeric ACCase is encoded by a small gene family in all the plants examined so far (Egli et al., 1993; Yanai et al., 1995; Podkowinski et al., 1996; Schulte et al., 1997). In Arabidopsis, *ACC1* and *ACC2*, two genes arranged in tandem within 25-kb on chromosome 1, code the homomeric ACCase (Yanai et al., 1995). It has been reported that *ACC1* gene is required for very long chain fatty acid elongation and is essential for embryo development (Baud et al., 2003).

Heteromeric ACCase

The plant heteromeric ACCase (htACCase) is composed of four subunits, BCCP subunit (Choi et al., 1995; Elborough et al., 1996; Ke et al., 1997; Reverdatto et al., 1999; Thelen et al., 2000), BC subunit (Alban et al., 1995; Shorrosh et al., 1995; Bao et al., 1997; Sun et al., 1997; Reverdatto et al., 1999), and α (Shorrosh et al., 1996; Reverdatto et al., 1999; Ke et al., 2000) and β subunits of CT (Sasaki et al., 1993; Elborough et al., 1996; Reverdatto et al., 1999; Ke et al., 2000). Genes coding three of these subunits are nuclear, but a plastome gene encodes the β-CT subunit. While multiple nuclear genes code for a given subunit in other plant species, in *Arabidopsis* single-copy genes code for all the subunits except BCCP, which is coded by two paralogous genes, *CAC1-A* and *CAC1-B* (Mekhedov et al., 2000; Thelen et al., 2000, 2001)(Table 1).

Table 1. Arabidopsis htACCase genes

Gene	Genomic Locus	subunit	Protein Size	Chromosome
CAC1-A	At5g16390	Biotin Carboxyl Carrier Protein 1 (BCCP-1)	280aa	V
CAC1-B	At5g15530	Biotin Carboxyl Carrier Protein 2 (BCCP-2)	255aa	V
CAC2	At5g35360	Biotin Carboxylase (BC)	537aa	V
CAC3	At2g38040	α subunit of Carboxyltransferase (α-CT)	796aa	II
accD	AtCg00500	β subunit of Carboxyltransferase (β-CT)	488aa	Chloroplast

To date, plant htACCase holoenzyme complexes have not been purified because they are unstable and dissociate during purification. Given the existence of multiple genes coding for

a given subunit, the htACCase complexes could be highly heterogenous. In the simplest case of *Arabidopsis*, the holoenzyme complexes could potentially contain either BCCP-1 or BCCP-2, or both. However, it is not known whether all of them exist *in vivo*.

Regulation of htACCase

Studies to date indicate that regulation of htACCase is complex and may occur at multiple levels. It has been found that htACCase activity is much higher in light-incubated spinach chloroplasts than in dark-incubated ones (Hunter and Ohlrogge, 1998). Further studies on the htACCase in pea revealed that htACCase is activated by light-dependent reduction of CT via a thioredoxin-mediated redox cascade (Sasaki et al., 1997; Kozaki and Sasaki, 1999; Kozaki et al., 2000). An intermolecular disulfide-dithiol exchange between the α- and β-CT subunits has been shown to be involved in the redox regulation of CT (Kozaki et al., 2001). There is also evidence showing that the htACCase activity can be modified by light-dependent phosphorylation of β-CT subunit (Savage and Ohlrogge, 1999). Besides the above post-translational regulatory mechanisms, a chloroplast RNA editing mechanism has also been reported to be required for functional htACCase in pea (Sasaki et al., 2001).

Plant htACCase is also developmentally regulated. It has been shown that expression of the *Arabidopsis CAC1-A, CAC2, CAC3* and *accD* genes is spatially and temporally coordinated with lipogenesis (Ke et al., 1997; Sun et al., 1997; Ke et al., 2000). Since htACCase is composed of multiple subunits, it is expected that these subunits are produced in stoichiometric amount. Indeed, the four mRNAs maintain a constant molar ratio during plant development (Ke et al., 2000). Moreover, a recent study indicates that there is a higher level

of coordination between htACCase and other enzymes involved in fatty acid and lipid biosynthesis pathway (O'Hara et al., 2002). But the mechanisms of such coordinate regulations remain unknown.

DISSERTATION ORGANIZATION

This dissertation is composed of four chapters. The first chapter provides a general introduction of fatty acid biosynthesis and acetyl-CoA carboxylase in plants. The following two chapters are two manuscripts prepared for submission to journals. Chapter 2 is on functional analysis of the two BCCP-coding genes in *Arabidopsis thaliana*. I did the knockout mutant isolation (the *cac1-a-1* allele was identified by Ping Che) and genetic characterization, protein analysis, and fatty acid analysis. The microscopic examination of the mutants and the pollen germination experiment were done collaboratively with Hilal Ilarslan. The *in situ* hybridization of *CAC1-A* and *CAC1-B* mRNAs during embryo development was performed by Ling Li and Carol Foster. CAC1A antisense plants were generated and characterized by Hui-rong Qian. Chapter 3 concerns the coordination of the expression of htACCase subunit genes. I produced all the data presented in this chapter. Chapter 4 summarizes the results presented in chapters 2 and 3, and discusses future research.

REFERENCES

Alban, C., Jullien, J., Job, D., and Douce, R. (1995). Isolation and Characterization of Biotin Carboxylase from Pea Chloroplasts. Plant Physiol **109,** 927-935.

Bao, X., Shorrosh, B.S., and Ohlrogge, J.B. (1997). Isolation and characterization of an Arabidopsis biotin carboxylase gene and its promoter. Plant Mol Biol **35,** 539-550.

Baud, S., Guyon, V., Kronenberger, J., Wuilleme, S., Miquel, M., Caboche, M., Lepiniec, L., and Rochat, C. (2003). Multifunctional acetyl-CoA carboxylase 1 is essential for very long chain fatty acid elongation and embryo development in Arabidopsis. Plant J **33,** 75-86.

Choi, J.K., Yu, F., Wurtele, E.S., and Nikolau, B.J. (1995). Molecular cloning and characterization of the cDNA coding for the biotin- containing subunit of the chloroplastic acetyl-coenzyme A carboxylase. Plant Physiol **109,** 619-625.

Egli, M.A., Gengenbach, B.G., Gronwald, J.W., Somers, D.A., and Wyse, D.L. (1993). Characterization of Maize Acetyl-Coenzyme A Carboxylase. Plant Physiol **101,** 499-506.

Elborough, K.M., Winz, R., Deka, R.K., Markham, J.E., White, A.J., Rawsthorne, S., and Slabas, A.R. (1996). Biotin carboxyl carrier protein and carboxyltransferase subunits of the multi-subunit form of acetyl-CoA carboxylase from Brassica napus: cloning and analysis of expression during oilseed rape embryogenesis. Biochem J **315,** 103-112.

Hunter, S.C., and Ohlrogge, J.B. (1998). Regulation of spinach chloroplast acetyl-CoA carboxylase. Arch Biochem Biophys **359,** 170-178.

Ke, J., Wen, T.N., Nikolau, B.J., and Wurtele, E.S. (2000). Coordinate regulation of the nuclear and plastidic genes coding for the subunits of the heteromeric acetyl-coenzyme A carboxylase. Plant Physiol **122,** 1057-1071.

Ke, J., Choi, J.K., Smith, M., Horner, H.T., Nikolau, B.J., and Wurtele, E.S. (1997). Structure of the CAC1 gene and in situ characterization of its expression. The Arabidopsis thaliana gene coding for the biotin- containing subunit of the plastidic acetyl-coenzyme A carboxylase. Plant Physiol **113,** 357-365.

Konishi, T., and Sasaki, Y. (1994). Compartmentalization of two forms of acetyl-CoA carboxylase in plants and the origin of their tolerance toward herbicides. Proc Natl Acad Sci U S A **91,** 3598-3601.

Konishi, T., Shinohara, K., Yamada, K., and Sasaki, Y. (1996). Acetyl-CoA carboxylase in higher plants: most plants other than gramineae have both the prokaryotic and the eukaryotic forms of this enzyme. Plant Cell Physiol **37,** 117-122.

Kozaki, A., and Sasaki, Y. (1999). Light-dependent changes in redox status of the plastidic acetyl-CoA carboxylase and its regulatory component. Biochem J **339,** 541-546.

Kozaki, A., Mayumi, K., and Sasaki, Y. (2001). Thiol-disulfide exchange between nuclear-encoded and chloroplast-encoded subunits of pea acetyl-CoA carboxylase. J Biol Chem **276,** 39919-39925.

Kozaki, A., Kamada, K., Nagano, Y., Iguchi, H., and Sasaki, Y. (2000). Recombinant carboxyltransferase responsive to redox of pea plastidic acetyl-CoA carboxylase. J Biol Chem **275,** 10702-10708.

Mekhedov, S., de Ilarduya, O.M., and Ohlrogge, J. (2000). Toward a functional catalog of the plant genome. A survey of genes for lipid biosynthesis. Plant Physiol **122,** 389-402.

O'Hara, P., Slabas, A.R., and Fawcett, T. (2002). Fatty acid and lipid biosynthetic genes are expressed at constant molar ratios but different absolute levels during embryogenesis. Plant Physiol **129,** 310-320.

Podkowinski, J., Sroga, G.E., Haselkorn, R., and Gornicki, P. (1996). Structure of a gene encoding a cytosolic acetyl-CoA carboxylase of hexaploid wheat. Proc Natl Acad Sci U S A **93,** 1870-1874.

Post-Beittenmiller, D. (1996). Biochemistry and molecular biology of wax production in plants. Annu. Rev. Plant Physiol. Plant Mol. Biol. **47,** 405-430.

Reverdatto, S., Beilinson, V., and Nielsen, N.C. (1999). A multisubunit acetyl coenzyme A carboxylase from soybean. Plant Physiol **119,** 961-978.

Sasaki, Y., Kozaki, A., and Hatano, M. (1997). Link between light and fatty acid synthesis: thioredoxin-linked reductive activation of plastidic acetyl-CoA carboxylase. Proc Natl Acad Sci U S A **94,** 11096-11101.

Sasaki, Y., Kozaki, A., Ohmori, A., Iguchi, H., and Nagano, Y. (2001). Chloroplast RNA editing required for functional acetyl-CoA carboxylase in plants. J Biol Chem **276,** 3937-3940.

Sasaki, Y., Hakamada, K., Suama, Y., Nagano, Y., Furusawa, I., and Matsuno, R. (1993). Chloroplast-encoded protein as a subunit of acetyl-CoA carboxylase in pea plant. J Biol Chem **268,** 25118-25123.

Savage, L.J., and Ohlrogge, J.B. (1999). Phosphorylation of pea chloroplast acetyl-CoA carboxylase. Plant J **18,** 521-527.

Schulte, W., Topfer, R., Stracke, R., Schell, J., and Martini, N. (1997). Multi-functional acetyl-CoA carboxylase from Brassica napus is encoded by a multi-gene family: indication for plastidic localization of at least one isoform. Proc Natl Acad Sci U S A **94,** 3465-3470.

Shorrosh, B.S., Savage, L.J., Soll, J., and Ohlrogge, J.B. (1996). The pea chloroplast membrane-associated protein, IEP96, is a subunit of acetyl-CoA carboxylase. Plant J **10,** 261-268.

Shorrosh, B.S., Roesler, K.R., Shintani, D., van de Loo, F.J., and Ohlrogge, J.B. (1995). Structural analysis, plastid localization, and expression of the biotin carboxylase subunit of acetyl-coenzyme A carboxylase from tobacco. Plant Physiol **108,** 805-812.

Sun, J., Ke, J., Johnson, J.L., Nikolau, B.J., and Wurtele, E.S. (1997). Biochemical and molecular biological characterization of CAC2, the Arabidopsis thaliana gene coding for the biotin carboxylase subunit of the plastidic acetyl-coenzyme A carboxylase. Plant Physiol **115,** 1371-1383.

Thelen, J.J., Mekhedov, S., and Ohlrogge, J.B. (2000). Biotin carboxyl carrier protein isoforms in Brassicaceae oilseeds. Biochem Soc Trans **28,** 595-598.

Thelen, J.J., Mekhedov, S., and Ohlrogge, J.B. (2001). Brassicaceae express multiple isoforms of biotin carboxyl carrier protein in a tissue-specific manner. Plant Physiol **125,** 2016-2028.

Weber, H. (2002). Fatty acid-derived signals in plants. Trends Plant Sci **7,** 217-224.

Yanai, Y., Kawasaki, T., Shimada, H., Wurtele, E.S., Nikolau, B.J., and Ichikawa, N. (1995). Genomic organization of 251 kDa acetyl-CoA carboxylase genes in Arabidopsis: tandem gene duplication has made two differentially expressed isozymes. Plant Cell Physiol **36,** 779-787.

CHAPTER 2. FUNCTIONAL ANALYSIS OF THE TWO PARALOGOUS GENES CODING FOR THE BCCP SUBUNIT OF THE HETEROMERIC ACETYL-COA CARBOXYLASE OF ARABIDOPSIS

A manuscript to be submitted to The Plant Cell

Xu Li[a], Hui-Rong Qian[b], Hilal Ilarslan[b], Ling Li[b], Carol Foster[b], Ping Che[a], Eve Syrkin Wurtele[b], and Basil J. Nikolau[a]

[a]Department of Biochemistry, Biophysics and Molecular Biology, and [b]Department of Genetics, Development and Cell Biology, Iowa State University, Ames, IA 50011

ABSTRACT

The heteromeric acetyl-CoA carboxylase (htACCase) catalyzes the first and committed reaction of *de novo* fatty acid synthesis in plastids. This enzyme is composed of four subunits: biotin carboxyl-carrier protein (BCCP), biotin carboxylase (BC), alpha-carboxyltransferase (α-CT) and beta-carboxyltransferase (β-CT). Genes coding three of these subunits are nuclear, but a plastome gene encodes the beta-CT subunit. In *Arabidopsis*, single-copy genes encode all these subunits, with the exception of the BCCP subunit. We have identified a T-DNA knockout mutant for the α-CT-coding gene (*CAC3*, At2g38040); the fact that the *cac3* mutant is recessive embryo lethal is consistent with the essential role of htACCase for lipid biosynthesis during embryogenesis. The two BCCP-coding genes, *CAC1-A* (At5g16390, codes for BCCP-1) and *CAC1-B* (At5g15530, codes for BCCP-2), have similar spatial and temporal expression patterns during embryo development, but their individual functional significance is unknown. To test the potential redundant role of the two BCCP isoforms, we have identified and characterized T-DNA knockout mutants for both *CAC1-A* and *CAC1-B*

genes. While *CAC1-A* mutant is recessive embryo lethal, the *CAC1-B* knockout mutant has no discernable phenotype. The composition and quantity of fatty acids in seeds, as well as the accumulation of the other subunits of htACCase, was not affected by loss of BCCP-2 subunits. *CAC1-A* antisense plants with reduced BCCP-1 possessed different degrees of changes. They are smaller than the wild-type plants, and their late vegetative and cauline leaves are crinkly and variegated yellow, indicating premature cell death. *CAC1-A* antisense plants have reduced leaf cell size, altered leaf organelle morphology and retarded embryo development. The severity of the morphological change in *CAC1-A* antisense plants is correlated with the magnitude of the reduction of BCCP-1 protein. However, the mRNA and protein abundance of the other three subunit proteins of htACCase are not altered. Fatty acid contents in leaves and seeds of each *CAC1-A* antisense plant are reduced, but the fatty acid composition is indistinguishable from wild type plants. These results indicate that BCCP-1 is an essential subunit of htACCase and cannot be substituted by BCCP-2. In contrast, BCCP-2 appears to be redundant to BCCP-1, and is dispensable for the function of htACCase.

INTRODUCTION

Acetyl-CoA carboxylase (ACCase) [EC 6.4.1.2] catalyzes the ATP-dependent carboxylation of acetyl-CoA to produce malonyl-CoA. There are two forms of ACCase in plants. One isoform generates malonyl-CoA for *de novo* fatty acid synthesis in plastids, and the other is responsible for generating the cytosolic malonyl-CoA pool, which is required by many metabolic pathways, such as fatty acid elongation and flavonoid biosynthesis. In most plants (with the exception of the Graminae) the plastidic ACCase is a heteromeric isoform and the cytosolic isoform is homomeric (Konishi and Sasaki, 1994; Konishi et al., 1996).

The heteromeric acetyl-CoA carboxylase (htACCase) is composed of three nuclear-gene-encoded subunits, biotin carboxyl-carrier protein (BCCP), biotin carboxylase (BC), α-carboxyltransferase (α-CT) and one plastome-gene-encoded subunit, β-carboxyltransferase (β-CT). In *Arabidopsis thaliana*, single-copy genes encode BC (*CAC2*) (Sun et al., 1997), α-CT (*CAC3*) (Ke et al., 2000a), and β-CT (*accD*) (Ke et al., 2000a), but there are two BCCP-coding genes. *CAC1-A* (At5g16390) codes for BCCP-1 and *CAC1-B* (At5g15530) codes for BCCP2 (Choi et al., 1995; Ke et al., 1997; Thelen et al., 2001). *CAC1-A* and *CAC1-B* genes are located within 0.32 Mb of each other on chromosome 5. There are four potential explanations for this apparent redundancy in BCCP genes: 1) One of the BCCP-coding genes is non-functional and is thus a pseudogene; 2) the two BCCP-coding genes provide the identical function in the same tissue, i.e., the genes are redundant; 3) the two BCCP-coding genes provide different functions in the same tissues; 4) the two BCCP-coding genes provide the same function in different tissues; or 5) the two BCCP-coding genes provide different functions in different tissues. The first of these hypotheses can probably be discounted based upon initial observations, which indicate that both genes are expressed (Thelen et al., 2001). To distinguish between the latter four hypotheses we have characterized the spatial and temporal pattern of expression of each BCCP gene during seed development by *in situ* hybridization using gene-specific probes to each mRNA. In addition, we characterized T-DNA knockout mutants for the two BCCP-coding genes as well as the α-CT-coding gene. These characterizations indicate that the htACCase is essential for plant seed development, and that BCCP-1 is an essential subunit for htACCase, but BCCP-2 appears to be redundant to BCCP-1 and dispensable.

The embryonic lethality of *CAC1-A* knockout mutant prevents further studies on the functions of BCCP-1 in other developmental stages. To overcome this problem, we have used antisense RNA technology to reduce the expression of *CAC1-A* gene. Characterization of the *CAC1-A* antisense plants confirmed the important role of BCCP-1 in embryo development and also revealed the dramatic morphological consequences of reducing the accumulation of BCCP-1 subunit of htACCase during vegetative development.

RESULTS

Generation of BCCP-1 and BCCP-2 specific antibodies

To develop the tools for studying the individual functional significance of BCCP-1 and BCCP-2, polyclonal antibodies specific for each BCCP subunit were generated by immunizing rabbits with BCCP-1- or BCCP-2-specific recombinant proteins. The amino acid sequences of BCCP-1 and BCCP-2 were aligned using GCG software (Genetics Computer Group, Madison, WI). The cDNA sequence of each gene for the region with low amino acid similarity between the two polypeptides was PCR amplified and cloned into pET-30 vector (Novagen, Madison, WI) (Figure 1A). Recombinant proteins were produced by overexpression of these two constructs in *E. coli*. Western blot analyses of the protein extracts from *Arabidopsis* flowers with these two antibodies as well as with streptavidin were performed to test the specificity of the two antibodies produced. While streptavidin revealed BCCP-1 and BCCP-2 as two protein bands of about 35 kD and 25 kD, BCCP-1 antibody only detected the 35 kD band, and BCCP-2 antibody only detected the 25kD band (Figure 1B and C). This demonstrates that monoreactive antibodies for the BCCP-1 and BCCP-2 proteins were generated.

Identification of T-DNA knockout mutants for htACCase subunit genes

To investigate how the different subunit genes of the htACCase genetically interact with each other to affect ACCase activity and potentially regulate fatty acid biosynthesis, and to understand the physiological significance of htACCase in plants, we identified and characterized T-DNA tagged mutant alleles for three of the subunit genes (*CAC1-A*, *CAC1-B*, and *CAC3*) (Table 1). The *cac1-a-1* allele was isolated from the T-DNA insertion lines of Arabidopsis Knockout facility at University of Wisconsin-Madison (Sussman et al., 2000). Other candidate alleles were found by searching SALK Insertion Sequence Database (http://signal.salk.edu/cgi-bin/tdnaexpress) for each gene (Alonso et al., 2003). Plant genomic DNA sequences flanking the T-DNA borders were amplified by PCR and sequenced. The molecular structure of the mutant alleles was deduced by aligning these flanking DNA sequences against the *Arabidopsis* genome sequence.

Based on the information at the SALK database, the T-DNA (or transposon in the case of GT lines) is located within coding region of *CAC1-A* gene in three lines (SALK_138637, GT_3_38620, and SALK_050082), but we could not find the T-DNA or transposon insertion by PCR-based assays for SALK_138637 and GT_3_38620 lines. We were however, able to identify the T-DNA left border for SALK_050082 line. Segregation analysis indicated an unusual behavior for this allele. Specifically, all progeny (48 plants analyzed) from a single heterozygote were heterozygous for the T-DNA allele and no wild-type or homozygous mutant plants were recovered. When heterozygous mutants were crossed with wild-type plants, all the F1 (20 plants) were heterozygotes. We concluded therefore that in this line a

translocation of the T-DNA carrying partial *CAC1-A* gene occurred, and no further analysis was carried out.

In agreement with the SALK database, we found the T-DNA insertion located within 300 bp upstream of the start codon of *CAC1-A* gene for SALK_023225 and SALK_120571 lines. Homozygous mutants from these two lines were obtained. However, western blot analysis with BCCP-1 anti-serum showed that homozygous mutant plants carrying these alleles accumulate similar level of BCCP-1 as wild-type plants (data not shown). The T-DNA flanking sequences in SALK database indicate that the insertion in SALK_025081 and GABI_217E08 lines is further upstream from the *CAC1-A* coding region than in the SALK_023225 and SALK_120571 alleles, therefore they are unlikely to be knockout alleles. In similar analyses, we also failed to detect the T-DNA insertion in the *CAC3* gene for the SALK_045127 line. Therefore out of all the lines analyzed, four mutant alleles (*cac1-a-1*, *cac1-b-1*, *cac1-b-2*, and *cac3-1*) were subjected to further characterization.

The *cac1-a-1* allele has two copies of T-DNA inserted head-to-head in the first intron of *CAC1-A* gene (Figure 2A). There is a small (4bp) deletion of genomic DNA at the insertion site. One end of the T-DNA in the *cac1-b-1* allele (SALK_056228) is located in the third intron of *CAC1-B* gene, and the other end was not defined (Figure 2B). In the *cac1-b-2* allele (SALK_070569), the T-DNA insertion resulted in a 64bp deletion of the first exon-intron junction of *CAC1-B* gene (Figure 2B). The *cac3-1* allele (SALK_045139) has two copies of T-DNA inserted head-to-head in the first exon of *CAC3* gene (Figure 2C).

Both *cac1-a-1* and *cac3-1* alleles are recessive lethal, but the two *cac1-b* alleles are not

As the first step to characterize a loss-of-function mutation, seeds from a single heterozygous mutant plant were sowed on MS plates and segregation analysis was carried out by genotyping the progeny seedlings. For the *cac1-a-1* and the *cac3-1* alleles, homozygous mutant plants were never recovered. Thus, out of 204 *cac1-a-1* progeny and 40 *cac3-1* progeny that were genotyped, only heterozygotes or wild-type progeny were recovered (Table 2). Hence, both *cac1-a-1* and *cac3-1* appear to be recessive lethal. Observations of the *cac1-a-1* mutant showed that there are more seeds aborted after fertilization in siliques from heterozygous plants than in siliques from wild-type siblings (Figure 3A). Eighteen siliques from heterozygous mutant plants and fifteen siliques from wild-type siblings were dissected under a stereomicroscope. Aborted and normal seeds were counted (Table 3). The proportion of aborted seeds in siliques from heterozygous plants is significantly higher (0.175±0.05) than that from wild-type siblings (χ^2= 43.85, *p* value<0.0001). Therefore, at the 95% confidence level, 12.5% to 22.5% of seeds from heterozygous mutant plants were aborted due to effects other than environmental influences. Similarly, more aborted seeds were observed within siliques of heterozygous *cac3-1* mutant plants than in the siliques of their wild-type siblings (Figure 3B). We therefore deduce that these aborted seeds are homozygous mutants (genotype: *cac1-a-1/cac1-a-1* or *cac3-1/cac3-1*).

In contrast, homozygous mutant plants were recovered for both *cac1-b-1* and *cac1-b-2* alleles. Both alleles were inherited with a normal Mendelian ratio (1:2:1) (Table 2). The *cac1-b-1* and *cac1-b-2* mutants showed no apparent phenotypic differences from wild-type plants. Seeds develop normally independent of the *CAC1-B* allele (Figure 3C). Western blot analysis with BCCP-2-specific antibody showed that BCCP-2 protein was not detectable in

both *cac1-b-1* and *cac1-b-2* homozygous mutants (Figure 4). Therefore, these two *cac1-b* alleles are nulls.

Genetic complementation of *cac1-a-1* mutant

Since no other knockout alleles for *CAC1-A* gene were available, we carried out complementation experiments to prove that the lethal phenotype is due to loss of *CAC1-A* gene function. A 4.5 kb *Arabidopsis* genomic fragment containing the *CAC1-A* gene was transformed into heterozygous *cac1-a-1* plants with Bar gene as a selective marker. Since the T-DNA of the *cac1-a-1* allele has a Kan selection marker, it does not interfere with the screening for the newly transformed genomic *CAC1-A* fragment. Gene-specific primers flanking the T-DNA insertion site of *cac1-a-1* allele were designed with one primer residing in the genome region beyond the 4.5 kb fragment, so the native genomic *CAC1-A* allele can be distinguished from the one on the transformed 4.5 kb fragment. We were able to recover T2 generation plants homozygous for *cac1-a-1* allele, which also carry the transformed *CAC1-A* genomic fragment. This demonstrates that the *cac1-a-1* allele is a loss-of-function allele and responsible for the lethal phenotype.

Effect of the *cac1-a-1* allele on embryo and endosperm development

To further characterize the phenotype of the *cac1-a-1* mutant allele, detailed microscopic examinations of developing seeds were carried out on heterozygous plants (Figure 5). Mutant embryos showed a delay of development and aborted prematurely. Specific differences associated with the *cac1-a-1* allele are as follows: At 3 DAF, delays in embryo and endosperm development are apparent. When wild-type embryos are at the 32-cell stage, mutant embryos

are at the 8-cell stage. At 5 DAF, mutant embryos are at the globular stage, and embryo cells are highly vacuolated. Furthermore, the embryo sac is collapsed. Endosperm remains uncellularized in aborted seeds, showing abnormal peripheral free nuclear and no radial microtubules. At 7 DAF, whereas normal embryos are at the torpedo stage, aberrant embryos have not grown or undergone polarization, rather they are shriveled and the embryo sac has collapsed, and the endosperm has degenerated. At 9 DAF, normal embryos are at the mature stage, but mutant embryos are at the heart stage.

cac1-a-1 allele reduces male gamete transmission

From the segregation analysis, the ratio of progeny from a heterozygous plant with the genotype *CAC1-A/cac1-a-1* versus *CAC1-A/CAC1-A* was found to be 1.4 (119:85) instead of 2, as would be expected for a normal Mendelian recessive lethal allele. The observed deviation from the 2:1 segregation ratio is statistically significant (χ^2 test, p value = 0.012). This indicates that the transmission of gametes carrying the *cac1-a-1* mutant allele is reduced.

To determine whether the transmission of the male or female gamete is affected by the *cac1-a-1* allele, we crossed heterozygous mutant plants as either males or females (genotype *CAC1-A/cac1-a-1*) with wild-type plants (genotype *CAC1-A/CAC1-A*). The genotypes of the progeny from these crosses were scored by PCR analysis (Table 4). The *cac1-a-1* and *CAC1-A* alleles are equally transmitted (50% for each) through the female gametes. However, transmission of the mutant allele is at 30% and wild-type allele 70% when transmitted through the male gamete. Thus, the *cac1-a-1* allele affected the transmission of the male gametes.

Effect of the *cac1-a-1* allele on morphology and germination of pollen grains and on pollen tube growth

To further characterize the reduced transmission of the *cac1-a-1* allele through male gametes, the morphology of pollen grains was examined by microscopy. Pollen grains from heterozygous (*CAC1-A/cac1-a-1*) plants (Figure 6B and D) were a mixture of normal-looking grains (white arrowed) and grains which have an abnormal shape (yellow arrowed). On these abnormally shaped pollen grains the exine pattern is also abnormal, especially around the aperture, where the exine has a smooth appearance (the aperture is the spot on the pollen grain where the pollen tube will expand from upon pollen germination). Such aberrant pollen grains were not recovered from sibling wild-type plants (Figure 6A and C).

To investigate the effect of *cac1-a-1* allele on pollen germination, an *in vitro* germination assay was performed with pollen collected from heterozygous (*CAC1-A/cac1-a-1*) and wild-type (*CAC1-A/CAC1-A*) sibling plants. Pollen grains were placed on slides that contain germination medium and incubated at 22 °C under continuous illumination for twenty hours. Then pollen grains were examined and categorized as germinated, not germinated, or burst. For each category, the number of pollen was counted and the percentages calculated (Figure 7). While 90% of the pollen from wild-type siblings germinated, only about 60% of pollens from *cac1-a-1* heterozygous plants germinated. Thus, the germination rate of pollen from *cac1-a-1* heterozygous mutant is significantly reduced (about 30% lower than wild-type). Moreover, 6% of pollen grains from *cac1-a-1* heterozygous plants generated pollen tubes that burst during germination and so were classified as burst, but less than 1% of the pollen from wild-type siblings were burst.

To ascertain the effect of the *cac1-a-1* allele on pollen germination *in vivo*, germinating self-pollen grains on pistils of heterozygous (*CAC1-A/cac1-a-1*) and wild-type (*CAC1-A/CAC1-A*) sibling plants were stained with Aniline Blue and DAPI and examined by florescence microscopy. Fewer pollen tubes germinate on the heterozygous plants (Figure 8B and D) than on the sibling wild-type plants (Figure 8A and C), and for those pollen grains that have germinated, pollen tube migration is slower through the style.

CAC1-A antisense plants show unique morphological changes

Since the *cac1-a-1* mutant allele is embryo lethal, we were unable to examine the role of the BCCP-1 protein in the plant following embryogenesis. Therefore, transgenic *Arabidopsis* plants expressing the *CAC1A* antisense RNA under the transcriptional control of the CaMV 35S promoter were generated and characterized. Forty-two independent transgenic lines were obtained, as indicated by inheritance of the tightly linked kanamycin-resistance trait, PCR amplification of the 35S::*CAC1-A* antisense transgene, and Southern blot hybridization analyses of genomic DNA isolated from individual plants from each transgenic line (data not shown).

About half of these transgenic lines show unique morphological alterations as compared to wild-type controls. These lines were grouped into five classes (very severe, severe, moderate, mild, or wild-type-like) depending upon the strength of the transgene-associated phenotype (Table 5, Figure 9A and B). A key feature of the *CAC1-A* antisense phenotype is that the timing of the appearance of the growth aberrations depends on the strength of the phenotype; the stronger the phenotype, the earlier its developmental onset.

The very severe phenotype is evident upon germination as stunted growth (Figure 9A, plants with white arrows) and yellow patches on the cotyledons (Figure 9G and J). These seedlings remain small and ultimately die within 7 days after germination. If rosette leaves appear on these plants, they are minute and crinkly with a mosaic green and yellow pattern of pigmentation.

Plants with a severe phenotype germinate normally and have normal-appearing cotyledons, but the growth rate of these seedlings is noticeably decreased 1-2 weeks after germination. These plants may have up to three wild-type-like true leaves, but subsequent emerging rosette and cauline leaves are significantly smaller, extremely undulated and mostly yellow variegated with small green areas (Figure 9C). By 30 days after imbibition (DAI) these plants are approximately one-fifth the size of wild-type plants (Figure 9F). A subset of the plants with a severe phenotype do not bolt.

In plants that show a moderate phenotype, the switch from wild-type-like leaves to aberrant leaves occurs sometime between the emergence of the fourth and seventh leaf (Figure 9D). Aberrant leaves are slightly crinkly and have distinct yellow patches (Figure 9H and I). By 30 DAI these plants are approximately two-thirds the size of wild-type plants.

Plants having a mild phenotype (Figure 9E) are indistinguishable from the wild-type plants until they bolt. After bolting, the rosette and cauline leaves that emerge are crinkly and have a mosaic pattern, characteristic of the *CAC1-A* antisense phenotype. Those transgenic lines that show no apparent alteration in morphology or development were classified as wild type-like transgenics.

Irrespective of the strength of the phenotype (which includes decreased plant size and leaf number), those plants that bolt do so with the same timing as their wild-type siblings (3-4

weeks after germination). The transgenic plants that survive until flowering produce viable seeds. However, seed yield varies inversely with the strength of the phenotype, ranging from only a few seeds for the severe phenotype, to between 0.3 and 0.65 g/plant for the mild phenotype, a yield similar to that of wild-type plants.

The morphological phenotype co-segregates with the *CAC1-A* antisense transgene

To confirm that the morphological changes in the *CAC1-A* antisense transgenic plants are caused by the transgene, PCR amplification was used to track the inheritance of the transgene. Progeny from three independent heterozygous *CAC1-A* antisense lines segregate approximately 3:1 (antisense phenotype:wild-type phenotype) (Table 6). DNA was isolated from individual offspring with and without the antisense phenotype and the presence of the antisense *CAC1-A* gene determined by PCR. Table 6 shows that all plants with an antisense phenotype carry the transgene, and no plant with a wild-type phenotype carries this transgene. These data indicate that the antisense *CAC1-A* transgene is incorporated at a single locus in the genome and that this transgene is the cause of the morphological changes in the transgenic plants.

***CAC1-A* antisense transgene decreases the accumulation of the BCCP-1 protein**

To determine whether *CAC1-A* expression is down-regulated in the antisense *CAC1-A* transgenic plants, the accumulation of the BCCP-1 protein was assessed by measuring immunoreactive BCCP-1 polypeptide and the biotin prosthetic group associated with this protein (Figure 10). The accumulation of the BCCP-1 protein in shoots of 30 day-old plants with a moderate phenotype is significantly lower than that in wild-type plants (about 35% of

wild-type levels; p value<0.0001, for both antisera and streptavidin detection); in plants with a severe phenotype BCCP-1 levels is even lower (about 20% of wild-type levels; p value=0.001 and 0.0002 for antisera and streptavidin detection, respectively). In transgenic plants with a mild or wild-type-like phenotype, BCCP-1 polypeptide and holoprotein levels are indistinguishable from wild-type plants (data not shown). The ratios of the band detected by BCCP-1 antisera to that detected by streptavidin are near identical regardless of the genotypes tested (cf., Figure 10B and C). These comparisons indicate that the biotinylation status of BCCP-1 is similar in wild-type and *CAC1-A* antisense plants.

Cellular size is diminished in leaves with reduced levels of BCCP-1

To assess the cellular basis for the striking change in leaf morphology associated with the *CAC1-A* antisense plants, leaves from wild-type plants and a series of *CAC1-A* antisense plants from four independent transgenic lines were examined microscopically (Figure 11). Leaves from *CAC1-A* antisense plants are thinner than wild-type leaves, in many cases being only 1/2 the thickness of the latter. This decrease in leaf thickness is the result of reduced cell size and near-absence of apoplastic space. Measurement of the dimensions of epidermal, mesophyll and palisade parenchyma cells indicates that all three-cell types are one-fourth to two-thirds smaller than the corresponding wild-type cells (Figure 12). Despite the reduction in cell and leaf size, the overall cellular organization within the leaf is retained, with one layer of elongated palisade cells and a spongy mesophyll layer of four to six cells delimited by elongated epidermal cells (Figure 11). Furthermore, the water content of rosette leaves is indistinguishable among wild-type and *CAC1-A* antisense plants with mild and severe

phenotypes (ratios of fresh weight to dry weight are: 10.9 ± 1.1, 11.3 ± 1.0, 9.7 ± 0.4, respectively).

The undulation that occurs in many leaves of *CAC1-A* antisense plants is due, in part, to a decrease in the size and number of mesophyll cells in discreet locations along the leaf lamellae, which is occasionally accentuated by a missing or malformed epidermal cell (Figure 11G, H).

There are also intracellular changes associated with the *CAC1-A* antisense plants. The size of the vacuoles is greatly reduced and there is a corresponding increase in the visible cytosol. Additionally, the mesophyll cells contain fewer chloroplasts (Figure 11D, F, H) than wild-type cells (Figure 11B).

Organelle morphology is altered in leaves with reduced levels of BCCP-1

Electron microscopy reveals that the plastids of leaves of *CAC1-A* antisense plants are smaller than normal and show structural aberrations (Figure 13). The outer envelope is undulate and the grana, when present, are disorganized. These plastids also lack conspicuous starch grains, and many contain numerous, large plastoglobuli (e.g., Figure 13C).

The mitochondria of these cells are also unusual. Approximately half of the mitochondria are aberrant, with the other half appearing normal. Affected mitochondria are enlarged (roughly doubled in diameter), with undulate outer membranes and fewer cristae, reminiscent of the disorganized and decreased membrane structure found in plastids. Intracristae spaces are swollen (visualized as large white vesicles), very uncharacteristic of wild-type mitochondria.

Embryo development is retarded in *CAC1-A* antisense plants

Mature seeds harvested from *CAC1-A* antisense plants appear normal and have a ~96% germination rate (compared to >99% for wild-type seeds). However, plants with the *CAC1-A* antisense phenotype have a greatly reduced seed yield (Table 5). To determine if embryos progress punctually through normal stages of development, siliques were examined histologically at seven and fourteen days after flowering (DAF) (Figure 14). At 7 DAF, siliques of wild-type plants contain uniformly torpedo-staged embryos (Figure 14A). In contrast, siliques from *CAC1-A* antisense plants contain a subset of embryos with an altered developmental profile (Figure 14B-E). Many of these altered embryos only reach the globular or heart stages (Figure 14C-E). In other cases, aberrant ovule-like structures were observed (Figure 14B). The *CAC1-A* antisense siliques also contain embryos that appear to be developing normally (Figure 14F), a conclusion further supported by the normal accumulation of oil bodies within these embryos (Figure 15). However, even these normal-appearing embryos contain a subpopulation of aberrant, bloated mitochondria, resembling those found in *CAC1-A* antisense leaves (c.f., Figure 15B vs. A). Within each 7 DAF ovule, the timing of endosperm development corresponds to that expected for the stage of the embryo within. For example, a wild-type or antisense *CAC1-A* ovule containing a heart stage embryo will also contain an endosperm that has just completed initial cellularization. This implies that the coordination between endosperm and embryo development is not disrupted.

In siliques at 14 DAF, embryos in wild-type plants are mature (Figure 14G). In contrast, 14 DAF siliques of *CAC1-A* antisense plants contain many ovules that have heart or earlier-staged embryos and degenerate endosperm (Figure 14H and I). The presence of these immature embryos with degenerate endosperm, together with an absence of intermediate

stages of embryos (e.g., torpedo and walking stick stages), indicates that these immature embryos are permanently paused in their developmental progression. These observations indicate that the reduced seed yield of *CAC1-A* antisense plants is in part due to embryo arrest.

In situ accumulation of *CAC1-A* and *CAC1-B* mRNAs during embryo development

Despite the apparent redundancy, *CAC1-B* genes cannot substitute *CAC1-A* gene function for embryo development. One possible explanation is that *CAC1-B* and *CAC1-A* have different expression patterns during seed development. To test this possibility, *in situ* hybridization was performed with gene-specific probes to detect the *CAC1-A* and *CAC1-B* mRNA accumulation during embryo development of wild-type *Arabidopsis*. The two genes showed similar spatial and temporal expression pattern (Figure 16). Both *CAC1-A* and *CAC1-B* mRNAs are evenly distributed among the maternal tissues of silique and developing embryos at the very early stage of development (1DAF). With the development of the embryos, the accumulation of *CAC1-A* and *CAC1-B* mRNAs is reduced in the silique walls and ovule integuments (3 DAF). During subsequent development of siliques, *CAC1-A* and *CAC1-B* mRNAs mainly accumulate in embryos (3 DAF to 7 DAF). *CAC1-A* mRNA reaches maximal level in heart-stage embryos (5 DAF), while *CAC1-B* mRNA is maximal at the globular stage (3 DAF). Both *CAC1-A* and *CAC1-B* mRNAs are not detectable at 12 DAF.

The expression of the other subunits is unaffected by the absence of either BCCP subunit

To investigate coordination of the expression of the subunits of heteromeric ACCase, the accumulation of each htACCase subunit was determined for wild-type and the two

homozygous *CAC1-B* knockout mutants by western blot analysis of extracts from flowers using antisera directed against BCCP-1, BCCP-2, BC, α-CT and β-CT (Figure 4). The elimination of BCCP-2 subunit has no effect on the accumulation of the other four subunits. Similarly, the abundance of the four subunits that accumulate in leaves, BCCP-1, BC, α-CT and β-CT, was determined in wild-type and *CAC1-A* antisense plants (Figure 17A). (BCCP-2 does not accumulate in leaves (Thelen et al., 2001) and was undetectable in any of our analyses (data not shown)). Regardless of the extent of down-regulation of BCCP-1 protein, the abundance of BCCP-2, BC, α-CT and β-CT in *CAC1-A* antisense plants is indistinguishable from that of wild-type plants (Figure 17B). Consistent with these findings, the abundance of the *CAC2*, *CAC3*, and *accD* mRNAs is indistinguishable between wild-type and *CAC1-A* antisense plants with a severe phenotype (Figure 18). (*CAC1-B* mRNA was not detectable in these analyses (data not shown)). Thus, a decrease in the expression of either the *CAC1-A* gene or the *CAC1-B* gene does not affect the expression of the other subunit genes of heteromeric ACCase.

Reduction of BCCP-1 levels but not of BCCP-2 affects fatty acids

To investigate the individual effect of BCCP-1 and BCCP-2 on fatty acid accumulation, lipids extracted from wild-type and *CAC1-A* antisense plants or *CAC1-B* knockout plants were compared. The concentration of fatty acids (on the basis of fresh weight and dry weight) in leaves of *CAC1-A* antisense plants is increased by about 20% in plants with a moderate phenotype and 30% in plants with a severe phenotype (Figure 19). However, because the *CAC1-A* antisense plants are considerably smaller (rosettes of plants with the severe phenotype weigh between 10 and 20% of wild-type rosettes), the total fatty acid content of

each individual *CAC1-A* antisense plant is considerably less than that of a wild-type plant. Seeds of *CAC1-A* antisense plants with a severe phenotype also express an increase in the concentration of fatty acids (337 μg mg-1 versus 278 μg mg-1 in wild-type plants) (Figure 20). However, because *CAC1-A* antisense plants yield fewer seeds, the total amount of seed fatty acids produced by each antisense plant is considerably reduced (186 μg of fatty acids per plant from the wild-type, and 34 and 8.4 μg of fatty acids per plant from *CAC1-A* antisense plants with moderate and severe phenotypes, respectively).

The fatty acid composition of the lipids of antisense *CAC1-A* and wild-type leaves (Table 7) and seeds (Table 8) were determined. There are no detectable differences in the relative amount of each fatty acid between leaves of wild-type and *CAC1-A* antisense plants. The fatty acid composition of seeds from wild-type and *CAC1-A* antisense plants is also indistinguishable. Hence, although reduction in the expression of the BCCP-1 protein quantitatively affects fatty acid accumulation, it does not affect fatty acid composition.

Since *CAC1-B* is mainly expressed in developing siliques, seed fatty acids were analyzed for *CAC1-B* knockout mutants. Both the amount and the composition of the seed fatty acids from either *cac1-b-1* or *cac1-b-2* homozygous plants are similar to that from wild-type plants (Figure 21).

DISCUSSION

Fatty acids are required for the formation of many important molecules including membrane lipids, waxes, and signal molecules. Therefore, it is expected that disruption of fatty acid biosynthesis will have severe physiological effect on plants. Indeed, mutations in the enoyl-acyl carrier protein (ACP) reductase which reduce *de novo* fatty acid biosynthesis

dramatically alters the growth morphology of plants (Mou et al., 2000). Moreover, it has been reported that the disruption of *plE2*, the gene for the E2 subunit of the plastidic pyruvate dehydrogenase which provides the acetyl-CoA for fatty acid biosynthesis, in *Arabidopsis* causes an embryo lethal phenotype (Lin et al., 2003). These findings are consistent with the concept that *de novo* fatty acid biosynthesis is an essential metabolic pathway. In plastids, the htACCase catalyzes the ATP-dependent formation of malonyl-CoA from acetyl-CoA and bicarbonate, the committed reaction for *de novo* fatty acid biosynthesis. However, the presence of a homomeric ACCase in the cytosol provides a possible redundancy of malonyl-CoA supply for fatty acid biosynthesis. Besides, it has been reported that in *Brassica napus* at least one isoform of hmACCase is located in plastids (Schulte et al., 1997). In *Arabidopsis*, there are two hmACCase-coding genes, *ACC1* and *ACC2* (Yanai et al., 1995). ACC1 protein is located in the cytosol, but ACC2 protein has a putative transit peptide and may target the ACC2 protein to plastids. To determine the importance of htACCase for *de novo* fatty acid biosynthesis *in planta*, we identified and characterized T-DNA tagged mutant alleles for three *Arabidopsis* htACCase subunit genes. Disruption of *CAC3*, the single-copy gene coding for α-CT subunit of htACCase, results in embryo lethality. This finding indicates that the malonyl-CoA produced by the cytosolic hmACCase is either unable to enter the plastids or insufficient for *de novo* fatty acid biosynthesis. It also suggests either that ACC2 protein is not located in plastids, or that even if it is located in plastids, its ACCase activity is insufficient to meet the requirement of malonyl-CoA for fatty acid biosynthesis. Given that the only known metabolic fate of malonyl-CoA in plastids is to make fatty acids, our finding demonstrates that htACCase is essential for *de novo* fatty acid biosynthesis in plants.

Two BCCP-coding genes, *CAC1-A* and *CAC1-B*, have been found in *Arabidopsis* (Ke et al., 1997; Thelen et al., 2001). *CAC1-A* and *CAC1-B* are located within 0.32 Mb of each other on chromosome 5. Their protein sequences have 42% amino acid identity. *CAC1-A* gene is ubiquitously expressed (Ke et al., 1997), but *CAC1-B* gene is mainly expressed in flowers and siliques (Thelen et al., 2001). The presence of two paralogous BCCP-coding genes raises the question about their individual significance to the htACCase function and the consequent effect on fatty acid biosynthesis. To address this question, we have examined the expression of the *CAC1-A* and *CAC1-B* genes in developing embryos where large amounts of fatty acids are biosynthesized for deposition as seed oil. Previous study has shown that the accumulation of *CAC1-A*, *CAC2*, *CAC3*, and *accD* mRNAs are coordinate with the accumulation of seed oil during seed development (Ke et al., 2000a). In this paper, we have shown that the *CAC1-B* has a similar spatial and temporal expression pattern to *CAC1-A* during seed development. However, to our surprise, the two *CAC1-B* knockout mutants appear similar to wild-type plants, but *cac1-a-1* mutant is homozygous embryo lethal. The accumulation of BCCP-1, BC, α-CT, and β-CT subunits is not changed in the homozygous *CAC1-B* knockout plants. Moreover, the amount and composition of seed fatty acids were not affected by loss of BCCP-2 subunit.

One possible explanation for the above observations is that BCCP subunit is not a limiting factor of the htACCase activity. Considering that the *CAC1-A* antisense plants accumulating 35% of wild-type level of BCCP-1 in leaves only showed a moderate phenotype, it is likely that the htACCase activity is affected only when the accumulation of BCCP subunits decreases to a limiting level. Western analysis with streptavidin showed that biotinylated BCCP-2 is only about 25% as much as of biotinylated BCCP-1 in developing siliques. The

total BCCP level in *CAC1-B* knockout mutant only decreases by about 20% of the wild-type level in siliques and much less in leaves, which probably is not low enough to result in a phenotype. On the contrary, when the *CAC1-A* gene is completely knocked out, only about 20% of wild-type total BCCP level remains in the developing embryos. The *CAC1-A* antisense plants accumulating 20% of wild-type level of BCCP-1 in leaves has already shown a severe phenotype. It is possible that the BCCP-2 level in the *CAC1-A* knockout embryo is not sufficient to rescue the lethal phenotype.

An alternative explanation is that BCCP-1 can form holoenzyme complex with other htACCase subunits independent of BCCP-2, but BCCP-2 can only do so in the presence of BCCP-1. Overexpression of *CAC1-B* gene in the *CAC1-A* antisense plants can be used to distinguish the above two explanations. If the BCCP-1 and BCCP-2 are equivalent to each other, overexpression of *CAC1-B* gene will rescue the *CAC1-A* antisense plants with different severity of phenotype equally well. If the latter explanation is correct, then the plants with severe phenotype can not be rescued to the same level as the plants with moderate phenotype.

There are two physically distinct malony-CoA pools in plants: one located in plastids and the other in the cytosol. The plastidic ACCase, which in most plants (except Graminea), is of heteromeric form, produces the plastidic malonyl-CoA pool. The homomeric ACCase (hmACCase) is responsible for the production of cytosolic malonyl-CoA pool. While the only known metabolic fate of plastidic malonyl-CoA is for fatty acid biosynthesis, cytosolic malonyl-CoA is required for a variety of pathways including fatty acid elongation and flavonoids biosynthesis. It has been reported that knockout of *ACC1*, the hmACCase-coding gene, in *Arabidopsis* results in abnormal embryo development (Baud et al., 2003). In these mutants the defects of the embryo morphogenesis are the lack of cotyledons and disruption of

cellular organization of the apical region of the embryo. In spite of this, the abnormal embryo still matures. In contrast, the *cac1-a-1* mutant showed delayed development and premature abortion of the embryo without any specific alteration of its morphogenesis. These phenotypic differences suggest that the role of BCCP-1 during embryo development is related to a fundamental metabolic process providing structural components such as membrane lipids, rather than a signaling process, which is most likely the case for hmACCase. Indeed, the defects associated with the cytosolic malonyl-CoA generation appear to be associated with fatty acid elongation and biosynthesis of sphingolipid, a molecule with many signaling properties (Smith and Merrill, 2002; Sperling and Heinz, 2003; Worrall et al., 2003; Dietrich et al., 2005; Zheng et al., 2005).

The generation of transgenic *CAC1-A* antisense plants with reduced level of BCCP-1 enabled us to further investigate the physiological significance of BCCP-1 and htACCase. *CAC1-A* antisense plants showed a range of pleiotropic morphological and subcellular changes, and the severity of the phenotype correlated with the magnitude of the reduction in BCCP-1 accumulation. The most likely interpretation of the phenotypic alterations associated with reduced BCCP-1 is that htACCase activity is reduced, which limits the availability of fatty acids for membrane biogenesis. Thus, many of the morphological and ultrastructural changes associated with reduced BCCP-1 are consistent with the adaptation of plant growth to decreased ability to generate membranes. This is primarily expressed by alterations in cellular structures that decrease the size and invaginations of membrane bounded structures, which would have the consequence of reducing membrane area and conserving membrane lipids. For example, cells and vacuoles are smaller and rounder, there are fewer and smaller plastids with reduced thylakoid membranes and reduced and disorganized grana, and invaginations of

mitochondrial cristae are greatly reduced. The unusual ultrastructure of the mitochondria (expanded intercristae space) is probably the consequence of the reduced cristae membranes, maintaining intercristae volume despite reduction in intercristae membrane area. Because cells are smaller and rounder, they are packed closer together, which reduced the apoplastic spaces of the leaves. All these alterations result in thinner and smaller leaves on the *CAC1-A* antisense plants.

In spite of the reduction in cell and leaf size, the overall cellular organization as well as water content of rosette leaves in the *CAC1-A* antisense plant is unchanged. Moreover, although the total fatty acid content of each individual *CAC1-A* antisense plant is considerably less than that of a wild-type plant, the fatty acid content in leaves of the *CAC1-A* antisense plant does not decrease when measured on the basis of weight. All these observations can be explained by the model that the *CAC1-A* antisense plants adapt to the limiting supply of fatty acids for membrane biogenesis by reducing the cell size to maintain the normal cell structure and metabolism.

The small size and cellular structure of *CAC1-A* antisense plants with a severe phenotype has several aspects in common with *fab2 Arabidopsis* mutants. The miniaturization of *fab2* plants is associated with a decrease in activity of the enzyme producing 18:1-acyl-carrier-protein:18:0-acyl-carrier-protein desaturase, resulting in additional stearate in their membranes (Lightner et al., 1994). However, the *CAC1-A* phenotype develops without alteration in fatty acid composition. Thus, the subset of alterations that the two mutants have in common - reduced cell size, reduced apoplastic space, and disorganized plastids, while due to altered stearate levels in *fab2* plants, are not due to changes in membrane fatty acid ratios in *CAC1-A* antisense plants.

Reduction of the levels of BCCP-1 diminishes activity of htACCase and decreases *de novo* fatty acid biosynthesis. Fatty acid availability is required for normal cell growth and expansion. If reduced, these processes may be delayed and cell expansion rate decreased. Thus, it might be expected that any mutant with a decreased ability to synthesize fatty acids would have a similar phenotype. Indeed, *CAC1-A* plants share many gross morphological traits with *mod1* mutants (Mou et al., 2000). *MOD1* encodes ACP reductase, the enzyme catalyzes the final reaction of the four cyclical series of reactions that constitute *de novo* fatty acid biosynthesis. The similarity in phenotype between *CAC1-A* antisense and the *mod1* mutant may indicate that a reduction in the availability of fatty acids has a distinct impact on the successful growth and development of the plant. Both lesions yield cells that appear to be undergoing autophagic response.

Ultrastructurally, *mod1* mutant and *CAC1-A* antisense plants share a subset of cellular characteristics: aberrant plastid structure, fewer plastids and decreased mesophyll cell size. However, the *CAC1-A* antisense phenotype is more extensive including compact cells greatly reduced in size, smaller vacuoles, more visible cytoplasm, and alterations in mitochondrial structure, characteristics not typically associated with autophagy or cell death. These features are absent in *mod1*. These differences in cellular structure between the *CAC1-A* antisense and *mod1* plants imply alternative factors are at play in the development of *CAC1-A* antisense cells, and may reflect the subtle interplay between down regulation of a single gene (*CAC1-A*) and gene expression.

During the attempts to complement the *cac1-a-1* mutant, we found *CAC1-A* cDNA driven by the CaMV 35S promoter failed to complement the embryo lethal phenotype (data not shown). It has also been reported that *plE2* cDNA driven by the CaMV 35S promoter cannot

rescue the similar embryo lethal phenotype caused by knockout of *plE2*, which encodes a subunit of the plastidic pyruvate dehydrogenase (Lin et al., 2003). The plastidic pyruvate dehydrogenase has a similar expression pattern to htACCase within the developing embryo, and this enzyme provides acetyl-CoA for htACCase to use for fatty acid biosynthesis (Ke et al., 2000b). So our finding is consistent with this previous report and both are consistent with the idea that the CaMV 35S promoter failed to express during the early stages of embryogenesis, which was demonstrated by a study of the expression profile of the CaMV 35S promoter during embryo development in cotton using green fluorescent protein (GFP) reporter (Sunilkumar et al., 2002). With the same consideration, *CAC1-A* antisense cDNA driven by the 35S promoter is unlikely to affect the early embryo development and seed oil accumulation, since the *CAC1-A* gene as well as other htACCase subunit genes are mainly expressed in early-stage (globular, heart, and torpedo) embryos. Consistent with this, mature seeds collected from *CAC1-A* antisense plants appear normal and have similar fatty acid content to wild-type plants. However, there are also some embryos showing delayed development and premature abortion, similar to those from *cac1-a-1* mutant. This perhaps is due to the limiting supply of carbon source from maternal part to these embryos.

METHODS

Plant material and growth conditions

All the wild-type and mutant *Arabidopsis thaliana* lines were obtained from ABRC (Arabidopsis Biological Resource Center, Columbus, OH). The *cac1-a-1* mutant line is in the Wassilewskija (WS) ecotype background. The *cac1-b-1*, *cac1-b-2*, and *cac3-1* lines are in Columbia ecotype background.

Seeds were sown either in LC1 Sunshine Mix soil (Sun Gro Horticulture, Bellevue, WA) or on Murashige and Skoog argar medium (Invitrogen, Carlsbad, CA). To break dormancy, sown seeds were placed at 4 °C for 2 days, and then moved into a growth room maintained at 22 °C with 24h continuous illumination. When sown on MS media, seeds were first sterilized by a short wash of 95% ethanol and a 10-min incubation in 50% bleach solution containing 0.1% tween-20. If needed, the seedlings were transferred from MS media to soil at 7-10 days after germination.

Antisense plants were grown under a controlled photoperiod of 16 h of illumination followed by 8 h of darkness. All studies of rosettes were from plants between 28 and 30 DAI, and all plant materials were harvested between 3 to 5 hours after the start of the illumination period.

To developmentally stage siliques, color threads were used to tag flowers on the day of flowering (day 0) when petals just appeared. The siliques developed from those tagged flowers were collected at specific time points thereafter.

PCR genotyping and DNA gel blotting

Plant DNA extraction and PCR reactions were conducted with the protocols provided by the Arabidopsis Knockout facility at University of Wisconsin-Madison (http://www.biotech.wisc.edu/arabidopsis/). Two PCR reactions were performed to genotype a single plant. One reaction used a T-DNA border primer and a gene-specific primer to detect the T-DNA tagged allele, the other reaction used a pair of gene specific primers that flank the T-DNA insertion site to detect the wild-type allele. Table 9 listed the primers used in this study for genotyping of the T-DNA tagged mutants.

CAC1-A cDNA specific primers (pC-F and pC-R) were designed to track the *CAC1-A* antisense transgene (Table 9). This PCR reaction amplified a 933-bp fragment from the endogenous *CAC1-A* genomic gene, and a 462-bp fragment from the *CAC1-A* antisense transgene. Thus, a PCR reaction using these primers yields a 933-bp product from wild-type plants, and 933-bp and 462-bp products from transgenic plants.

For DNA gel blot analysis, DNA was isolated from plant leaves based on the method of (Rogers and Bendich, 1994). To confirm the incorporation of the *CAC1-A* antisense transgene in the plant genome, DNA was digested with restriction enzymes *EcoR*I and *Hind*III, and fractionated on by electrophoresis in 0.8% agarose gels. The DNA was then transferred onto MAGNA nylon membrane (Osmonics, Westborough, MA) and hybridized with ^{32}P-labeled *CAC1-A* cDNA. Blots were prehybridized and hybridized under standard conditions (Sambrook et al., 1989), and were washed at 65 °C for 10 min in 2 x SSC, 0.1% SDS, and 10 min in 1 x SSC, 0.1% SDS.

In situ Hybridization

Arabidopsis siliques were harvested at 1, 3, 5, 7, 12 DAF, cut into 4 mm pieces, fixed, embedded and sectioned as previously described (Ke et al., 1997). DIG-labeled RNA probe (antisense and sense) were transcribed from the following insert + vector combinations: 676 nucleotides at 3'-end (positions 451-1114) of *CAC1-A* cDNA in pBluescript SK (+/-) and 789 nucleotides at 3'-end (positions 451-1217) of *CAC1-B* cDNA in pSPORT 1 (GIBCO, Rockville, Maryland). After Proteinase K digestion, hybridization and washing at 65 °C, slides were treated with RNaseA to remove the RNA probe that had not hybridized with mRNA. The Boehringer Mannheim DIG nucleic acid detection kit (Boehringer Mannheim,

Indianapolis, Indiana) was used for immunological detection (Canas et al., 1994). About 30 silique pieces were used in total. For each developmental stage, about 8 ovules per silique piece were examined, and the entire experiment was repeated 3 times.

Binary vector construction

To express the *CAC1-A* antisense RNA, a plant transformation vector was constructed. The binary vector pBI121 (Clontech, Palo Alto, CA) was modified by removing the *GUS* gene and replacing it with an oligonucleotide containing *Xho*I and *Sst*I restriction enzyme sites. A reverse-orientated full length *CAC1-A* cDNA (Choi et al., 1995) was then inserted into the modified pBI121 vector using *Xho*I/*Sst*I restriction enzymes such that the antisense *CAC1-A* cDNA was under the control of the CaMV 35S promoter.

The construct used for complementation of *cac1-a-1* mutant was made by subcloning the 4.5 kb genomic *Bam*HI fragment containing *CAC1-A* gene (Ke et al., 1997) into pCAMBIA3300.

Plant transformation and screening

The binary vectors were transferred into *Agrobacterium tumefaciens* (strain C58C1) by electroporation. Plant transformation was performed with a simplified *Arabidopsis* transformation protocol (Clough and Bent, 1998). Kanamycin or glufosinate ammonium was used to screen the transformants of the antisense *CAC1-A* cDNA construct or genomic *CAC1-A* construct, respectively. To screen for kanamycin resistance, the T1 seeds were sown on MS medium containing 50 μg/ml kanamycin. After ~12 days the kanamycin-resistant seedlings were transferred into soil. To screen with glufosinate ammonium, T1 seeds were

sown in soil and 14-day seedlings were sprayed with 1:1500 dilution of Finale Concentrate (Farnam Companies, Inc. Phoenix, AZ).

Complementation of *cac1-a-1* mutant

Heterozygous *cac1-a-1* plants were transformed with the pCAMBIA-CAC1A construct. Seeds were collected from the individual T1 tansformants. To test whether the construct complements the *cac1-a-1* mutant, the T2 plants were PCR genotyped by using the primers listed in Table 10.

Generation of BCCP-1 and BCCP-2 specific antibodies

Primers A-F: CCTCAACCTCAAGCTCCT and A-R: AACAGTAGGAAGTGACGATT were used to amplify *CAC1-A*-specific cDNA region. Primers B-F: CAGCAAGCTGTACCACCA and B-R: GAGTGGAGGATGAGACGA were used to amplify *CAC1-B*-specific cDNA region. The PCR products were cloned into pET30 vector (Novagen, Madison, WI). These two constructs were named CAC1A-pET and CAC1B-pET. Overexpression of these constructs in *E. coli* strain BL21 produced recombinant proteins with both an S-tag and a His-tag located at the N-terminus. BCCP-2-specific recombinant protein was purified with a His·bind column, as described by the manufacturer (Novagen, Madison, WI). Affinity purification of BCCP-1-specific recombinant protein with either S-tag or His-tag was not successful in either non-denaturing condition or denaturing condition. Thus the total proteins were fractionated by SDS-PAGE, the band that contains the BCCP-1-specific recombinant protein was cut out for antibody generation. The antibodies

were generated in New Zealand White female rabbits by following the procedure previously described (Ke et al., 2000a).

Immunoblot analysis

Proteins were extracted from plant tissue as described previously (Che et al., 2002). The protein concentration in the extracts was determined with the Bradford method (Bradford, 1976). Proteins were separated by 10% SDS-PAGE (Laemmli, 1970) and transferred to a nitrocellulose membrane (Towbin et al., 1979) using Mini-PROTEAN II Electrophoresis and Mini Trans-Blot system (Bio-Rad Laboratories, Hercules, CA). The BCCP-1, BCCP-2, BC, α-CT and β-CT subunits of heteromeric ACCase were immunologically detected with antisera that had been generated and characterized previously (Sun et al., 1997; Ke et al., 2000a) or during the course of this work. The antigen-antibody complexes were detected by either autoradiography with ^{125}I-Protein A or ECL chemiluminescent detection system with horseradish peroxidase (HRP) linked anti-rabbit IgG (Amersham Biosciences, Piscataway, NJ). The biotin-containing proteins were detected using ^{125}I-labeled or HRP linked streptavidin (Nikolau et al., 1985). For quantitative analysis, a Storm 840 scanner (Amersham Biosciences, Piscataway, NJ) was used to scan the membrane. The signal intensities were quantified by ImageQuant software (Molecular Dynamics, Sunnyvale, CA).

Fatty acid analysis

Extraction and methylation of fatty acids was conducted with the direct transesterification method (Lewis et al., 2000). Triheptadecanoate was used as internal standard. Analysis of the fatty acid methyl esters (FAMEs) was performed with a gas chromatograph (Model 6890

series, Agilent Technologies, Palo Alto, CA), equipped with a mass detector Model 5973 (Agilent Technologies, Palo Alto, CA). Chromatography was conducted with HP-1 column, using helium as the carrier gas. The injection temperature was at 300 °C. The oven temperature was initially at 80 °C for 2 minutes and then increased to 150 °C at a rate of 40 °C /min. Then the temperature was ramped to 200 °C at a rate of 2 °C/min. After holding this temperature for 2 minutes, it was ramped to 300 °C at a rate of 5 °C / min and held there for 2 min. Peak identification was facilitated by using the HP enhanced chemical analysis software G1701BA (version B.01.00) with Windows NT™ operating system.

Cytological and phenotypic analysis of pollen and siliques

Cytological preparations of pollen

Flowers that were either fully or nearly fully open, with anthers that were freshly dehiscent were collected from heterozygous *cac1-a-1* plants and their wild-type siblings. Flowers and pollen were fixed in Farmer`s fixative (ethanol:acetic acid, 3:1 [v/v]), and stored in 70% ethanol at 4 °C.

Fixed or freshly collected anthers were disrupted on a microscope slide using dissecting needles and gently placed under a cover-slip in stain solutions. Another way to collect sufficient pollen was by placing 3-4 open flowers in a microcentrifuge tube containing 300 µl of stain solutions. After briefly vortexing and centrifugation, the pollen pellet was transferred to a microscope slide and viewed by light and by UV epi-illumination.

Five different staining assays were used to compare pollen viability and germination. These stains were (Alexander's stain, iodine-potassium iodide (IKI), DAPI, Aniline Blue, and Nile Blue). Staining of fixed pollen with Alexander's stain was carried out for 30 min. After

washing flowers in 50 mM Tris-HCl buffer (pH 6.8), released pollen grains were mixed directly with Alexander stain (Alexander, 1969). Alexander's stain differentially colors viable pollen grains as dark purple and nonviable pollen grains as either a pale green or a splotchy dark purple and pale green. IKI stains viable pollen with as dark red/brownish and aborted pollen as slightly red. Nile Blue stains free fatty acids and phospholipids, and aborted pollen appear greenish-blue. Aniline blue (0.1% [w/v] was prepared in 0.1 M phosphate buffer [pH 8.5]) was used for viewing pollen tube walls under epi-fluorescence. The stain was applied for at least 30 min prior to microscopic examination. Mature pollen grains were stained for 1 to 2 h in the dark with DAPI solution (0.4 μg/ml DAPI in 0.1 M sodium phosphate (pH 7), 1 mM EDTA, 0.1% Triton X-100) to visualize nuclei by UV epi-illumination. After pollen samples were placed on slides in each solution, samples were examined with bright field microscopy (Alexander's stain, IKI, Nile Blue stain), UV epi-illumination (DAPI and Aniline Blue stain). Each slide contained 100 to 400 pollen grains was visually counted, scoring pollen grains as germinated (pollen tube longer than pollen grain diameter) or non-germinated or burst. Light microscopy was performed on a Zeiss Axiovert microscope bright field and with a UV filter set for observing the DAPI and Aniline Blue fluorescent stains. Digital images were acquired using a camera and *AxioVision* software.

Pollen germination

Pollen was germinated *in vivo* and *in vitro* on medium containing 30 ppm boric acid, 25% sucrose. For *in vitro* germination, glass slides were dipped into warm medium, and then cooled to form a thin layer on the slide. Pollen was placed on these slides, and the slides were placed in a sealed box and incubated overnight at 22 °C at 100% humidity under continuous illumination.

To determine *in vivo* germination efficiency, stigmas from heterozygous *cac1-a-1* plants and wild-type sibling were cut at the base and inserted vertically into germination medium (30ppm boric acid, 25% sucrose) in a 9-cm Petri dish. Plates were sealed and incubated overnight at 22°C, at 100% humidity, under continuous illumination. For each genotype about 300-400 pollen grains deposited on 20 stigmas were analyzed. Pollen grains were scored and length of pollen tubes measured by direct observation of plates using a Zeiss Axiovert inverted microscope.

Anther and the path of pollen tubes inside the pistil were visualized by fixing whole pistils and staining with Aniline Blue and DAPI. The tissue was then cleared for 24 hours at room temperature with a drop of clearing solution (240 g of chloral hydrate and 30 g of glycerol in 90 ml water). Pollen was examined with Zeiss Axioplan 2 light microscope with a Zeiss AxioCamHRc digital camera (Carl Zeiss,Inc., Thornwood, NY) and images were captured using an AxioCamMR camera and AxioVision 4.3 software. The microscope was equipped with a DAPI filter set comprising of an excitation filter (BP 365/12 nm), a beam splitter (395 nm), and an emission filter (LP 397 nm). The objectives used for imaging were the Neofluar 40x oil, the Apochromat 63x oil, and the Neofluar 100x oil.

Clearing of siliques for differential interference contrast microscopy (Nomarski optics)

Siliques at between 1 and 13 DAF were collected and fixed with FAA (50 ml of 50% ethanol (v/v), 10 ml of 37% formalin (v/v), 5 ml of acetic acid (v/v), and 35 ml water), under vacuum at 15 psi (6.89 kPa) for 48 h at room temperature (Sass, 1958). Siliques were taken through a series of 50 and 70% ethanol, and stored in 70% ethanol (v/v) at 4 °C. Fixed siliques were cleared for 1-20 hr with Herr's fluid (85% lactic acid:chloral hydrate:phenol:clove

oil:xylene (2:2:2:2:1 w/w) (Herr, 1971) and then viewed with a Zeiss Axioplan 2 light microscope) equipped with Nomarski optics and a Zeiss AxioCamHRc digital camera (Carl Zeiss, Inc., Thornwood, NY). Another clearing technique that was used was as follows. Developing seed were fixed in ethanol:acetic acid (3:1) for 1 day, followed by a partial rehydration series in ethanol. Clearing was obtained after 24h in a derivative of Hoyer's medium (7.5 g gum Arabic; 100 g chloral hydrate; 5 ml glycerol in 30 ml water). The preparations could then be conserved at 4 °C more than 24 hrs.

Clearing of siliques for confocal scanning laser microscopy (CSLM)

Fifteen siliques from each stage of development (from 1 to 13 DAF) were collected from heterozygous *cac1-a-1* plants and their wild-type siblings were collected. Siliques were fixed in FAA, placed under vacuum, dehydrated, and stored in 70% ethanol. Siliques were then hydrated in a descending 50%, 30% ethanol series (20 min per step) and water, and then thoroughly washed in deionized water. Modified Kasten's fluorescent Feulgen reaction and Kasten's fluorescent periodic acid-Schiff reaction (Kasten, 1981) were used to stain nuclei and walls, respectively. For the Feulgen reaction, siliques were subjected to hydrolysis for 20 min in 6 N HCl at RT, and then rinsed with deionized water. For the PAS reaction, siliques were hydrolyzed with 0.5% periodic acid for 25 min at RT, thoroughly rinsed with deionized water, and stained for 20-30 min at RT in a 0.1-0.25% fluorescent acriflavine-Schiff-type reagent (Kasten, 1981). The stained siliques were rinsed with deionized water until very little acriflavine leached out (1-4 h). The siliques were dehydrated in a graded ethanol series (25% to 100% ethanol, 1 h per step), and cleared in an ethanol-methyl salicylate series (3:1, 1:1, 1:3) followed by two changes of 100% methyl salicylate; at least one h per step. The siliques were mounted in methyl salicylate on slides, a cover-slip was gently added, and siliques were

sealed with nail polish or liquid transparent glue. Slides were stored at 4 °C to decrease evaporation prior to viewing. Ovules at each developmental stage were viewed using a Leica TCS-NT laser-scanning microscope with an Argon/Krypton laser (the excitation wavelength was 488 nm and 518) (Omnichrome, Chino, CA). Images (40-60 1 μm optical images/ per ovule, the serial 1μm optical-section images) were collected digitally.

Scanning electron microscopy (SEM) of flowers/pollen and seeds/ovules

Flowers and siliques were fixed in 2% glutaraldehyde and 2% paraformaldehyde in 0.1 M sodium cacodylate buffer, pH 7.2, under vacuum (pressure: 18 psi Hg) for 7 h at room temperature, and then overnight at 4 °C. Fixed samples were washed three times in the same buffer, post-fixed in buffered 1% OsO_4 for 2 h, washed two times in the same buffer followed by deionized water, and dehydrated in an ethanol series to absolute ethanol and placed in 100% ethanol. Samples were subsequently critical point-dried in a DCP-1 Denton critical point-drying apparatus (Denton Vacuum Inc., Cherry Hill NJ), and mounted on aluminum stubs with double-sided sticky tape and silver cement. For viewing inside the seeds/ovules, seeds/ovules were fractured using a fine surgery razor blade. Flowers and seeds/ovules were sputter coated with gold and palladium in a Denton Vacuum LLC Desk II Cold Sputter Unit (Denton Vacuum Inc., Moorestown, NJ) for 120 seconds, and viewed with JEOL 5800LV SEM (JEOL=Japan Electron Optics Laboratory, USA Inc., Peabody, Mass.) at 10 kV. Additional way for scanning electron microscopy, released pollen grains were directly mounted on stubs and sputter-coated with gold particles before specimens were examined with a scanning electron microscope. All digitally collected images including the LM and SEM images were processed in Adobe PhotoShop 7.0 and made into plates using Adobe Illustrator 10.

Microscopic examination of leaves

Leaves were fixed in 2% paraformaldehyde and 2% glutaraldehyde in a 0.1 M cacodylate buffer, pH 7.2. Leaf punches, 1 mm in diameter, were taken from the mid-section of each leaf. The longitudinal mid-point was determined as the mid-point between the first set of marginal lobes and the leaf tip. The tissue was fixed overnight at 4 °C, post-fixed with 1% osmium, dehydrated in a progressive ethanol series and embedded in Spurr's resin (EM Sciences, Fort Washington, PA). One micrometer sections from 3-10 leaf discs per leaf sample were cut, stained with 1% in Toluidine Blue, and examined and photographed under bright-field optics on a Leitz orthoplan microscope. Sixty nanometer thin sections were cut and stained with 5% uranyl acetate in methanol and Sato's lead for observation under a JEOL (Japan Electron Optics Laboratory, Akishima, Japan) 1200 EX scanning transmission electron microscope.

Cell size measurement

Three light micrographs of transverse sections from the tenth true leaf of wild-type plants and the tenth true leaf from three independent *CAC1-A* antisense transgenic lines with a severe phenotype were enlarged. For each of the 12 micrographs, the dimensions of 15-49 epidermal, 14-49 spongy and 10-30 palisade parenchyma cells were measured with an mm ruler. The measurements were converted to actual cell size via print magnification calculation.

REFERENCES

Alexander, M.P. (1969). Differential staining of aborted and nonaborted pollen. Stain Technol **44,** 117-122.

Alonso, J.M., Stepanova, A.N., Leisse, T.J., Kim, C.J., Chen, H., Shinn, P., Stevenson, D.K., Zimmerman, J., Barajas, P., Cheuk, R., Gadrinab, C., Heller, C., Jeske, A., Koesema, E., Meyers, C.C., Parker, H., Prednis, L., Ansari, Y., Choy, N., Deen, H., Geralt, M., Hazari, N., Hom, E., Karnes, M., Mulholland, C., Ndubaku, R., Schmidt, I., Guzman, P., Aguilar-Henonin, L., Schmid, M., Weigel, D., Carter, D.E., Marchand, T., Risseeuw, E., Brogden, D., Zeko, A., Crosby, W.L., Berry, C.C., and Ecker, J.R. (2003). Genome-wide insertional mutagenesis of Arabidopsis thaliana. Science **301,** 653-657.

Baud, S., Guyon, V., Kronenberger, J., Wuilleme, S., Miquel, M., Caboche, M., Lepiniec, L., and Rochat, C. (2003). Multifunctional acetyl-CoA carboxylase 1 is essential for very long chain fatty acid elongation and embryo development in Arabidopsis. Plant J **33,** 75-86.

Bradford, M.M. (1976). A rapid and sensitive method for the quantitation of microgram quantities of protein utilizing the principle of protein-dye binding. Anal Biochem **72,** 248-254.

Canas, L.A., Busscher, M., Angenent, G.C., Beltran, J.-P., and van Tunen, A.J. (1994). Nuclear localization of the petunia MADS box protein FBP1. The Plant Journal **6,** 597-604.

Che, P., Wurtele, E.S., and Nikolau, B.J. (2002). Metabolic and environmental regulation of 3-methylcrotonyl-coenzyme A carboxylase expression in Arabidopsis. Plant Physiol **129,** 625-637.

Choi, J.K., Yu, F., Wurtele, E.S., and Nikolau, B.J. (1995). Molecular cloning and characterization of the cDNA coding for the biotin- containing subunit of the chloroplastic acetyl-coenzyme A carboxylase. Plant Physiol **109,** 619-625.

Clough, S.J., and Bent, A.F. (1998). Floral dip: a simplified method for Agrobacterium-mediated transformation of Arabidopsis thaliana. Plant J **16,** 735-743.

Dietrich, C.R., Perera, M.A., M, D.Y.-N., Meeley, R.B., Nikolau, B.J., and Schnable, P.S. (2005). Characterization of two GL8 paralogs reveals that the 3-ketoacyl reductase component of fatty acid elongase is essential for maize (Zea mays L.) development. Plant J **42,** 844-861.

Herr, J.M., Jr. (1971). A New Clearing-Squash Technique for the Study of Ovule Development in Angiosperms. American Journal of Botany **58,** 785-790.

Kasten, F.H. (1981). Methods for fluorescence microscopy. In Staining procedures, G. Clark and Biological Stain Commission., eds (Baltimore: Published for the Biological Stain Commission by Williams & Wilkins), pp. 39-103.

Ke, J., Wen, T.N., Nikolau, B.J., and Wurtele, E.S. (2000a). Coordinate regulation of the nuclear and plastidic genes coding for the subunits of the heteromeric acetyl-coenzyme A carboxylase. Plant Physiol **122,** 1057-1071.

Ke, J., Choi, J.K., Smith, M., Horner, H.T., Nikolau, B.J., and Wurtele, E.S. (1997). Structure of the CAC1 gene and in situ characterization of its expression. The Arabidopsis thaliana gene coding for the biotin- containing subunit of the plastidic acetyl-coenzyme A carboxylase. Plant Physiol **113,** 357-365.

Ke, J., Behal, R.H., Back, S.L., Nikolau, B.J., Wurtele, E.S., and Oliver, D.J. (2000b). The role of pyruvate dehydrogenase and acetyl-coenzyme A synthetase in fatty acid synthesis in developing Arabidopsis seeds. Plant Physiol **123,** 497-508.

Konishi, T., and Sasaki, Y. (1994). Compartmentalization of two forms of acetyl-CoA carboxylase in plants and the origin of their tolerance toward herbicides. Proc Natl Acad Sci U S A **91,** 3598-3601.

Konishi, T., Shinohara, K., Yamada, K., and Sasaki, Y. (1996). Acetyl-CoA carboxylase in higher plants: most plants other than gramineae have both the prokaryotic and the eukaryotic forms of this enzyme. Plant Cell Physiol **37,** 117-122.

Laemmli, U.K. (1970). Cleavage of structural proteins during the assembly of the head of bacteriophage T4. Nature **227,** 680-685.

Lewis, T., Nichols, P.D., and McMeekin, T.A. (2000). Evaluation of extraction methods for recovery of fatty acids from lipid-producing microheterotrophs. J Microbiol Methods **43,** 107-116.

Lightner, J., James, D.W., Dooner, H.K., and Browse, J. (1994). Altered body morphology is caused by increased stearate levels in a mutant of Arabidopsis. The Plant Journal **6,** 401-412.

Lin, M., Behal, R., and Oliver, D.J. (2003). Disruption of plE2, the gene for the E2 subunit of the plastid pyruvate dehydrogenase complex, in Arabidopsis causes an early embryo lethal phenotype. Plant Mol Biol **52,** 865-872.

Mou, Z., He, Y., Dai, Y., Liu, X., and Li, J. (2000). Deficiency in fatty acid synthase leads to premature cell death and dramatic alterations in plant morphology. Plant Cell **12,** 405-418.

Nikolau, B.J., Wurtele, E.S., and Stumpf, P.K. (1985). Use of streptavidin to detect biotin-containing proteins in plants. Anal Biochem **149,** 448-453.

Rogers, S.O., and Bendich, A.J. (1994). Extraction of Total Cellular DNA from Plants, Algae and Fungi. In Plant Molecular Biology Manual, S.B. Gelvin and R.A. Schilperoort, eds (Dordrecht, The Netherlands: Kluwer Academic Press), pp. D1:1-8.

Sambrook, J., Fritsch, E.F., and Maniatis, T. (1989). Molecular cloning : a laboratory manual. (Cold Spring Harbor, N.Y.: Cold Spring Harbor Laboratory).

Sass, J.E. (1958). Botanical microtechnique. (Ames,: Iowa State College Press).

Schulte, W., Topfer, R., Stracke, R., Schell, J., and Martini, N. (1997). Multi-functional acetyl-CoA carboxylase from Brassica napus is encoded by a multi-gene family: indication for plastidic localization of at least one isoform. Proc Natl Acad Sci U S A **94,** 3465-3470.

Smith, W.L., and Merrill, A.H., Jr. (2002). Sphingolipid metabolism and signaling minireview series. J Biol Chem **277,** 25841-25842.

Sperling, P., and Heinz, E. (2003). Plant sphingolipids: structural diversity, biosynthesis, first genes and functions. Biochim Biophys Acta **1632,** 1-15.

Sun, J., Ke, J., Johnson, J.L., Nikolau, B.J., and Wurtele, E.S. (1997). Biochemical and molecular biological characterization of CAC2, the Arabidopsis thaliana gene coding for the biotin carboxylase subunit of the plastidic acetyl-coenzyme A carboxylase. Plant Physiol **115,** 1371-1383.

Sunilkumar, G., Mohr, L., Lopata-Finch, E., Emani, C., and Rathore, K.S. (2002). Developmental and tissue-specific expression of CaMV 35S promoter in cotton as revealed by GFP. Plant Mol Biol **50,** 463-474.

Sussman, M.R., Amasino, R.M., Young, J.C., Krysan, P.J., and Austin-Phillips, S. (2000). The Arabidopsis knockout facility at the University of Wisconsin-Madison. Plant Physiol **124,** 1465-1467.

Thelen, J.J., Mekhedov, S., and Ohlrogge, J.B. (2001). Brassicaceae express multiple isoforms of biotin carboxyl carrier protein in a tissue-specific manner. Plant Physiol **125,** 2016-2028.

Towbin, H., Staehelin, T., and Gordon, J. (1979). Electrophoretic transfer of proteins from polyacrylamide gels to nitrocellulose sheets: procedure and some applications. Proc Natl Acad Sci U S A **76,** 4350-4354.

Worrall, D., Ng, C.K., and Hetherington, A.M. (2003). Sphingolipids, new players in plant signaling. Trends Plant Sci **8,** 317-320.

Yanai, Y., Kawasaki, T., Shimada, H., Wurtele, E.S., Nikolau, B.J., and Ichikawa, N. (1995). Genomic organization of 251 kDa acetyl-CoA carboxylase genes in Arabidopsis: tandem gene duplication has made two differentially expressed isozymes. Plant Cell Physiol **36,** 779-787.

Zheng, H., Rowland, O., and Kunst, L. (2005). Disruptions of the Arabidopsis Enoyl-CoA Reductase Gene Reveal an Essential Role for Very-Long-Chain Fatty Acid Synthesis in Cell Expansion during Plant Morphogenesis. Plant Cell **17,** 1467-1481.

Table 1. Characterization of T-DNA tagged alleles of htACCase subunit genes

Gene Name	Gene locus	Allele	Insert Position	Characterization	T-DNA border	
					5'	3'
CAC1-A (BCCP-1)	At5g16390	*cac1-a-1*	1st intron, 4nt deletion	Embryo lethal	LB	LB
		SALK_120571	-181, 1nt deletion	No phenotype, normal level BCCP-1	LB	LB
		SALK_023225	-288 to -234, 54nt deletion	No phenotype, normal level BCCP-1	LB	RB
		SALK_050082	1st exon	Possible T-DNA rearrangement [a]	Not found	LB
		SALK_138637	Not found	T-DNA not found	Not found	Not found
		GT_3_38620	Not found	T-DNA not found	Not found	Not found
		SALK_025081	N/A	NOT CHARACTERIZED	N/A	N/A
		GABI_217E08	N/A	NOT CHARACTERIZED	N/A	N/A
CAC1-B (BCCP-2)	At5g15530	*cac1-b-1* (SALK_056228)	3rd intron	No phenotype	Not found	LB
		cac1-b-2 (SALK_070569)	1st exon and intron junction, 64nt deletion	No phenotype	LB	RB
CAC3 (α-CT)	At2g38040	*cac3-1* (SALK_045139)	-403 to -372, 31nt deletion	Embryo lethal	LB	LB
		SALK_045127	Not found	T-DNA not found	Not found	Not found

[a] see text for more details.

Table 2. Segregation analysis of T-DNA tagged alleles

Allele	Genotype	Number of plants	$\chi^2_{2:1}$	$\chi^2_{1:2:1}$	*p* value
cac1-a-1	*cac1-a-1/cac1-a-1*	0	6.375		0.012
	cac1-a-1/CAC1-A	119			
	CAC1-A/CAC1-A	85			
cac1-b-1 (SALK_056228)	*cac1-b-1/cac1-b-1*	48		0.01	0.995
	cac1-b-1/CAC1-B	95			
	CAC1-B/CAC1-B	47			
cac1-b-2 (SALK_070569)	*cac1-b-2/cac1-b-2*	56		4.40	0.11
	cac1-b-2/CAC1-B	79			
	CAC1-B/CAC1-B	41			
cac3-1 (SALK_045139)	*cac3-1/cac3-1*	0	3.61		0.057
	cac3-1/CAC3	21			
	CAC3/CAC3	19			

Table 3. Number of aborted seeds in siliques from heterozygous *cac1-a-1* plants and wild-type siblings

Genotype	Aborted (percentage)	Normal (percentage)	Total
cac1-a-1/CAC1-A[a]	229 (36.5%)	399 (63.5%)	628
CAC1-A/CAC1-A[b]	104 (19%)	443 (81%)	547

[a] Seeds in 18 siliques from multiple plants were counted.
[b] Seeds in 15 siliques from multiple plants were counted.

Table 4. Gamete transmission of *cac1-a-1*

Cross[a]	Number of F1 progeny			$\chi^2_{1:1}$	*p* value
	Total	*CAC1-A/cac1-a-1*	*CAC1-A/CAC1-A*		
CAC1-A/CAC1-A ♀ × *CAC1-A/cac1-a-1* ♂	47	14	33	7.68	0.006
CAC1-A/cac1-a-1 ♀ × *CAC1-A/CAC1-A* ♂	64	30	34	0.25	0.62

[a] 15 plants for each genotype were crossed.

Table 5. Severity of morphological changes in *CAC1-A* antisense plants[a]

Severity[a]	Time of Phenotype Onset	Leaf Morphology	Mature Plant Size (40 DAP)	Seed Yield
Very Severe	Upon germination	Yellow patches on cotyledons. None or less than four rosette leaves, which are all crinkly and yellow variegated.	Survive less than a week. Rosette diameter is less than 0.5 cm when die.	None
Severe	About one week after germination	Normal cotyledons. One to four WT-like rosette leaves. Most leaves undulated and yellow variegated with small green areas. All cauline leaves undulated and yellow patched.	Rosette diameter is less than 3 cm. Height is less than 5 cm. Total rosette leaf weight is 0.1-0.2 g.	Less than 0.05 g
Moderate	About two weeks after germination	Normal cotyledons. More than four WT-like rosette leaves. One-half to two-thirds of rosette leaves undulated and yellow variegated. All cauline leaves yellow patched.	Rosette diameter is about 3 to 6 cm. Height is about 5 to 12 cm. Total rosette leaf weight is 0.2-0.6 g.	About 0.05 to 0.3 g
Slight	After bolting or flowering (about 4 weeks after germination)	Normal cotyledons. All rosette leaves are WT-like before bolting. After bolting and flowering, newly developed rosette leaves show crinkly and yellow variegation. Most cauline leaves are yellow patched. Yellow patches may only appear on the tips of cauline leaves.	Slightly smaller than or close to WT plants.	About 0.3 to 0.65 g
WT Plant			Plant diameter is about 10 to 12 cm. Height is about 28 to 35 cm. Total rosette leaf weight is 0.8-1 g.	About 0.5 to 0.65 g

[a] Compared to WT plants. *CAC1-A* antisense plants without noticeable morphological changes not listed.

Table 6. Association of antisense mutant phenotype with *CAC1-A* antisense transgene

Transgenic Line	Phenotypic Segregation[a]			Phenotype/PCR Product[b]			
	CAC	WT	$\chi^2_{3:1}$ (p-value)[c]	CAC/462	CAC/933	WT/462	WT/933
9-1-3	33	14	0.266 (0.61)	11	0	0	9
8-2-2	24	10	0.235 (0.63)	7	0	0	7
1-5-6	48	22	0.114 (0.74)	14	0	0	12

[a] Three transgenic lines showing 3:1 segregating ratio of antisense transgenic morphological changes were chosen to test the association of the antisense phenotype with *CAC1-A* transgene. CAC, plants showing antisense morphological changes: crinkly and yellow variegated leaves; WT, plants without any morphological changes.

[b] Leaves were harvested from individual plants and PCR reaction was carried out to amplify *CAC1-A*. 462, plants with PCR products of 462 bp (transgene) and 933 bp (genomic DNA); 933, plants with PCR product of 933 bp only.

[c] Calculation based on 3:1 segregation ratio. In parenthesis is the corresponding p-value of χ^2 with degree of freedom of 1.

Table 7. Fatty acid composition of leaves from WT and *CAC1-A* antisense plants

Leaf	Fatty Acid Percentage (SE)					
	16:0	16:1	18:0	18:1	18:2	18:3
WT[a]	17.2 (0.9)	3.7 (0.5)	16.6 (0.8)	3.7 (0.4)	16.1 (0.4)	42.7 (2.6)
Antisense WT-like[b]	16.3 (0.9)	3.6 (0.2)	17.2 (0.7)	4.1 (0.8)	16.0 (0.7)	42.8 (0.8)
Antisense Crinkly[c]	17.4 (0.9)	3.7 (0.5)	17.4 (1.9)	4.7 (0.4)	16.1 (0.8)	40.7 (0.9)

[abc] n = 3, 7 and 3, respectively.

Table 8. Fatty acid composition of seeds from WT and *CAC1-A* antisense plants

Seed	Fatty Acid Percentage (SE)									
	16:0	16:1	18:0	18:1	18:2	18:3	20:0	20:1	22:0	22:1
WT[a]	8.8 (1.0)	0.55 (0.04)	3.7 (0.2)	15.6 (0.1)	30.1 (0.3)	19.8 (0.2)	2.0 (0.3)	15.9 (1.0)	1.7 (0.2)	1.7 (0.4)
Antisense M[b]	8.2 (0.04)	0.46 (0.06)	3.2 (0.2)	14.1 (0.9)	29.3 (0.7)	22.1 (0.7)	1.9 (0.04)	16.7 (0.5)	2.2 (0.1)	1.9 (0.02)
Antisense S[c]	8.9 (0.8)	0.63 (0.2)	3.3 (0.2)	14.4 (1.7)	29.6 (1.2)	21.9 (0.1)	1.8 (0.1)	15.6 (0.7)	2.0 (0.07)	1.8 (0.1)

[a] n = 2.

[b] Antisense plants with moderate phenotype (Figure 10A). n = 3.

[c] Antisense plants with severe phenotype (Figure 10A). n = 2.

Table 9. PCR primers used to characterize *CAC1-A* antisense plants and T-DNA tagged alleles for htACCase subunit genes

Primer	Sequence	Purpose
JL-202	5'-CATTTTATAATAACGCTGCGGACATCTAC-3'	T-DNA left border for Wisconsin lines
XR-2	5'-TGGGAAAACCTGGCGTTACCCAACTAAT-3'	T-DNA right border for Wisconsin lines
LB	5'-CGTTCTTTAATAGTGGACTCTTGTTCCAA-3'	T-DNA left border for SALK lines
RB	5'-GCAATAATGGTTTCTGACGTATGTGCTTA-3'	T-DNA right border for SALK lines
inv6-2	5'-GCTAAGCACATACGTCAGAAACCATTATT-3'	transposon left border primer for GT lines
spm31	5'-GCTTGTTGAACCGACACTTTTAACATAAG-3'	transposon right border primer for GT lines
CAC1A-1	5'-GTTGAGAAAAATCAGTTTGCCTCTCTTTT-3'	*CAC1-A* gene 5' primer
CAC1A-2	5'-CAAAAAGATTCATGTATCCTCAACATCCT-3'	*CAC1-A* gene 3' primer
CAC1B-5	5'-GACTAATGGTGGGTATATGAACGGAAAAG-3'	*CAC1-B* gene 5' primer used for *cac1-b-1*
CAC1B-3	5'-CATTACAGGAGGCATTGAGTGATAAACTG-3'	*CAC1-B* gene 3'primer used for *cac1-b-1*
CAC1B-a	5'-GCGGTTTGGTGAAGTTAGTTAAAAGAGTT-3'	*CAC1-B* gene 5' primer used for *cac1-b-2*
CAC1B-b	5'-GCAGGAGAAGAACAGAACAGAGAATTATG-3'	*CAC1-B* gene 3'primer used for *cac1-b-2*
CAC3-1	5'-AAGAAGCAAGGAAGAAGACTCAGAAATGT-3'	*CAC3* gene 5' primer
CAC3-2	5'-CAAGTAATCTGAAGCAGAAGCAGAAGAAG-3'	*CAC3* gene 3' primer
pC-F	5'-CATCTTATGCCCAGCAAATGGC-3'	*CAC1-A* cDNA 5' primer
pC-R	5'-CAGTGACAACGAAGGGGAAACG-3'	*CAC1-A* cDNA 3' primer

Table 10. PCR primers used to detect genetic complementation of *cac1-a-1* mutant

Primer	Sequence	Purpose
JL-202	5'-CATTTTATAATAACGCTGCGGACATCTAC-3'	to detect the *cac1-a-1* allele
CAC1A-KO-5	5'-TACACGATTCCTTCCTCGATTAAGATAAG-3'	
CAMBIA-1	5'-TAACAATTTCACACAGGAAACAGCTATGA-3'	to detect the *CAC1-A* transgene
CAC1A-X	5'-TGTTAGGTTTGTTAGTTTGGTGAGGAAGA-3'	
CAC1A-L	5'-CTTTCCGTTATTCTCCGATTACATCTACC-3'	to detect the native wild-type *CAC1-A* allele
CAC1A-3	5'-CTTCAATGAGTTTTTCTCCTTTCCTTCAG-3'	
CAC1A-KO-5	5'-TACACGATTCCTTCCTCGATTAAGATAAG-3'	to detect the native wild-type *CAC1-A* allele
CAC1A-R	5'-TATTGTAGTCGAAGTGGAACTGATTCTCG-3'	

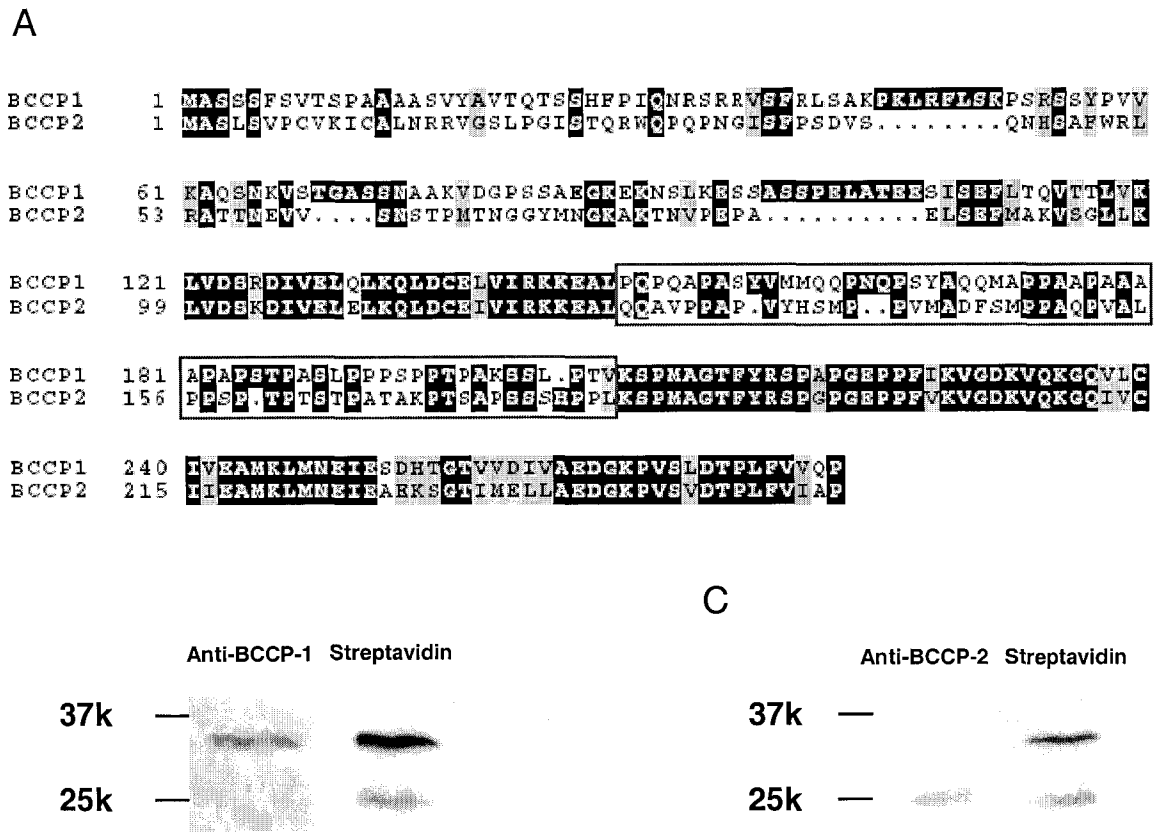

Figure 1. Generation of BCCP-1- and BCCP-2-specific antibodies.

(A) Alignment of BCCP-1 and BCCP-2 protein sequences. The sequence within the red box indicates the region with low amino acid similarity. The BCCP-1 and BCCP-2 cDNAs coding for this region were amplified and cloned into an expression vector.

Proteins were extracted from Arabidopsis flowers and subjected to SDS-PAGE and western blot analysis.
(B) Western blotting with streptavidin and with anti-BCCP-1 antibody.
(C) Western blotting with streptavidin and with anti-BCCP-2 antibody.

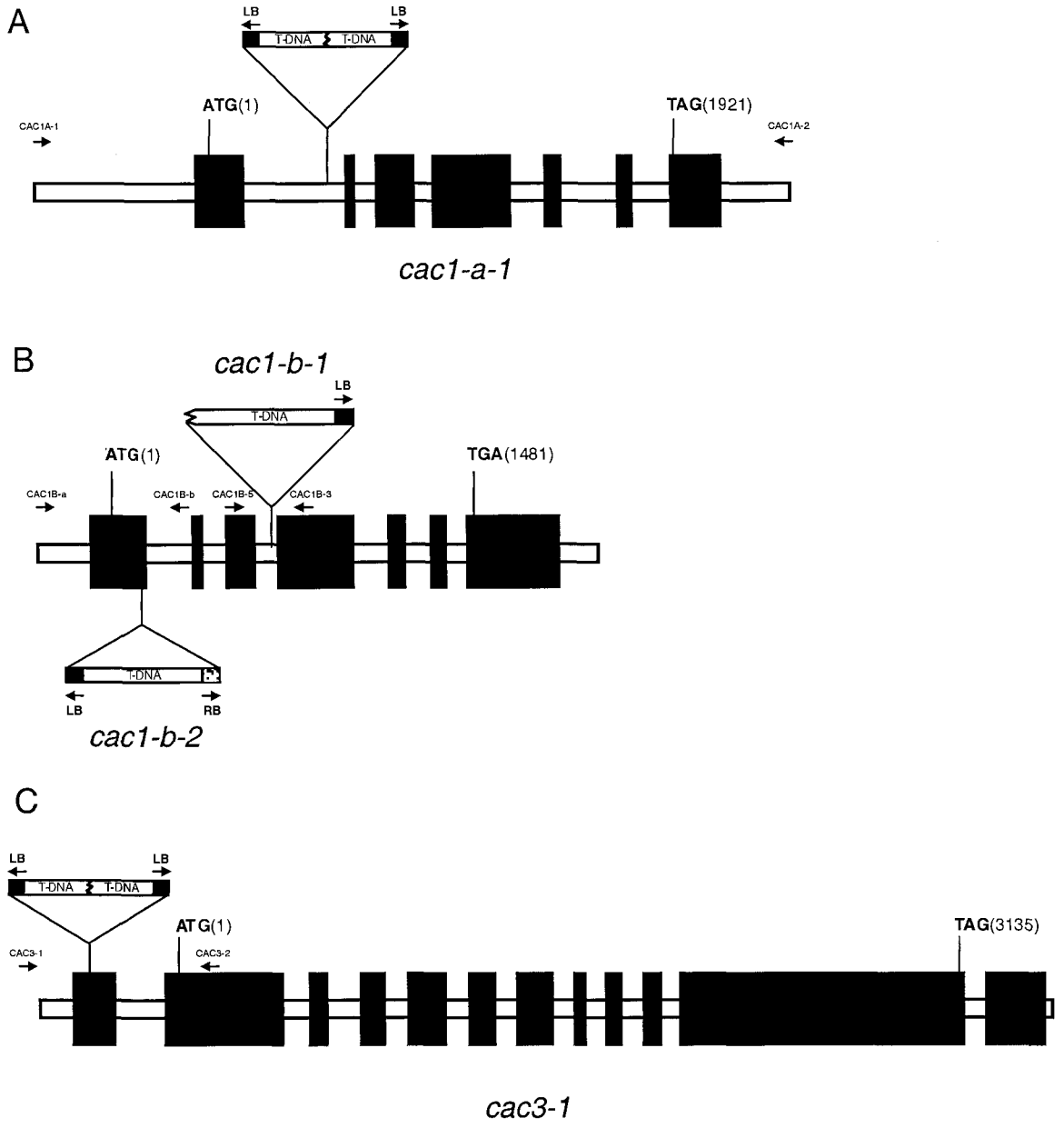

Figure 2. Molecular structure of the *cac1-a-1*, *cac1-b-1*, *cac1-b-2*, and *cac3-1* mutant alleles.

(A) Structure of the *CAC1-A* gene showing the position of the T-DNA insertion in *cac1-a-1*. Exons are represented by black boxes; introns are represented by white boxes. Nucleotides are numbered relative to the translational start site.
(B) Structure of the *CAC1-B* gene showing the position of the T-DNA insertions in *cac1-b-1* and *cac1-b-2*.
(C) Structure of the *CAC3* gene showing the position of the T-DNA insertion in *cac3-1*.

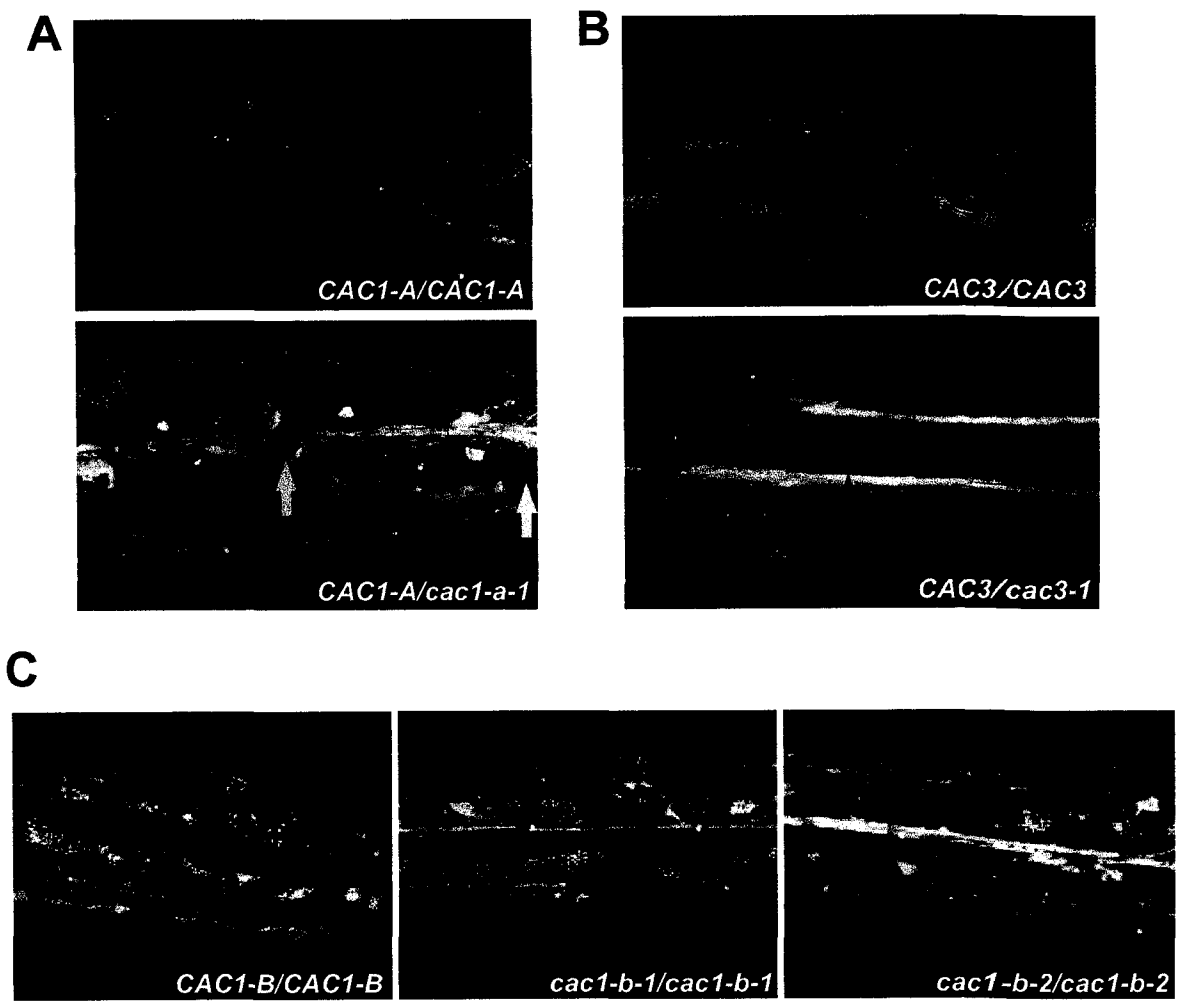

Figure 3. Stereomicroscopic images of developing seeds on sibling wild-type and heterozygous mutant plants for **(A)** *CAC1-A*, **(B)** *CAC3*, and **(C)** *CAC1-B*. The yellow arrows point to the aborted seeds.

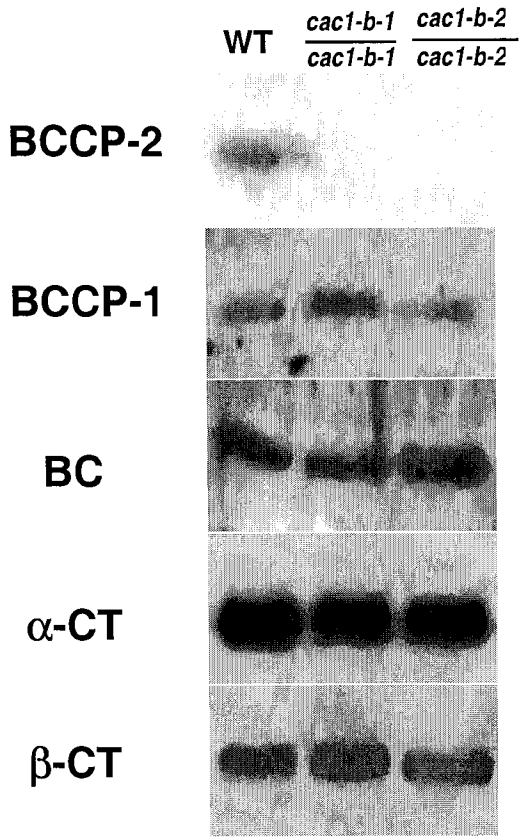

Figure 4. Effect of the *cac1-b* mutations on the accumulation of the htACCase subunits.

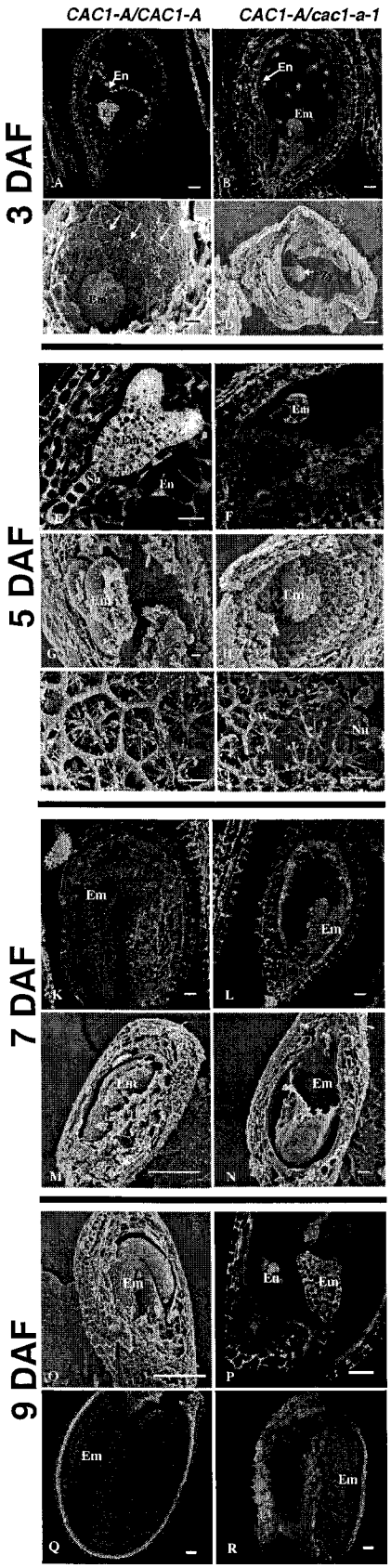

Figure 5. Effect of the *cac1-a-1* allele on embryo and endosperm development.

Developing seeds were examined by confocal scanning laser microscopy (A, B, E, F, K, L, P-R) and scanning electron microscopy (C, D, G-J, M-O). Microscopy was conducted at different stages of development (3, 5, 7, and 9 DAF). Seeds were examined within siliques from siblings that are either wild-type (*CAC1-A/CAC1-A*) or heterozygous mutant (*CAC1-A/cac1-a-1*). On the wild-type siblings, embryos and endosperm developed uniformly as shown in the left set of panels (A, C, E, G, I, K, M, O, Q), whereas on the heterozygous mutant siblings, approximately 17% of the embryos and endosperm developed abnormally as shown in the right set of panels (B, D, F, H, J, L, N, P). We presume that these latter seeds are the segregating homozygous mutants.
Bars= 50μm (A, B, E, F, K, L, P, Q, R); 10 μm (C, D, G, H, I, J, M, N, O).

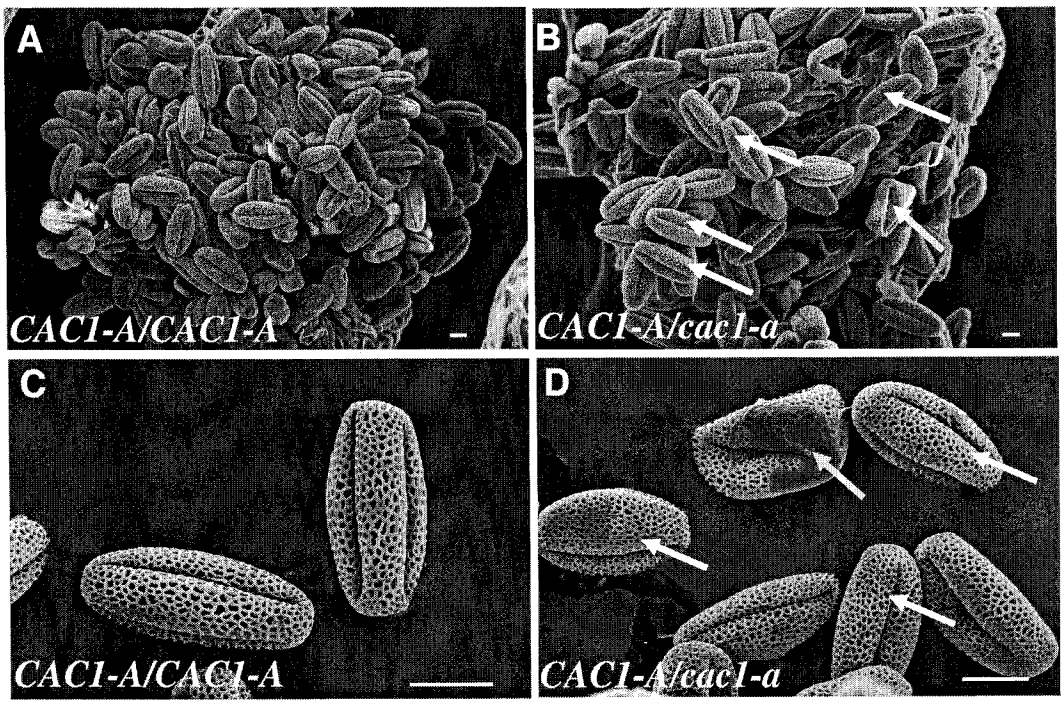

Figure 6. Scanning electron micrographs of pollen grains from sibling wild-type (*CAC1-A/CAC1-A*) (**A** and **C**), and heterozygous (*CAC1-A/cac1-a-1*) plants **(B and D)**. White arrows point to normal shaped pollen grains; yellow arrows point to abnormal shaped pollen grains. Bars = 10μm.

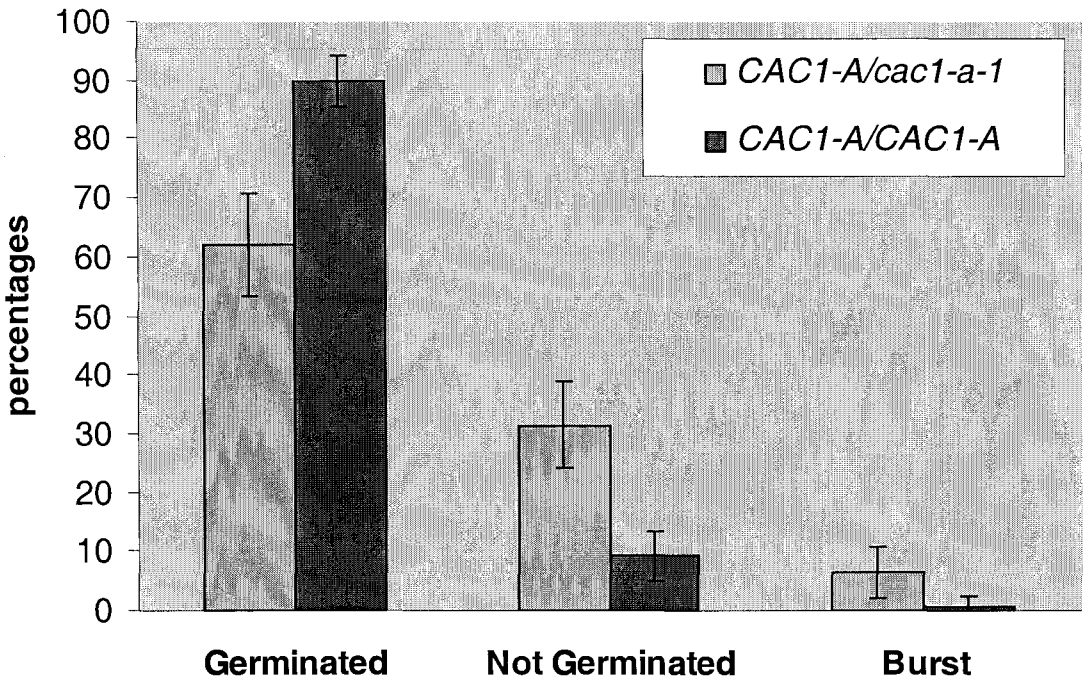

Figure 7. *In vitro* germination rate of pollen grains from heterozygous (*CAC1-A/cac1-a-1*) and wild-type (*CAC1-A/CAC1-A*) sibling plants.

About 1000 pollen grains from either heterozygous mutant plants or wild-type siblings were counted on 20 slides. The error bar shows standard deviation.

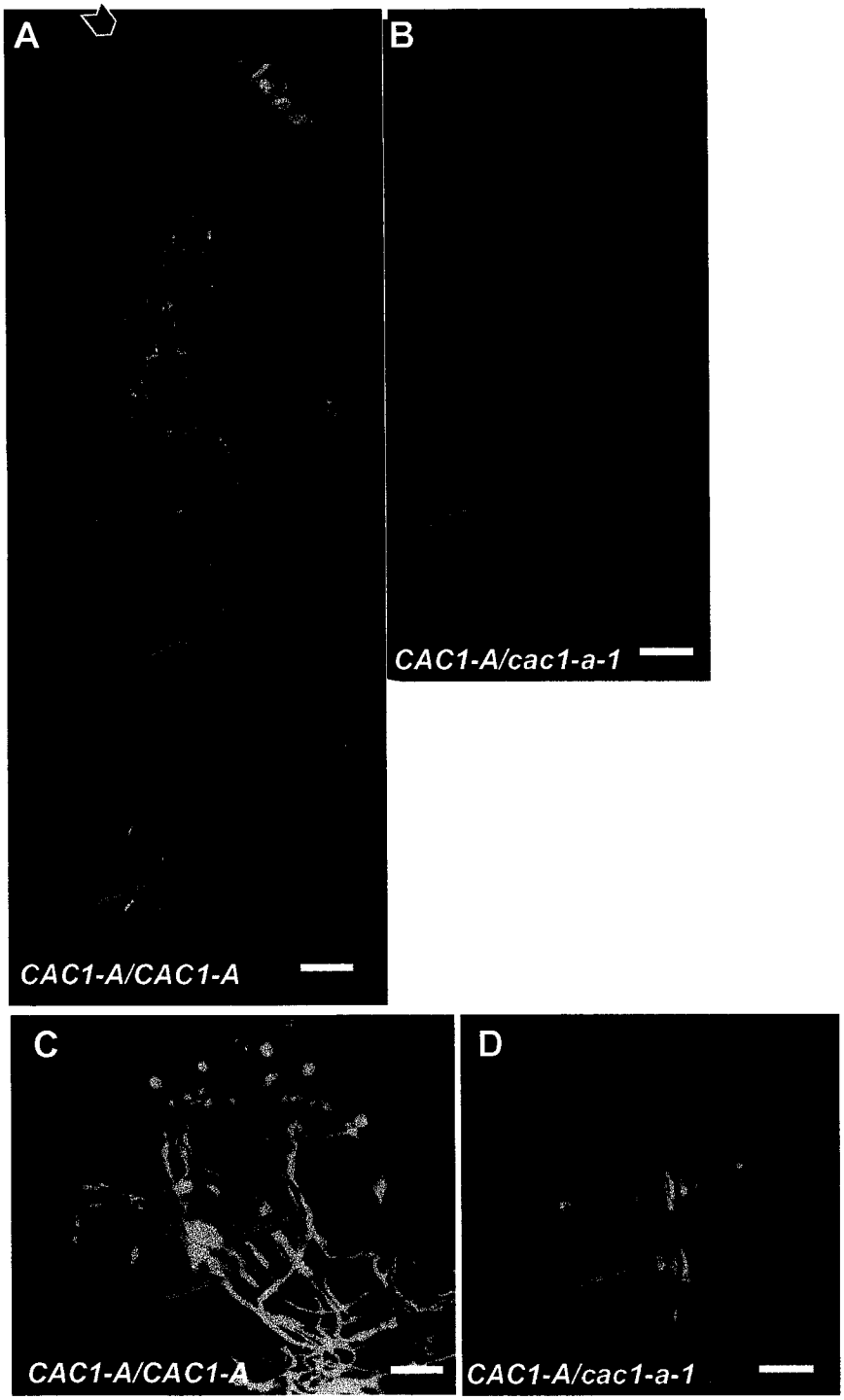

Figure 8. Germinating pollen on pistils of sibling wild-type (*CAC-1A/CAC1-A*) (**A** and **C**) and heterozygous mutant (*CAC-1A/cac1-a-1*) plants (**B and D**). (**A**) and (**B**) were stained with aniline blue; (**C**) and (**D**) were stained with aniline blue/DAPI. These stained pistils/pollen grains were viewed by fluorescence microscopy with a DAPI/FITC/Texas Red filters. Bars = 10 μm.

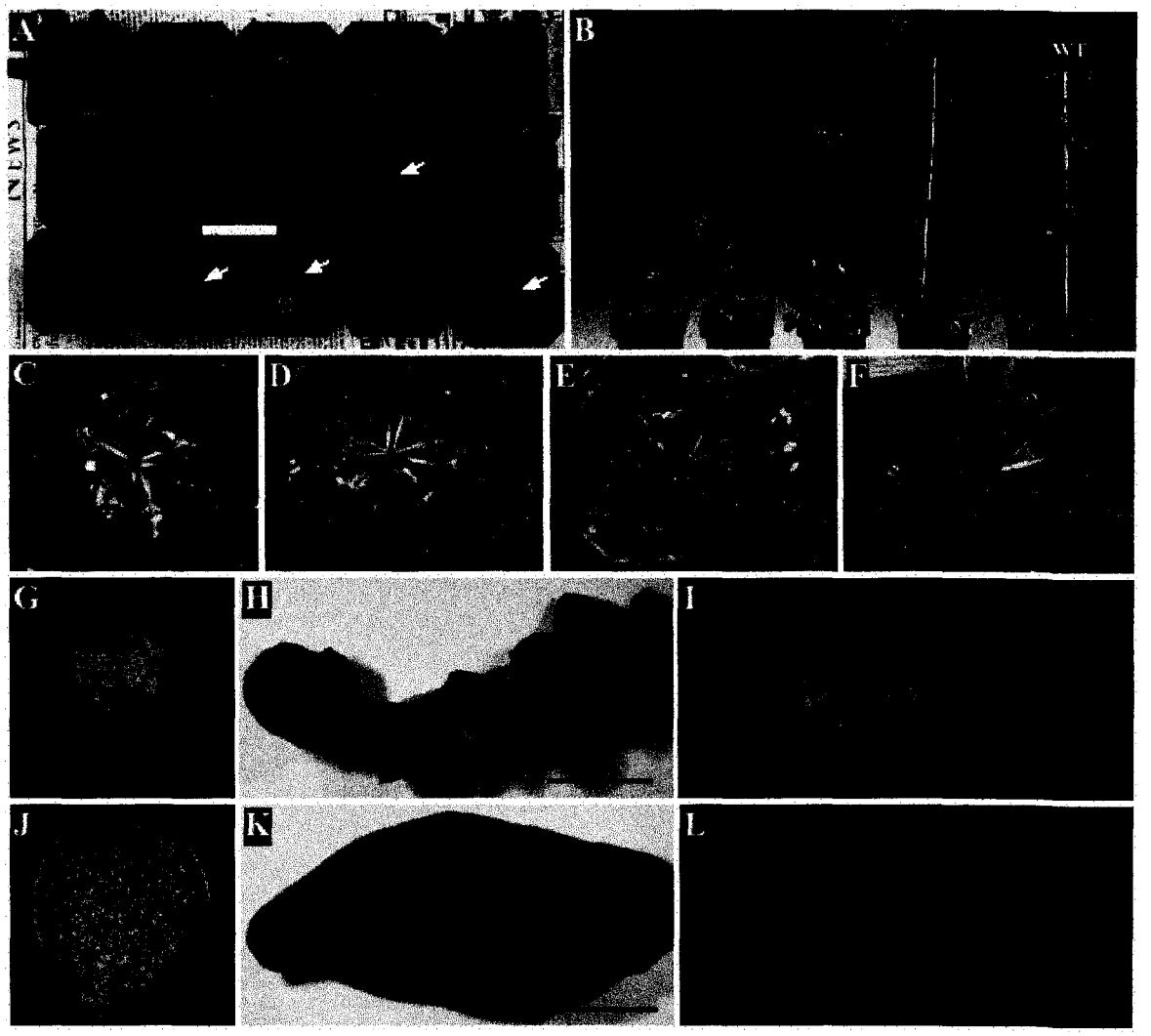

Figure 9. Morphological changes in *CAC1-A* antisense Arabidopsis plants.

(A) and **(B)** *CAC1-A* antisense and wild-type (WT) plants at 25 DAI **(A)** and 38 DAI **(B)**. White arrows in **(A)** point to tiny antisense plants with a very severe phenotype.

(C) to **(F)** Representative antisense plants with decreasing severity of phenotype (**[C]** to **[E]**) and WT plant **(F)** at 31 DAI. Bars = 1 cm.
(G) and **(J)** Cotyledon of antisense plant with severe phenotype **(G)** and WT **(J)** at 11 DAI. Bars = 0.1 cm.
(H) and **(K)** Rosette leaves of antisense **(H)** and WT plant **(K)** at 34 DAI. Bars = 1 cm.
(I) and **(L)** Cauline leaves of antisense **(I)** and WT plant **(L)** at 34 DAI. Bars = 1 cm.

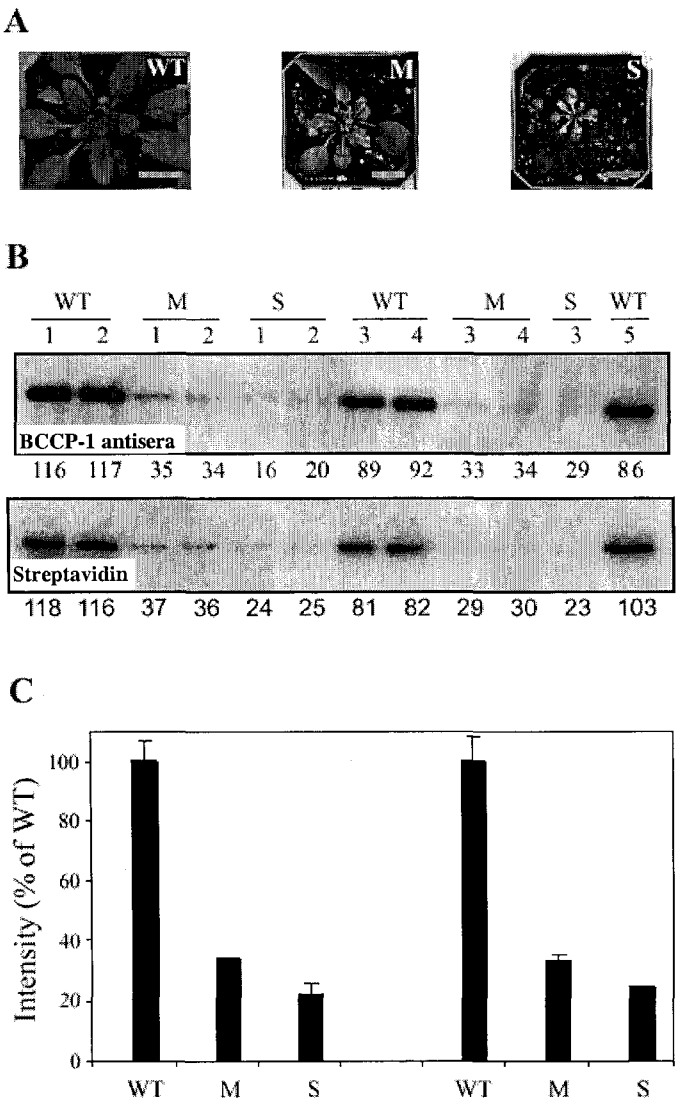

Figure 10. BCCP-1 abundance is reduced in *CAC1-A* antisense plants.

(A) Phenotype of plants used to investigate the relationship between BCCP-1 abundance and phenotype severity. Bars = 1 cm.
(B) BCCP-1 abundance in WT and *CAC1-A* antisense plants. Total protein was extracted from WT, *CAC1-A* antisense plants with a moderate and a severe phenotype. Equal amount of protein (50 μg) from each plant was loaded and blotted with antisera against BCCP-1 followed by ^{125}I-labeled protein A or ^{125}I-labeled streptavidin. Numbers below each blot are signal intensities relative to the average intensity of the WT (100).
(C) Comparison of BCCP-1 abundance in WT and *CAC1-A* antisense plants. BCC-1 signal intensities from WT (n = 5), moderate (M) (n = 4) and severe (S) (n = 3) *CAC1-A* antisense plants in **(B)** were averaged. The error bars indicate the SEM.
(A) to **(C)** WT, WT plant; M, *CAC1-A* antisense plant with moderate phenotype; S, *CAC1-A* antisense plant with severe phenotype. Three repeats of this experiment displayed similar results.

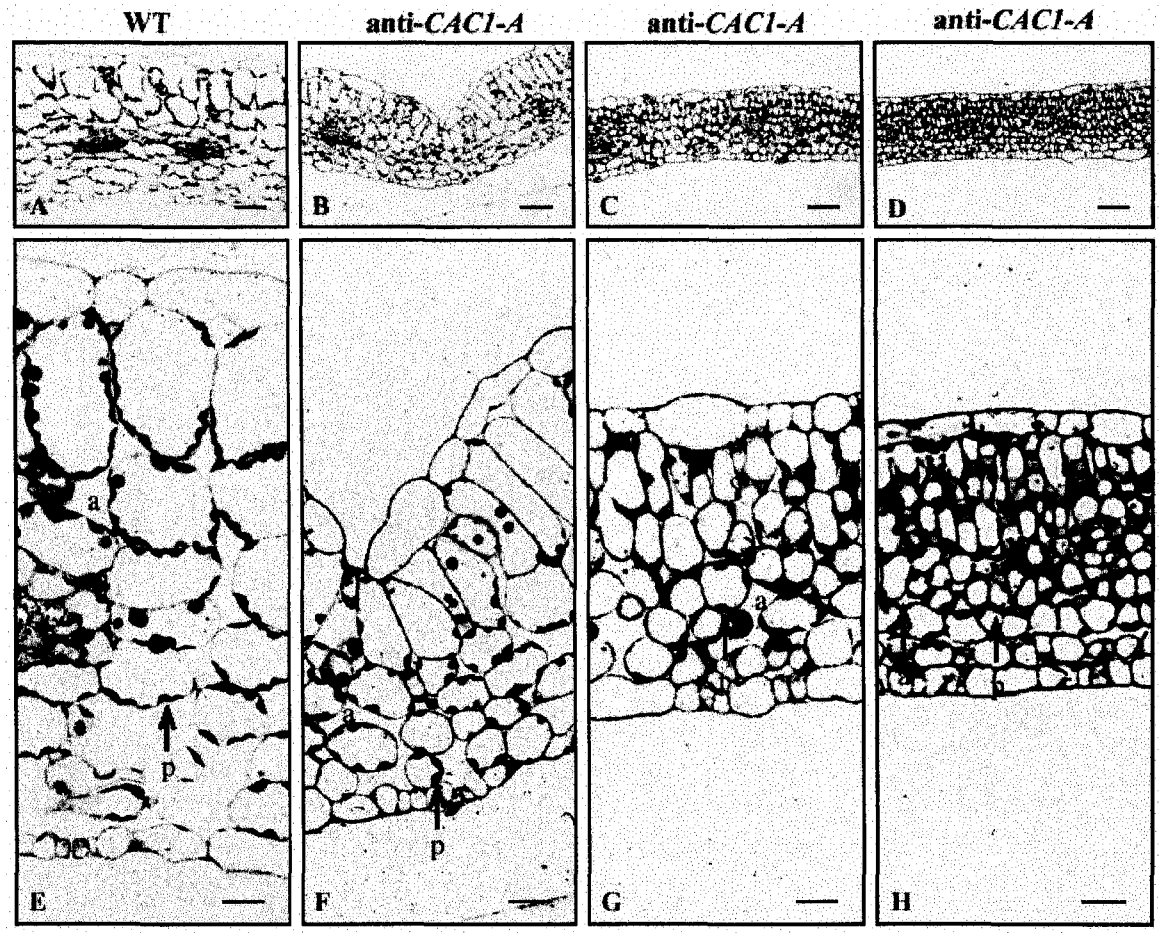

Figure 11. *CAC1-A* antisense ultrastructural phenotype corresponds to severity of leaf phenotype.

(A) and **(E)** WT leaves (control).
(B) and **(F)** Moderate leaf from *CAC1-A* antisense plants.
(C) and **(G)** Moderate leaf from *CAC1-A* antisense plants.
(D) and **(H)** Severe leaf from *CAC1-A* antisense plants.
(A) to **(D)** Bars = 50 μm. **(E)** to **(H)** Bars = 15 μm.

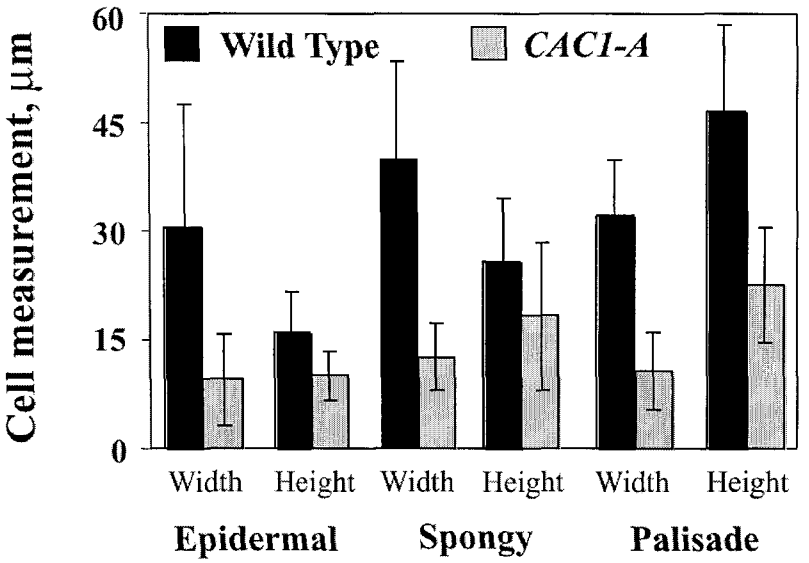

Figure 12. Average cell size of leaves from WT vs. *CAC1-A* antisense plants.

Values are averaged measurements taken from three leaf cross-sections each from an independent transgenic line.

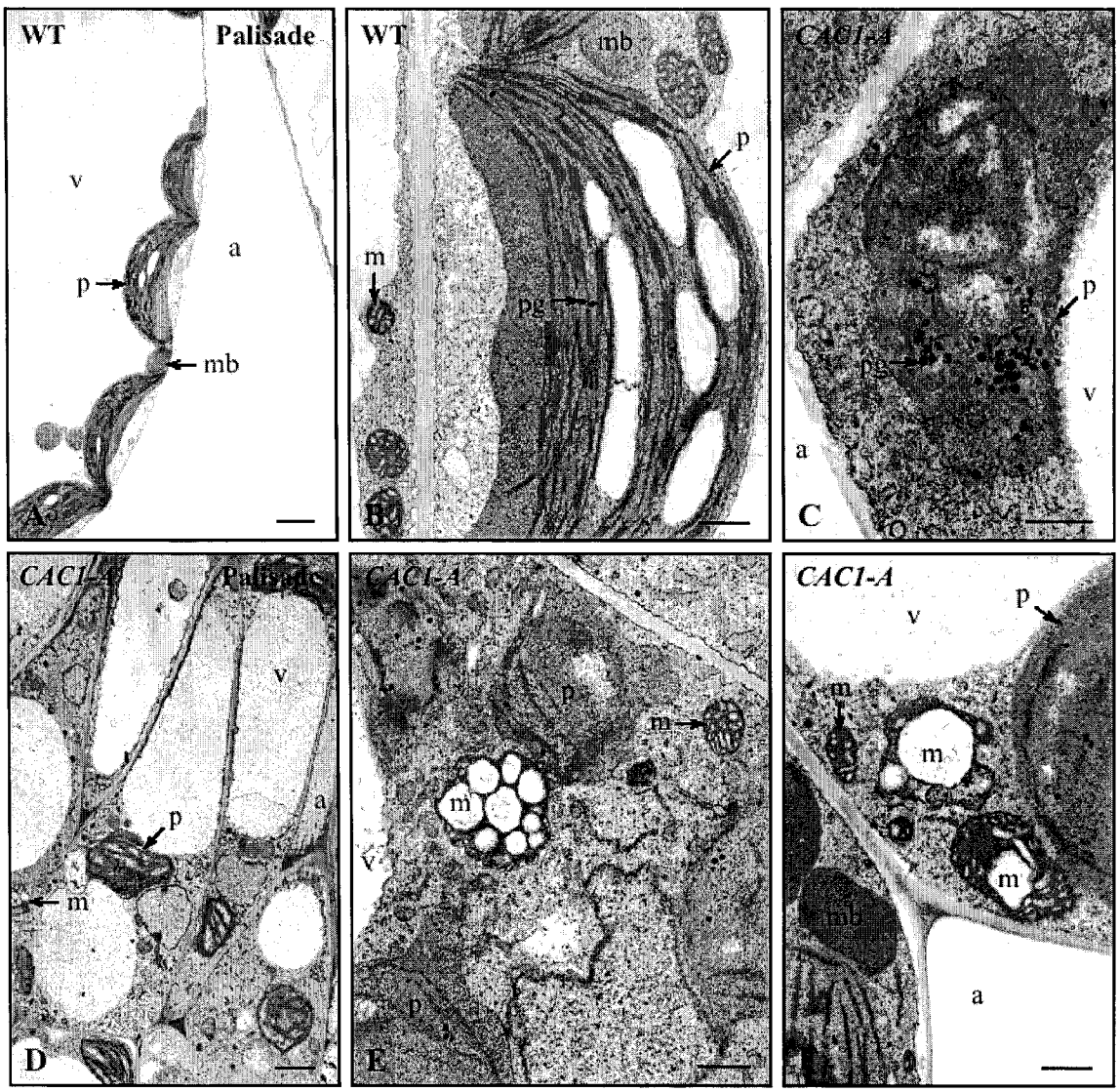

Figure 13. Cells of *CAC1-A* antisense leaves contain altered plastids and mitochondria with aberrant membrane structure.

(A) Cells from the palisade layer of a WT plant.
(B) Representative plastid and mitochondria from WT mesophyll cells.
(C) Representative plastids found in *CAC1-A* antisense plants. Plastids have disorganized membranes and a numerous plastoglobuli.
(D) Cells from the palisade layer of a severely-affected *CAC1-A* antisense leaf.
(E) and **(F)** Representative subcellular alterations found in *CAC1-A* antisense leaves.
(A) and **(D)** Bars = 2 μm. **(B)**, **(C)**, **(E)** and **(F)** Bars = 500 nm.
a = apoplastic space, m = mitochondria, mb = microbody, p = plastid, pg = plastoglobuli, v = vacuole.

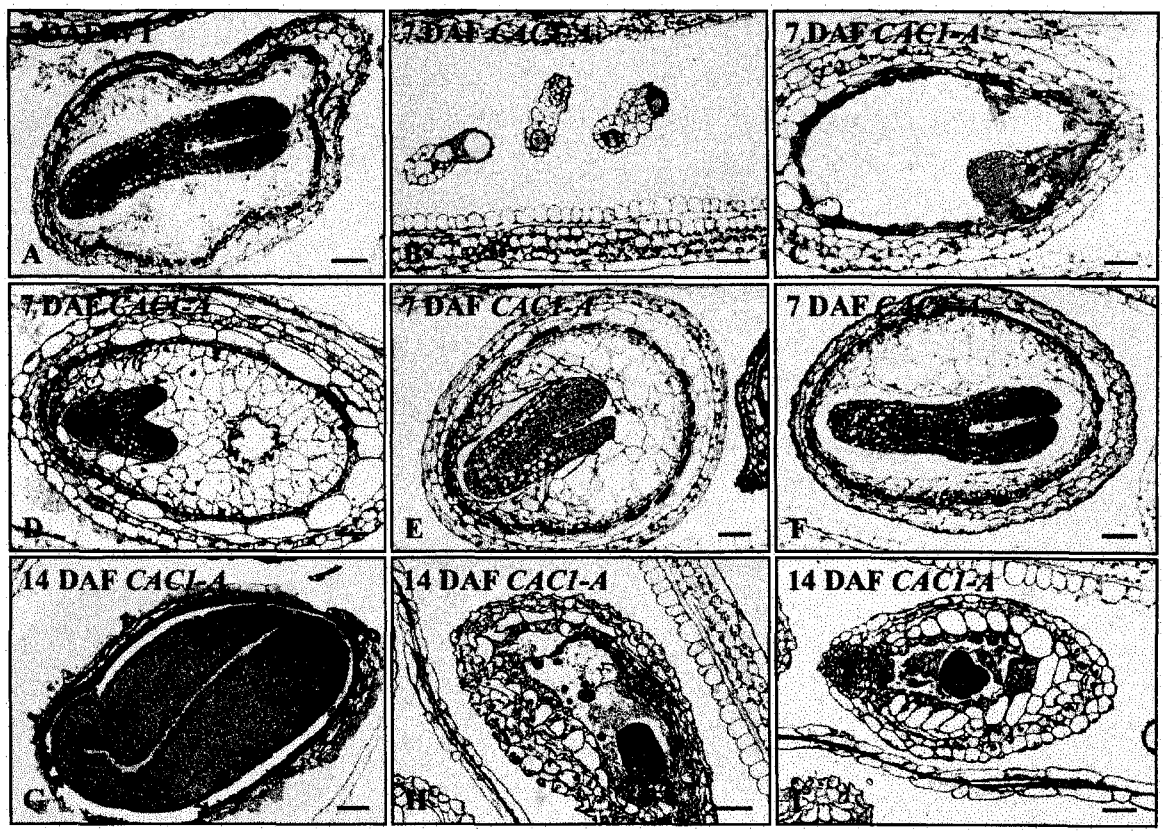

Figure 14. *CAC1-A* antisense siliques 7 and 14 DAF contain embryos at developmental stages far behind those of WT siliques.

The altered developmental profile for a portion of antisense *CAC1-A* embryos may be a product of the morphologically altered mitochondria.
(A) Representative of WT torpedo embryos found within siliques 7 DAF.
(B) to **(F)** Range of embryo stages found within *CAC1-A* siliques 7 DAF.
(G) Representative embryo found in WT 14 DAF siliques.
(H) and **(I)** Embryos found within 14 DAF *CAC1-A* antisense siliques.
(A) to **(I)** Bars = 40 μm.

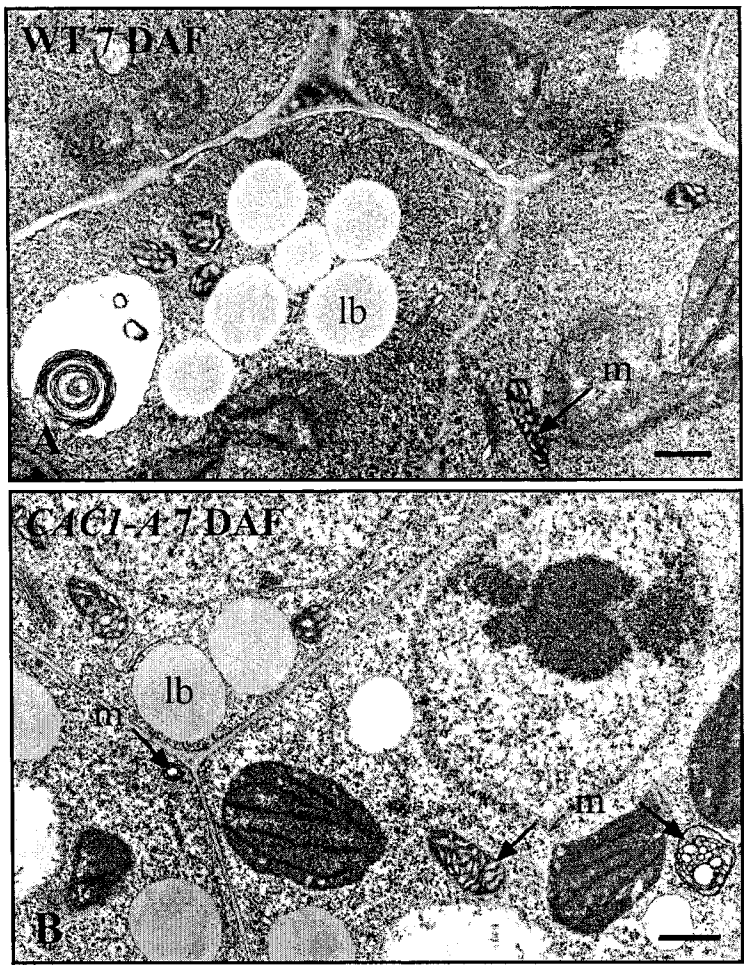

Figure 15. Developmentally lagging embryos from 7 DAF siliques of *CAC1-A* antisense plants contain aberrant mitochondria.

(A) Developing cotyledon from a torpedo-stage embryo in siliques of WT plant.
(B) Developing cotyledon from a torpedo-stage embryo in siliques of *CAC1-A* antisense plant. While both WT and *CAC1-A* embryo cotyledons appear to contain lipid bodies similar in size, distinct alterations in mitochondria structure are apparent in the *CAC1-A* embryo. These aberrant mitochondria are phenotypically consistent with those found in mature leaves.
lb = lipid body, m = mitochondria. Bars = 500 nm.

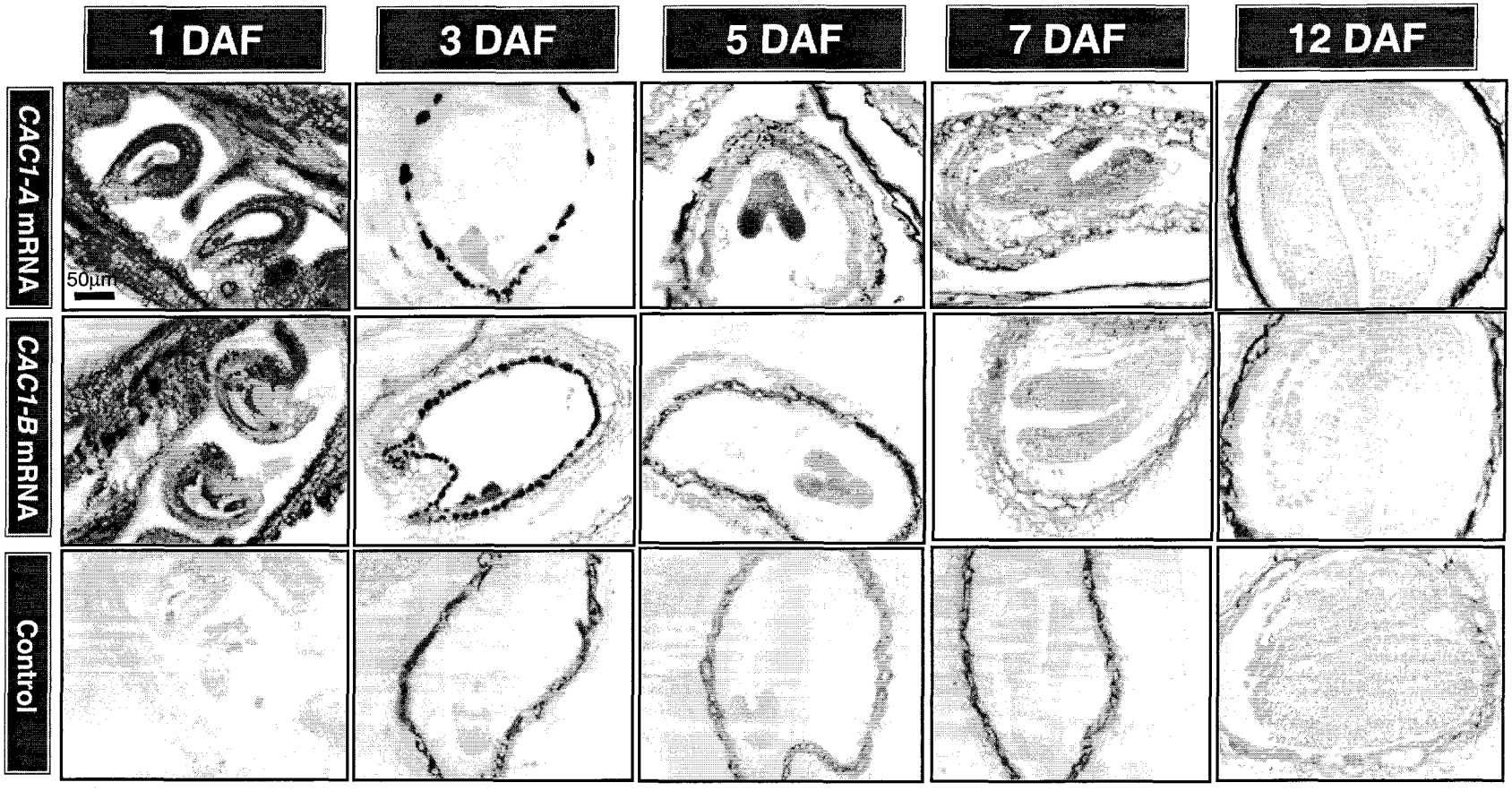

Figure 16. *In situ* location of the *CAC1-A* and *CAC1-B* mRNAs during embryo development.

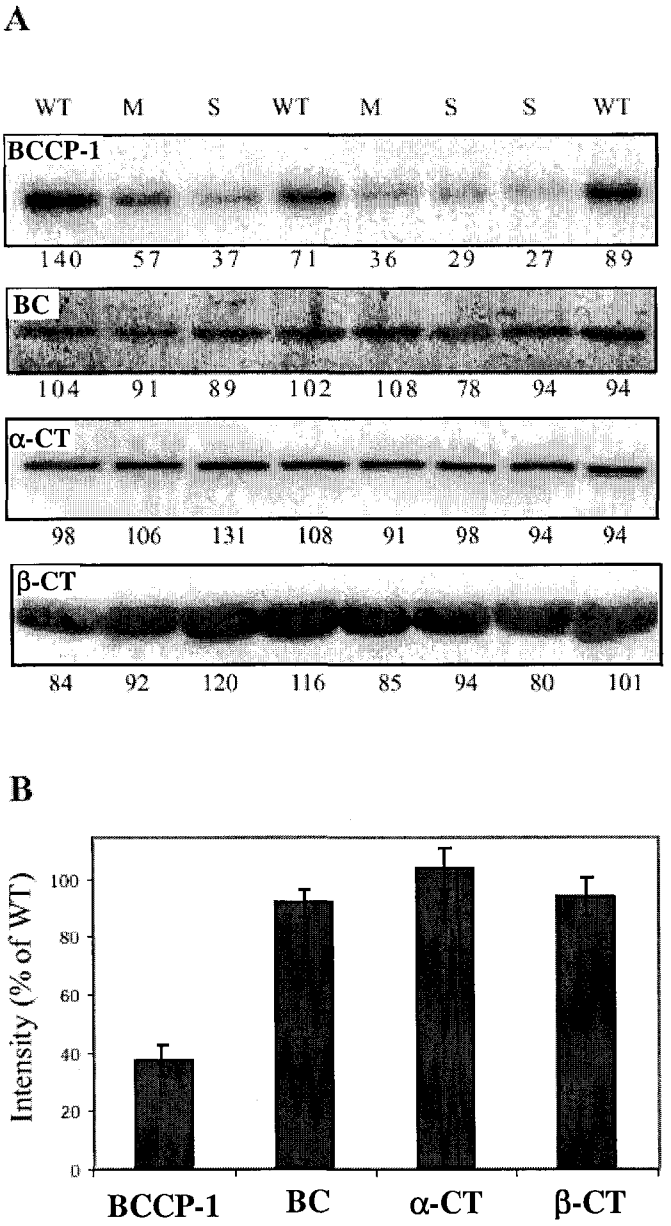

Figure 17. Accumulation of the four subunit proteins of heteromeric ACCase in *CAC1-A* antisense plants.

(A) Total proteins were extracted from leaves of three WT plants and five antisense transgenic plants with moderate and severe phenotypes. Equal amount of each independent protein sample (50 μg) was loaded and fractionated by SDS-PAGE. The blots were then incubated with antisera against BCCP-1, BC, α-CT or β-CT, followed by ^{125}I-labelled protein A. Bands were quantitated using ImageQuant software. Numbers below each blot are signal intensities relative to the average intensity of the WT (100).
(B) The mean intensity relative to WT of the four subunit proteins of ACCase in the five antisense plants from **(A)**. The error bars indicate the SEM.
(A) and **(B)** WT, WT plants; M, *CAC1-A* antisense plant with moderate phenotype; S, *CAC1-A* antisense plant with severe phenotype. Three repeats of this experiment displayed similar results.

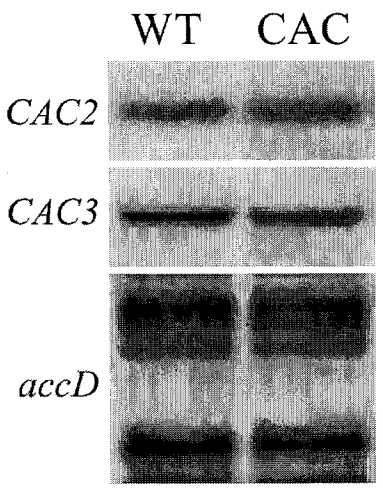

Figure 18. mRNA abundance of heteromeric ACCase in *CAC1-A* antisense plants

Total RNA was extracted from leaves of WT and crinkly leaves of *CAC1-A* antisense plants. Equal amounts of RNA (10 μg) were fractioned and blotted with P^{32}-labeled *CAC2*, *CAC3* and *accD* cDNAs. WT, WT plant; CAC, *CAC1-A* antisense plant with moderate to severe phenotypes. Three repeats of this experiment showed similar results.

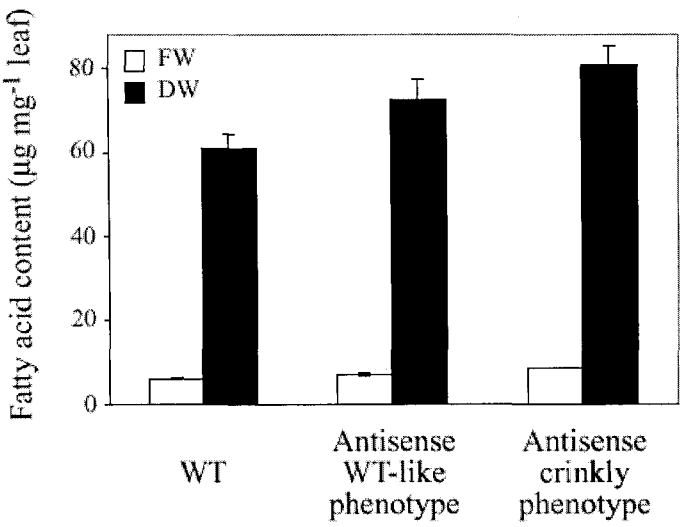

Figure 19. Fatty acid contents in leaves of WT and *CAC1-A* antisense plants.

Mean fatty acid content per FW (open bar) and DW (solid bar) of plant leaves. The error bars indicate the SEM (n = 3, 7, and 3 for WT, antisense WT-like, and antisense crinkly phenotypic leaves, respectively). FW, fresh weight; DW, dry weight.

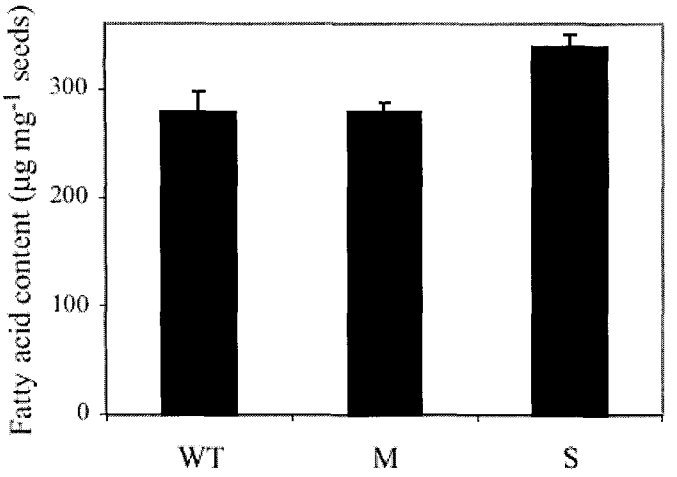

Figure 20. Fatty acid contents in seeds of WT and *CAC1-A* antisense plants.

Fatty acid content per weight of dry seeds. The error bars indicate the SEM (n = 2, 3, and 2 for WT, *CAC1-A* antisense M and S plants, respectively).

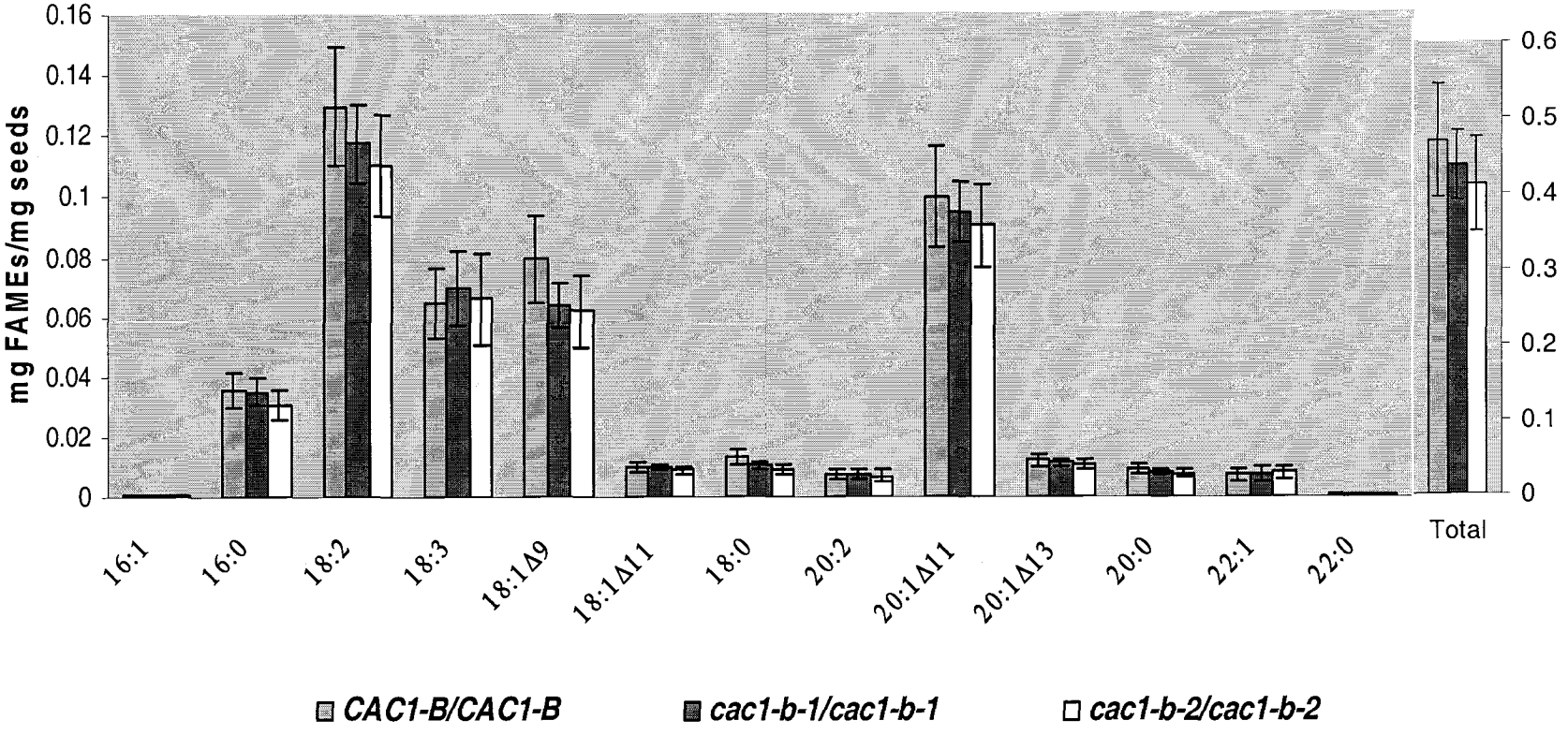

Figure 21. Effect of the *cac1-b* mutations on the accumulation of fatty acids in seeds.

Values represent the mean of six determinations and error bars represent standard deviation.

CHAPTER 3. BIOCHEMICAL AND EXPRESSION ANALYSIS OF HETEROMERIC ACCASE OF ARABIDOPSIS

A manuscript to be submitted to Plant Physiology

Xu Li[a], Eve Syrkin Wurtele[b] and Basil J. Nikolau[a]

[a]Department of Biochemistry, Biophysics and Molecular Biology, and [b]Department of Genetics, Development and Cell Biology, Iowa State University, Ames, IA 50011

ABSTRACT

In *Arabidopsis*, the plastidic heteromeric ACCase (htACCase) is reported to be composed of four nuclear-coded subunits (BCCP-1, BCCP-2, BC, and α-CT) and one plastome-coded subunit (β-CT). However, it is not clear how these subunits are organized in the holoenzyme complex. To investigate the subunit organization of htACCase, plant protein extracts were subjected to PAGE analysis under different conditions followed by western blot analysis with specific antibodies for each subunit. Native PAGE/western analysis failed to reveal an htACCase holoenzyme, instead BCCP-1 and BC, and α-CT and β-CT are associated in two separate complexes. SDS-PAGE/western analysis under reducing and non-reducing conditions reveals the presence of an α-CT homodimer and β-CT homodimer, held together by disulfide bonds. The formation of such disulfide bonds are not affected by illumination. To examine the possible coordinate expression among the subunits of htACCase, the expression of each subunit gene was measured at both the mRNA and the protein levels. The data show that BCCP-2 mRNA accumulates differently from the other htACCase subunit mRNAs, which accumulate at a constant molar ratio across a variety of different organs and development

stages. However, none of the subunit proteins accumulates at a constant ratio across all the plant materials examined.

INTRODUCTION

ACCase [EC 6.4.1.2] is a biotin-containing enzyme that catalyzes the first and committed reaction of *de novo* fatty acid biosynthesis: the ATP-dependent formation of malonyl-CoA from acetyl-CoA and bicarbonate. This reaction occurs in two steps: (1) carboxylation of the biotin prosthetic group; (2) transfer of the carboxyl group from carboxyl-biotin to acetyl-CoA to form malonyl-CoA. ACCase has three conserved functional domains: biotin carboxyl-carrier protein (BCCP), biotin carboxylase (BC), and carboxyl transferase (CT). BCCP acts as an intermediate carrier of the carboxyl group, whereas BC and CT catalyze the two half reactions respectively.

Two forms of ACCase have been found in nature: the homomeric ACCase (hmACCase), in which the three functional domains are on a single polypeptide, and the heteromeric ACCase (htACCase), in which those domains occur on separate dissociable proteins. Most eubacteria possess heteromeric form of ACCase (Guchhait et al., 1974; Li and Cronan, 1992, 1992; Gornicki et al., 1993; Marini et al., 1995), whereas fungi and animals have homomeric ACCase (Lopez-Casillas et al., 1988; Takai et al., 1988; Al-Feel et al., 1992; Ha et al., 1994; Barber and Travers, 1995). In contrast to other organisms, plants contain ACCases in two subcellular compartments, the cytosol and the plastids. Most plants (excluding Graminae) have the homomeric ACCase in cytosol and the heteromeric ACCase in plastids (Kannangara and Stumpf, 1972; Li and Cronan, 1992; Sasaki et al., 1993; Alban et al., 1994; Konishi and Sasaki, 1994; Shorrosh et al., 1995; Konishi et al., 1996; Reverdatto et al., 1999). In Graminae plants,

both cytosolic and plastidic ACCases are of the homomeric form (Egli et al., 1993; Konishi and Sasaki, 1994; Konishi et al., 1996; Gornicki et al., 1997).

E. coli ACCase is constituted of four different subunits: BCCP, BC, α-CT, and β-CT. The enzyme is very unstable and readily dissociates into three subcomplexes, BCCP, BC, and CT during extraction (Fall et al., 1971; Fall and Vagelos, 1972; Guchhait et al., 1974). The plant htACCase is also constituted of four distinct subunits. However, three of these (BCCP, BC, and α-CT) are encoded by nuclear genes, whereas β-CT is encoded by a plastidic gene (*accD*). The quaternary structure of the plant heteromeric ACCase is still not clear. Here, we report the biochemical characterization of the *Arabidopsis* htACCase and further investigation of the coordinate expression of the individual subunit genes at both mRNA level and protein level.

RESULTS

Native PAGE analysis of htACCase

To understand the subunit organization of the htACCase complex, protein extracts were subjected to native PAGE and western blot analysis with antibodies specific for each subunit. Two non-dissociating discontinuous buffer systems were used for native PAGE. Initially, the Tris-HCl-glycine system (Ornstein, 1964) was used to separate native protein complexes. Each subunit migrated at different rates on the gel, indicating that the enzyme complex dissociated during extraction and/or electrophoresis in these conditions (Figure 1). The molecular weights of the complexes for each subunit were estimated by comparing migration to molecular weight marker proteins. Two protein complexes (458 kD and 86 kD) contain BCCP-1. BCCP-2 is in a complex of 368 kD, and BC is in a complex of 388 kD. The α-CT subunit is found in three immunoreactive bands of different sizes (554 kD, 378 kD, and 89 kD). The 89 kD band is the

α-CT monomer. Apart from α-CT, all subunits were recovered at molecular weight greater than the monomeric molecular weights. Therefore, these immunoreactive "high" molecular weight proteins are complexes, probably of oligomers of each individual subunit. However, we can not exclude the possibility that other proteins are also in those complexes. What is clear is that they are constituted of only one type of htACCase subunit and not mixtures of these subunits.

The second electrophoresis system that was used in these analyses was the KOH-ACES-Hepes system (Jovin, 1973). In these conditions, BCCP-1 and BC comigrate as a complex of 600 kD, and α-CT and β-CT comigrate as complexes with a molecular weight ranging from 270 kD to 490 kD. BCCP-2 migrates at 242kD, a position distinct from any other subunits (Figure 2).

α-CT and β-CT form homodimers by disulfide bonding

To further investigate the subunit organization of htACCase, protein extracts were prepared and subjected to SDS-PAGE in the presence or absence of thiol-reducing reagent, and the resulting western blots were probed with antibodies specific for each subunit (Figure 3). Under reducing conditions, each subunit migrated as a monomer (BCCP-1: ~37kD, BCCP-2: ~25kD, BC: ~50kD, α-CT: ~75kD, and β-CT: ~50kD). However, under non-reducing conditions, while BCCP-1, BCCP-2, and BC migrate as monomers, the α-CT and β-CT subunits migrate both as monomers and as higher molecular weight homomeric complexes. These higher molecular weight complexes have an apparent molecular weight twice their monomers (i.e., ~150kD for α-CT, ~100kD for β-CT). These observations indicate that *in*

planta α-CT and β-CT can form homodimers that are held together by disulfide bond(s).

Light does not affect the accumulation of htACCase subunits

It has been reported that the ACCase activity is regulated by light-dependent redox change (Kozaki and Sasaki, 1999), so it is intriguing to determine whether light affects the disulfide bond formation of the α-CT and the β-CT subunits. To test this, proteins were extracted from plants grown under continuous illumination (31 days continuous illumination) and from dark-adapted plants (grown under 30 days continuous illumination, and then 24 hours of darkness). These extracts were subjected to SDS-PAGE under non-reducing conditions and subsequent western blot analyses with antibodies specific for each subunit; an additional blot was probed with streptavidin to detect biotin containing proteins. As shown in Figure 4A, in dark-adapted plants the accumulation of MCC-A, the biotinylated subunit of 3-methylcrotonyl-coenzyme A carboxylase, is about 3-fold of that found in plants grown under illumination, which is in agreement with previous finding (Che et al., 2002). However, there is no difference in BCCP-1, BC, α-CT, and β-CT subunit accumulation between the extracts from the light-adapted plants and the dark-adapted plants (Figure 4B). The BCCP-2 protein was not detectable with anti-BCCP-2 serum, but the accumulation of biotinylated BCCP-2 detected by streptavidin was independent of illumination (Figure 4A).

Accumulation of htACCase subunit mRNAs

Previous studies have demonstrated that *CAC1-A*, *CAC2*, *CAC3*, and *accD* mRNAs accumulate at a constant ratio in developing siliques, as well as expanding leaves, flower buds, and flowers (Ke et al., 2000). Later, another BCCP-coding gene (*CAC1-B*) was identified in

the Arabidopsis genome (Thelen et al., 2001). To investigate the possible coordinated expression among all five subunit genes, we quantified the mRNA and protein accumulation for each subunit gene in different organs and developmental stages.

Rosette leaves were collected from plants at growth stage 6.00 (when the first flower opened) (Boyes et al., 2001). Stems (above rosette leaves but below bottom cauline leaf), flower buds, 2-4 DAF siliques, 6-8 DAF siliques, and 10-12 DAF siliques were collected from older plants. To reduce biological variability, plant material collected from 8 individual plants was pooled together as one sample. The aerial parts and roots of 14-day seedlings were collected from plants grown on vertical MS plates. The above collection of tissue was applied to three batches of plants. Thus, three samples representing biological replications were obtained for each organ/developmental stage. Upon collection all samples were immediately flash frozen in liquid nitrogen and powderized under liquid nitrogen with a mortar and pestle, and stored in aliquots of 0.1 g at -80 °C until use.

The quantification of mRNA was conducted by real-time RT-PCR. 18S rRNA was used as a reference RNA to normalize the measured gene expression. The primers were designed so that the amplicon for each gene has the same size, therefore mRNA accumulation can be compared across different genes with a simple relative quantification method using SYBR Green I dye. As evidenced in Figure 5, the mRNA of *accD* gene is more abundant than that of the other subunit genes. Statistical analyses were performed to test whether the expression patterns (across organ) of any two of the five genes are different (Table 2). When Bonferroni correction for multiple comparison was used, *CAC1-A*, *CAC2*, *CAC3* and *accD* mRNA accumulation patterns are not statistically different at a significance level of 0.05. They accumulate at a constant molar ratio, which is *CAC1-A*:*CAC2*:*CAC3*:*accD* = 0.5:1.0:0.2:2.0,

across all the organs examined. But the *CAC1-B* mRNA accumulates differently from all the other subunits (Table 2).

Accumulation of htACCase subunit proteins

To measure the protein accumulation of htACCase subunits, for each subunit protein an S·tag fusion protein was produced from *E. coli* by recombinant DNA techniques. The concentration of the recombinant protein was determined by measuring the RNase activity reconstituted by the binding of S·tag with S-protein (Richards and Wyckoff, 1971). These recombinant proteins with known concentration were used as standard. Western blot with anti-serum for each subunit was performed with the unknown samples and a serial dilution of recombinant standard on the same gel/blot (Figure 6B). The standard curve was constructed from the recombinant protein standard (Figure 6A). Then the molar concentration of the target protein in the plant samples was determined using the standard curve. With this method, we were able to absolutely quantify the accumulation of each subunit protein.

The data are summarized in Table 3. Statistical analysis shows that none of the five subunits has the same accumulation pattern across the organs examined at a significance level of 0.05 (Table 2).

DISCUSSION

Plant htACCase catalyzes the first and committed reaction of de novo fatty acid biosynthesis in plastids. It consists of three nuclear-coded subunits (BCCP, BC, and α-CT) and one plastome-coded subunit (β-CT). Although the genes coding for individual subunits have been identified and characterized from many plant species, the quaternary structure of the plant

htACCase is still not clear.

Studies on *E. coli* ACCase showed that the holoenzyme complex is very unstable, dissociates and become inactivated during extraction (Fall et al., 1971; Fall and Vagelos, 1972; Guchhait et al., 1974). Although the overall ACCase activity is lost, the BC and CT subcomplexes retain the activities for their respective half reactions. BC has been purified to homogeneity and crystallized, and shown to be a homodimer (Guchhait et al., 1974). Purification of CT complex revealed that it is composed of $(\alpha\text{-CT})_2(\beta\text{-CT})_2$ (Guchhait et al., 1974; Li and Cronan, 1992). Recently, by a two-step affinity chromatography approach taking advantage of the natural affinity tag, biotin, on BCCP protein and an engineered His-tag on BC protein, the unstable BCCP•BC complex was purified and characterized as $(BCCP)_4(BC)_2$ (Choi-Rhee and Cronan, 2003).

Our current knowledge of the holoenzyme complex of the plant heteromeric ACCase comes mainly from biochemical studies of the pea and soybean enzymes. Gel filtration chromatography of chloroplast proteins indicated that the holoenzyme might be a 600-700 kDa complex (Sasaki et al., 1993; Alban et al., 1994; Reverdatto et al., 1999). The holoenzyme complex readily dissociates and loses activity during further purification. However, two subcomplexes, BCCP•BC and α-CT•β-CT can be recovered by ion exchange, native PAGE, or differential $(NH_4)_2SO_4$ fractionation (Alban et al., 1994; Shorrosh et al., 1996). The elucidation of the subunit stoichiometry of the enzyme complex from these experiments was further complicated by the existence of multiple paralogous genes for the nuclear-coded htACCase subunits (Elborough et al., 1996; Reverdatto et al., 1999; Mekhedov et al., 2000).

To overcome this genetic complexity, we have investigated the htACCase complex in *Arabidopsis* where single copy nuclear genes code for BC (Sun et al., 1997) and α-CT (Ke et

al., 2000), a plastome gene codes for β-CT (Ke et al., 2000) and two genes code for BCCP (Ke et al., 1997; Thelen et al., 2001). To understand the organization of these subunits in the htACCase holoenzyme, we fractionated plant protein extracts by native PAGE and detected each subunit by immunoblotting with specific antibodies. Protein complexes were separated at either pH 10 or pH 8.5. In neither condition were we able to detect htACCase holoenzyme. However, at pH 8.5, BCCP-1 and BC were found to be in the same complex of about 600 kD, and α-CT and β-CT in a range of complexes of different sizes (270 kD to 490 kD). This is consistent with previous observations from other plant species. The association of *Arabidopsis* α-CT and β-CT subunits has also been demonstrated by co-immunoprecipitation experiments (Ke et al., 2000). The observation that the α-CT and β-CT subunits appear in complexes of a wide range of sizes is consistent with the observation that α-CT and β-CT of soybean htACCase have a broad elution range from gel filtration or ion-exchange chromatography (Reverdatto et al., 1999). Interestingly, BCCP-2 was separate from the other subunits of htACCase at both pH 10 and pH 8.5.

The htACCase activity is increased by illumination (Hunter and Ohlrogge, 1998), but the mechanism of such regulation is not clear. It has previously been reported that the α-CT and β-CT subunits of pea htACCase form a heterodimer by disulfide bond and the dimerization is subject to light/dark regulation (Kozaki et al., 2001). However, in *Arabidopsis*, we found the α-CT and the β-CT subunits form homodimers that are covalently linked via disulfide bonds. Moreover, light does not appear to affect the disulfide bond formation for the α-CT and the β-CT dimers. Sequence alignment of β-CT sequences from different organisms including Arabidopsis shows the cystine residue that is involved in the formation of disulfide bond

between α-CT and β-CT subunits was only found in the pea sequence (Kozaki et al., 2001). This suggests that the light-dependent reduction of the disulfide bond formed between α-CT and β-CT subunits observed in pea is either irrelevant to the light activation of htACCase or it is a pea-specific mechanism.

It is expected that the synthesis of the individual subunits of htACCase would be coordinately regulated. Indeed, in *Arabidopsis*, quantitative northern blot analysis has shown that *CAC1-A*, *CAC2*, *CAC3* and *accD* mRNAs accumulate at a constant molar ratio of 0.14:1.0:0.17:0.06 in developing siliques, expanding leaves, flower buds, and flowers (Ke et al., 2000). Our real-time PCR data confirmed that the above four subunit mRNAs remain at a constant molar ratio across different organs including roots. However, the ratio we got (*CAC1-A*:*CAC2*:*CAC3*:*accD* = 0.5:1.0:0.2:2.0) is different from the previous report. This may be a reflection of the fact that the plants were grown under different growth conditions or may be a reflection of the different techniques used to quantify mRNAs.

It has been reported that the *CAC1-A* and *CAC1-B* genes have different expression patterns (Thelen et al., 2001). In agreement with this, our data showed *CAC1-B* mRNA does not have the same pattern as the other four subunit mRNAs.

Surprisingly, in spite of the coordinate accumulation of mRNAs, the htACCase subunit proteins do not accumulate at a constant ratio across the organs that we examined. This suggests translational and/or posttranslational processes are important in regulating expression of the subunit genes. The discrepancy between the steady-state levels of mRNA and those of protein is not uncommon. Large-scale analysis of gene expression at both the RNA and protein levels in yeast has revealed there is a poor correlation between the transcriptome and the proteome (Gygi et al., 1999).

MATERIALS AND METHODS

Plant materials

Arabidopsis (ecotype Columbia) seeds were sowed in LC1 Sunshine Mix soil (Sun Gro Horticulture, Bellevue, WA) or Murashige and Skoog medium (MS salt 4.3 g/L, B5 vitamins 1 ml/L, sucrose 10 g/L, MES 0.5 g/L, adjust pH to 5.7 with KOH, 0.8% agar) and placed at 4 °C for two days before moving to 22 °C under constant illumination.

To study the light effect on htACCase subunit status, wild-type plants were grown with 24-h illumination for 30 days, some plants were then covered by an opaque plastic container with three layers of black plastic bags for 24 hours. The aerial parts of the plants were collected in a dark room and immediately frozen in liquid nitrogen.

Real-time RT PCR

Total RNA was extracted from plant tissue by using RNeasy Plant Mini Kit (Qiagen, Valencia, CA). 1 μg RNA was incubated with 2 μl of RQ1 RNase-Free DNase (Promega, Madison, WI) at 37 °C for 1 hour to eliminate the trace amount of genomic DNA. First-strand cDNA synthesis using random hexamers was carried out with SuperScript™ II Reverse Transcriptase (Invitrogen, Carlsbad, CA) following the protocol provided by Invitrogen. The cDNAs were aliquoted and stored in -80 °C.

Primers for real-time PCR were designed using Primer Express software (Applied Biosystem, Foster City, CA) following the guideline provided. A relative quantification method was adapted to measure the expression of htACCase subunit genes with 18S rRNA as a reference gene (Pfaffl, 2001). Real-time PCR reactions were performed with GeneAmp 5700

Sequence Detection System using SYBR green PCR Master Mix (Applied Biosystem, Foster City, CA). The measurements of all 6 genes from a single sample were performed on the same plate. All the measurements were performed in triplicate. The averaged threshold cycle (C_T) value of the triplicate measurement was used to calculate the normalized expression value (Muller et al., 2002).

Preparation of protein standard for each htACCase subunit

Standard molecular cloning procedures (Sambrook et al., 1989) were used to make constructs that produce S·tag fusion proteins for each htACCase subunit in *E. coli*. The 1.1 kb *CAC1-A* cDNA (Choi et al., 1995) was released from pBlueScript vector with *Eco*RI and *Sau*3AI and cloned into *Eco*RI and *Bam*HI sites of pET30a vector (Novagen, Madison, WI). The *CAC1-B* cDNA clone 180M1T7 (GenBank accession No. H37386) was obtained from the Arabidopsis Biological Research Center (Columbus, OH). *Sal*I and *Not*I were used to subclone the *CAC1-B* cDNA into pET30a vector. The resulting plasmids were named pET-CAC1A and pET-CAC1B, respectively. The construction of pET-CAC2, pET-CAC3, and pET-accD has been described (Sun et al., 1997; Ke et al., 2000).

The above pET-derived plasmids were introduced into the *E.coli* strain BL21 (DE3) by using a MicroPulser electroporator (Bio-Rad Laboratories, Hercules, CA). The production of the recombinant proteins was induced with isopropylthio-β-galactoside (1 mM for pET-CAC1A, pET-CAC1B, and pET-CAC3; 0.4 mM for pET-CAC2 and pET-accD). The bacteria were harvested at 4 hours after induction by centrifugation. The cell pellets were re-suspended in extraction buffer (2% SDS, 2 mM EDTA, 20 mM Tris-HCl, pH 8.0), sonicated on ice, and then boiled for 3 minutes. After a 20 min, 10000 g centrifugation at 4 °C, the

supernatant was saved and stored in small aliquots at -80 °C.

The recombinant proteins resulting from the expression of pET-CAC1A, pET-CAC1B, pET-CAC2, pET-CAC3, and pET-accD were designated as S·tag-BCCP-1, S·tag-BCCP-2, S·tag-BC, S·tag-α-CT, and S·tag-β-CT, respectively. The presence of S·tag fusion proteins in the total protein extract was detected by SDS-PAGE and Western blotting with S-protein conjugates (Novagen, Madison, WI). Expression of pET-CAC1A, pET-CAC1B, and pET-CAC2 resulted in only S·tag fusion proteins of the expected size. However, pET-CAC3 and pET-accD, in addition to producing the expected size of fusion protein, also produced an additional smaller fusion protein (data not shown). The proteins were recovered from SDS-PAGE gel slices by electroelution using ElutaTube™ Protein Extraction Kit (Fermentas, Hanover, MD). The molar concentration of each S·tag fusion protein was determined by using FRETWorks S·tag assay kit (Novagen, Madison, WI).

Quantitative immunoblot analysis

About 0.1 g of frozen tissue powder was homogenized with 300-400 µl protein extraction buffer (0.1 M Hepes-KOH pH 7.0, 20 mM 2-mercaptoethanol, 0.1 mg/ml PMSF, 0.1% (v/v) Trition-X-100, 1 mM EDTA, and 20% (v/v) glycerol) using a Kontes pellet pestle (Fisher Scientific, Pittsburgh, PA). The extract was centrifuged at 18000 g for 15 minutes at 4 °C. The supernatant was recovered and protein concentration was determined by using Bradford Reagent (Bio-Rad Laboratories, Hercules, CA).

To quantify the BCCP-1 subunit in plants, plant protein samples and a serial dilution of the recombinant BCCP-1 standard were loaded in a single SDS polyacrylamide gel. After electrophoresis, the proteins were transferred onto a nitrocellulose membrane. Anti-serum of

BCCP-1 was used together with ECL chemiluminescent detection system (Amersham Biosciences, Piscataway, NJ) to detect the recombinant protein as well as native BCCP-1 in plant samples. The membrane was exposed to Kodak X-OMAT film. Several exposures of different length of time were made to control the signal intensity within the linear range of the film. A flatbed scanner was used to scan the film. The signal intensities of the target bands were quantified by using ImageJ software (National Institutes of Health, Bethesda, MD, http://rsb.info.nih.gov/ij/, 1997-2005). The standard curve was constructed by plotting the intensity of recombinant protein standard against its concentration. The BCCP-1 concentration in plant samples was determined from the standard curve. For each plant sample, the whole procedure was repeated at least twice. The average of the replicate measurements for a single sample was used as the BCCP-1 concentration in that sample. A similar procedure was followed to quantify the other htACCase subunits.

Statistical analysis

Two-way analysis of variance was performed on the logarithm of the normalized expression values produced from Real-time PCR experiments using SAS software (Version 9.1, SAS Institute Inc., Cary, NC). The gene-by-organ interaction effect is of our interest. The expression patterns of any two of the five genes across the organ were compared using *contrast* statements. A significance level of 0.05 was used to reject the null hypothesis and Bonferroni method was used for multiple-comparison. The same analysis was also applied to the logarithm of protein concentration data produced from quantitative western analysis.

Native PAGE analysis

For the Tris-HCl-glycine PAGE (Ornstein, 1964), proteins were extracted from 0.25 g of siliques with 500 µl extraction buffer (50 mM Tris-HCl pH8.0, 1 mM $MgSO_4$, 2 mM DTT, 10% glycerol). Protease inhibitor cocktail for plant cell and tissue extracts (Sigma, St. Louis, MO) was added at a rate of 5 µl per 100 µl of extraction buffer. The protein extract was subjected to electrophoresis in a 4-20% precast Tris-HCl Ready Gel (Bio-Rad Laboratories, Hercules, CA) with Tris-glycine running buffer at 160 V for 6 h at 4 °C. High molecular weight native protein marker was purchased from Amersham Biosciences (Piscataway, NJ). Subsequently the proteins were transferred onto a PVDF membrane in the Tris-glycine running buffer at 450 mA for 4 h. The membrane was stained with Ponceau S staining solution (0.5% (w/v) Ponceau S, 1% (v/v) glacial acetic acid).

For the KOH-ACES-Hepes PAGE system (Jovin, 1973), proteins were extracted from 0.25 g siliques with 500 µl extraction buffer (40 mM Hepes-KOH, pH 7.8, 10% glycerol). Protease inhibitor cocktail for plant cell and tissue extracts (Sigma, St. Louis, MO) was added at a rate of 5 µl per 100 µl extraction buffer. A 5%-20% resolving gel was prepared by using a Gradient Former (Bio-Rad Laboratories, Hercules, CA). A 4% stacking gel was prepared on top of the resolving gel.

Reducing and non-reducing SDS-PAGE

Protein extracts prepared with 50 mM Tris-HCl pH 8.0, 1 mM $MgSO_4$, were boiled with an SDS sample buffer in the presence or absence of 50 mM DTT for 5 minutes. The SeeBlue Plus2 Pre-stained protein standards (Invitrogen, Carlsbad, CA), which contains no reducing reagent, was used for non-reducing SDS-PAGE.

REFERENCES

Alban C, Baldet P, Douce R (1994) Localization and characterization of two structurally different forms of acetyl-CoA carboxylase in young pea leaves, of which one is sensitive to aryloxyphenoxypropionate herbicides. Biochem J **300:** 557-565.

Al-Feel W, Chirala SS, Wakil SJ (1992) Cloning of the yeast FAS3 gene and primary structure of yeast acetyl-CoA carboxylase. Proc Natl Acad Sci U S A **89:** 4534-4538

Barber MC, Travers MT (1995) Cloning and characterisation of multiple acetyl-CoA carboxylase transcripts in ovine adipose tissue. Gene **154:** 271-275

Boyes DC, Zayed AM, Ascenzi R, McCaskill AJ, Hoffman NE, Davis KR, Gorlach J (2001) Growth stage-based phenotypic analysis of Arabidopsis: a model for high throughput functional genomics in plants. Plant Cell **13:** 1499-1510

Che P, Wurtele ES, Nikolau BJ (2002) Metabolic and environmental regulation of 3-methylcrotonyl-coenzyme A carboxylase expression in Arabidopsis. Plant Physiol **129:** 625-637

Choi JK, Yu F, Wurtele ES, Nikolau BJ (1995) Molecular cloning and characterization of the cDNA coding for the biotin- containing subunit of the chloroplastic acetyl-coenzyme A carboxylase. Plant Physiol **109:** 619-625

Choi-Rhee E, Cronan JE (2003) The biotin carboxylase-biotin carboxyl carrier protein complex of Escherichia coli acetyl-CoA carboxylase. J Biol Chem

Egli MA, Gengenbach BG, Gronwald JW, Somers DA, Wyse DL (1993) Characterization of maize acetyl-coenzyme A carboxylase. Plant Physiol **101:** 499-506

Elborough KM, Winz R, Deka RK, Markham JE, White AJ, Rawsthorne S, Slabas AR (1996) Biotin carboxyl carrier protein and carboxyltransferase subunits of the multi-subunit form of acetyl-CoA carboxylase from Brassica napus: cloning and analysis of expression during oilseed rape embryogenesis. Biochem J **315:** 103-112.

Fall RR, Nervi AM, Alberts AW, Vagelos PR (1971) Acetyl CoA carboxylase: isolation and characterization of native biotin carboxyl carrier protein. Proc Natl Acad Sci U S A **68:** 1512-1515

Fall RR, Vagelos PR (1972) Acetyl coenzyme A carboxylase. Molecular forms and subunit composition of biotin carboxyl carrier protein. J Biol Chem **247:** 8005-8015

Gornicki P, Faris J, King I, Podkowinski J, Gill B, Haselkorn R (1997) Plastid-localized acetyl-CoA carboxylase of bread wheat is encoded by a single gene on each of the three ancestral chromosome sets. Proc Natl Acad Sci U S A **94:** 14179-14184.

Gornicki P, Scappino LA, Haselkorn R (1993) Genes for two subunits of acetyl coenzyme A carboxylase of Anabaena sp. strain PCC 7120: biotin carboxylase and biotin carboxyl carrier protein. J Bacteriol **175:** 5268-5272.

Guchhait RB, Polakis SE, Dimroth P, Stoll E, Moss J, Lane MD (1974) Acetyl coenzyme A carboxylase system of Escherichia coli. Purification and properties of the biotin carboxylase, carboxyltransferase, and carboxyl carrier protein components. J Biol Chem **249:** 6633-6645.

Gygi SP, Rochon Y, Franza BR, Aebersold R (1999) Correlation between protein and mRNA abundance in yeast. Mol Cell Biol **19:** 1720-1730

Ha J, Daniel S, Kong IS, Park CK, Tae HJ, Kim KH (1994) Cloning of human acetyl-CoA carboxylase cDNA. Eur J Biochem **219:** 297-306

Hunter SC, Ohlrogge JB (1998) Regulation of spinach chloroplast acetyl-CoA carboxylase. Arch Biochem Biophys **359:** 170-178

Jovin TM (1973) Multiphasic zone electrophoresis. 3. Further analysis and new forms of discontinuous buffer systems. Biochemistry **12:** 890-898

Kannangara CG, Stumpf PK (1972) Fat metabolism in higher plants. LIV. A procaryotic type acetyl CoA carboxylase in spinach chloroplasts. Arch Biochem Biophys **152:** 83-91.

Ke J, Choi JK, Smith M, Horner HT, Nikolau BJ, Wurtele ES (1997) Structure of the CAC1 gene and in situ characterization of its expression. The Arabidopsis thaliana gene coding for the biotin- containing subunit of the plastidic acetyl-coenzyme A carboxylase. Plant Physiol **113:** 357-365.

Ke J, Wen TN, Nikolau BJ, Wurtele ES (2000) Coordinate regulation of the nuclear and plastidic genes coding for the subunits of the heteromeric acetyl-coenzyme A carboxylase. Plant Physiol **122:** 1057-1071.

Konishi T, Sasaki Y (1994) Compartmentalization of two forms of acetyl-CoA carboxylase in plants and the origin of their tolerance toward herbicides. Proc Natl Acad Sci U S A **91:** 3598-3601

Konishi T, Shinohara K, Yamada K, Sasaki Y (1996) Acetyl-CoA carboxylase in higher plants: most plants other than gramineae have both the prokaryotic and the eukaryotic forms of this enzyme. Plant Cell Physiol **37:** 117-122

Kozaki A, Mayumi K, Sasaki Y (2001) Thiol-disulfide exchange between nuclear-encoded and chloroplast-encoded subunits of pea acetyl-CoA carboxylase. J Biol Chem **276:** 39919-39925

Kozaki A, Sasaki Y (1999) Light-dependent changes in redox status of the plastidic acetyl-CoA carboxylase and its regulatory component. Biochem J **339:** 541-546

Li SJ, Cronan JE, Jr. (1992) The gene encoding the biotin carboxylase subunit of Escherichia coli acetyl-CoA carboxylase. J Biol Chem **267:** 855-863.

Li SJ, Cronan JE, Jr. (1992) The genes encoding the two carboxyltransferase subunits of Escherichia coli acetyl-CoA carboxylase. J Biol Chem **267:** 16841-16847

Li SJ, Cronan JE, Jr. (1992) Putative zinc finger protein encoded by a conserved chloroplast gene is very likely a subunit of a biotin-dependent carboxylase. Plant Mol Biol **20:** 759-761.

Lopez-Casillas F, Bai DH, Luo XC, Kong IS, Hermodson MA, Kim KH (1988) Structure of the coding sequence and primary amino acid sequence of acetyl-coenzyme A carboxylase. Proc Natl Acad Sci U S A **85:** 5784-5788

Marini P, Li SJ, Gardiol D, Cronan JE, Jr., de Mendoza D (1995) The genes encoding the biotin carboxyl carrier protein and biotin carboxylase subunits of Bacillus subtilis acetyl coenzyme A carboxylase, the first enzyme of fatty acid synthesis. J Bacteriol **177:** 7003-7006.

Mekhedov S, de Ilarduya OM, Ohlrogge J (2000) Toward a functional catalog of the plant genome. A survey of genes for lipid biosynthesis. Plant Physiol **122:** 389-402.

Muller PY, Janovjak H, Miserez AR, Dobbie Z (2002) Processing of gene expression data generated by quantitative real-time RT-PCR. Biotechniques **32:** 1372-1374, 1376, 1378-1379

Ornstein L (1964) Disc Electrophoresis. I. Background and Theory. Ann N Y Acad Sci **121:** 321-349

Pfaffl MW (2001) A new mathematical model for relative quantification in real-time RT-PCR. Nucleic Acids Res **29:** e45

Reverdatto S, Beilinson V, Nielsen NC (1999) A multisubunit acetyl coenzyme A carboxylase from soybean. Plant Physiol **119:** 961-978.

Richards FM, Wyckoff HW (1971) Bovine pancreatic ribonuclease. *In* PD Boyer, ed, The Enzymes, Ed 3rd Vol IV. Academic Press, New York, pp 647-806

Sambrook J, Fritsch EF, Maniatis T (1989) Molecular cloning : a laboratory manual, Ed 2nd. Cold Spring Harbor Laboratory, Cold Spring Harbor, N.Y.

Sasaki Y, Hakamada K, Suama Y, Nagano Y, Furusawa I, Matsuno R (1993) Chloroplast-encoded protein as a subunit of acetyl-CoA carboxylase in pea plant. J Biol Chem **268:** 25118-25123.

Shorrosh BS, Roesler KR, Shintani D, van de Loo FJ, Ohlrogge JB (1995) Structural analysis, plastid localization, and expression of the biotin carboxylase subunit of

acetyl-coenzyme A carboxylase from tobacco. Plant Physiol **108:** 805-812.

Shorrosh BS, Savage LJ, Soll J, Ohlrogge JB (1996) The pea chloroplast membrane-associated protein, IEP96, is a subunit of acetyl-CoA carboxylase. Plant J **10:** 261-268.

Sun J, Ke J, Johnson JL, Nikolau BJ, Wurtele ES (1997) Biochemical and molecular biological characterization of CAC2, the Arabidopsis thaliana gene coding for the biotin carboxylase subunit of the plastidic acetyl-coenzyme A carboxylase. Plant Physiol **115:** 1371-1383

Takai T, Yokoyama C, Wada K, Tanabe T (1988) Primary structure of chicken liver acetyl-CoA carboxylase deduced from cDNA sequence. J Biol Chem **263:** 2651-2657

Thelen JJ, Mekhedov S, Ohlrogge JB (2001) Brassicaceae express multiple isoforms of biotin carboxyl carrier protein in a tissue-specific manner. Plant Physiol **125:** 2016-2028.

Table 1. Primers used for quantification of htACCase subunit mRNAs

Primer	Gene	Amplicon
5'-GACGGCAAGCCTGTCAGC-3' 5'-CATTTCTCATGGTGCCGATTC-3'	*CAC1-A*	71bp
5'-CCGCAACCCAATGGGAT-3' 5'-GCACGCAACCTCCAGAATG-3'	*CAC1-B*	71bp
5'-GGATTTGCCTCCTGCATTTG-3' 5'GGGTGGAGAAGTAATGGATTTGG-3'	*CAC2*	71bp
5'-AGAGATCAAGAGCATGGTGGAGTT-3' 5'-CGGTGACACCAGGCGTTT-3'	*CAC3*	71bp
5'-TGCATTTGCGGGTAAAAGAGT-3' 5'-CAGCCGCTTGTGAACCTTC-3'	*accD*	71bp
5'-GCCTTTGGTGTGCATTGGT-3' 5'-CGACCCGGCCAATTAAGAC-3'	18S rRNA	71bp

Table 2. *p* values for expression pattern comparison between two genes

Test		CAC1-A vs CAC1B	CAC1-A vs CAC2	CAC1-A vs CAC3	CAC1-A vs accD	CAC1-B vs CAC2	CAC1-B vs CAC3	CAC1-B vs accD	CAC2 vs CAC3	CAC2 vs accD	CAC3 vs accD
p Value	mRNA	<.0001	0.04	0.34	0.027	0.0004	<.0001	<.0001	0.68	0.054	0.16
	protein	<.0001	<.0001	<.0001	<.0001	<.0001	<.0001	<.0001	<.0001	<.0001	<.0001

Table 3. htACCase subunit protein levels in different organs[a]

	BCCP-1	BCCP-2	BC	α-CT	β-CT
Bud	6.5±1.5	0.9±0.1	7.4±0.9	0.2±0.01	99.2±9.1
2-4DAF	3.3±0.2	0.5±0.1	7.3±0.5	0.2±0.02	110.9±11.0
6-8DAF	7.0±1.2	0.9±0.3	8.9±2.0	0.1±0.03	159.5±44.9
10-12DAF	5.7±1.4	1.2±0.6	11.7±2.7	0.04±0.01	119.5±23.9
Leaf	4.4±0.3	n.d.	6.2±0.7	0.2±0.03	298.5±64.5
Aerial	5.0±0.9	n.d	3.5±1.1	0.1±0.01	219.2±48.2
Root	6.4±0.6	1.0±0.1	9.5±1.0	0.1±0.02	n.d.
Stem	15.1±3.5	0.4±0.1	7.2±1.8	0.3±0.03	56.3±7.7

[a] protein concentrations were calculated from three biological replicates and represented as mean±standard deviation (fmol/μg total protein).
n.d. – not detected.

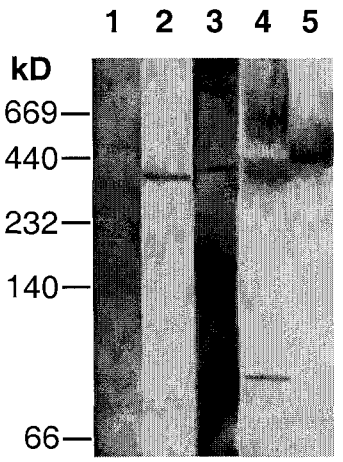

Figure 1. Tris-Glycine native gel / western analysis of htACCase.

Proteins extracts were subjected to electrophoresis in 4%-20% polyacrylamide gels using Tris-glycine running buffer. Proteins were transferred to a PVDF membrane and the blot was probed with antibodies specific to BCCP-1 (1), BCCP-2 (2), BC (3), α-CT (4), and β-CT (5).

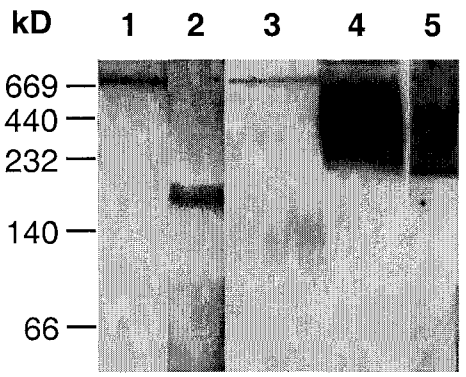

Figure 2. Hepes-KOH native gel / Western analysis of htACCase.

Proteins extracts were subjected to electrophoresis in 5%-20% polyacrylamide gels using Hepes-KOH running buffer. Proteins were transferred to a PVDF membrane and the blot was probed with antibodies specific to BCCP-1 (1), BCCP-2 (2), BC (3), α-CT (4), and β-CT (5).

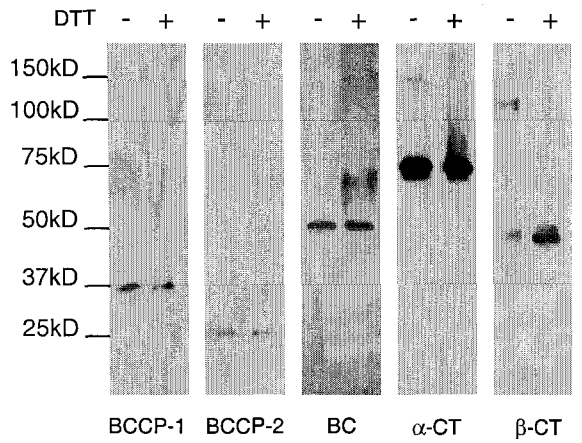

Figure 3. SDS-PAGE / Western analysis of htACCase subunits in the presence or absence of DTT.

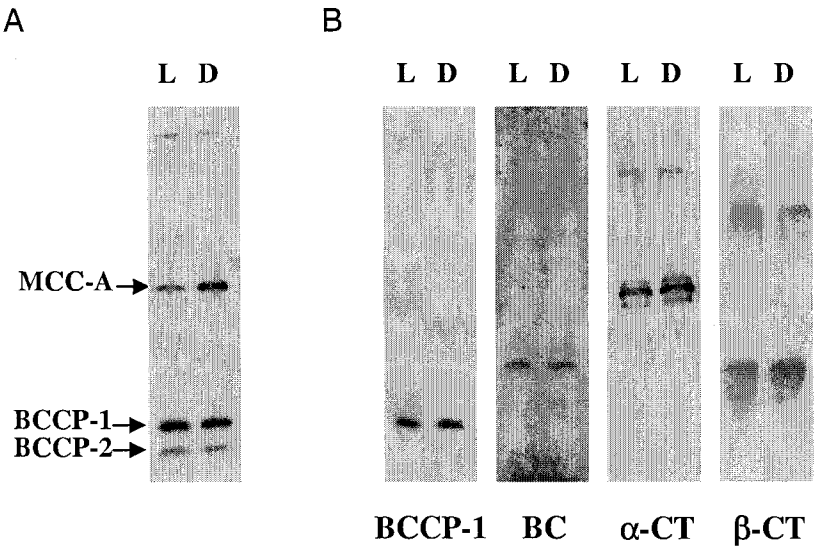

Figure 4. Effects of illumination on htACCase subunit proteins.

Arabidopsis plants were grown either under continuous illumination for 31 days (L) or under 30-day continuous illumination followed by 24-hours of darkness (D). Equal amount of proteins extracted from the two groups of plants were subjected to SDS-PAGE under non-reducing condition and subsequent western analysis with either (A): streptavidin or (B): antisera of BCCP-1, BC, α-CT, and β-CT.

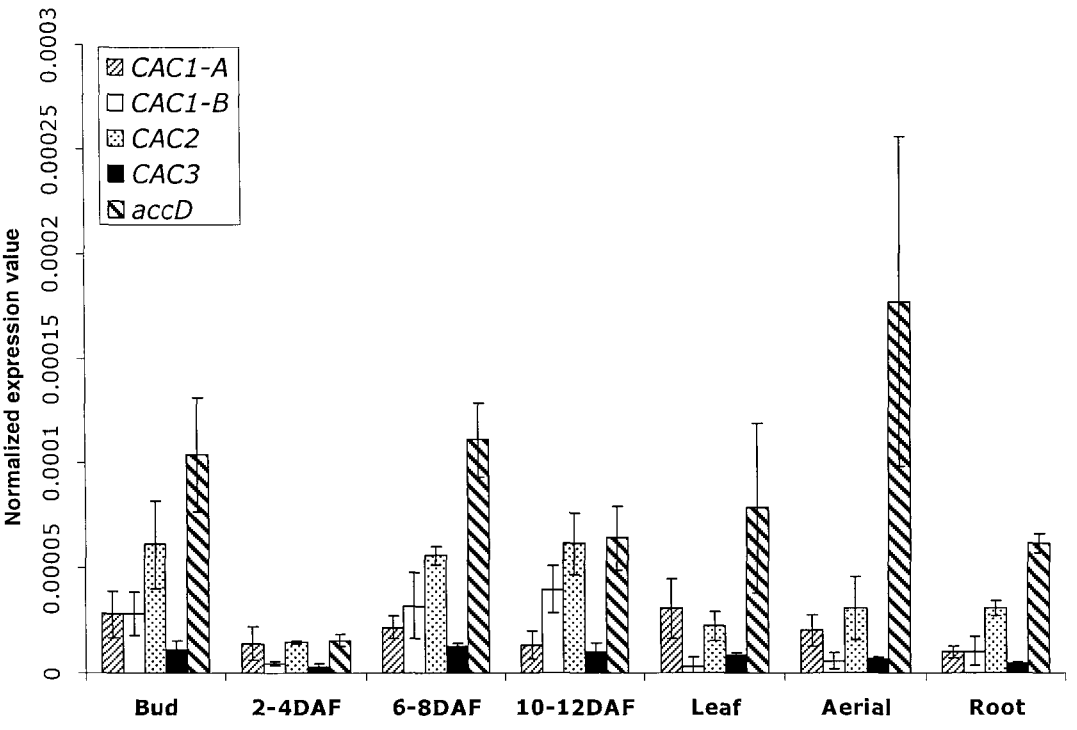

Figure 5. mRNA levels of htACCase subunit genes in different organs.

The accumulation of htACCase subunit mRNAs were measured by real-time RT PCR and normalized to 18S rRNA.. Each value represents the mean of three biological replicates. The error bars represent standard deviation.

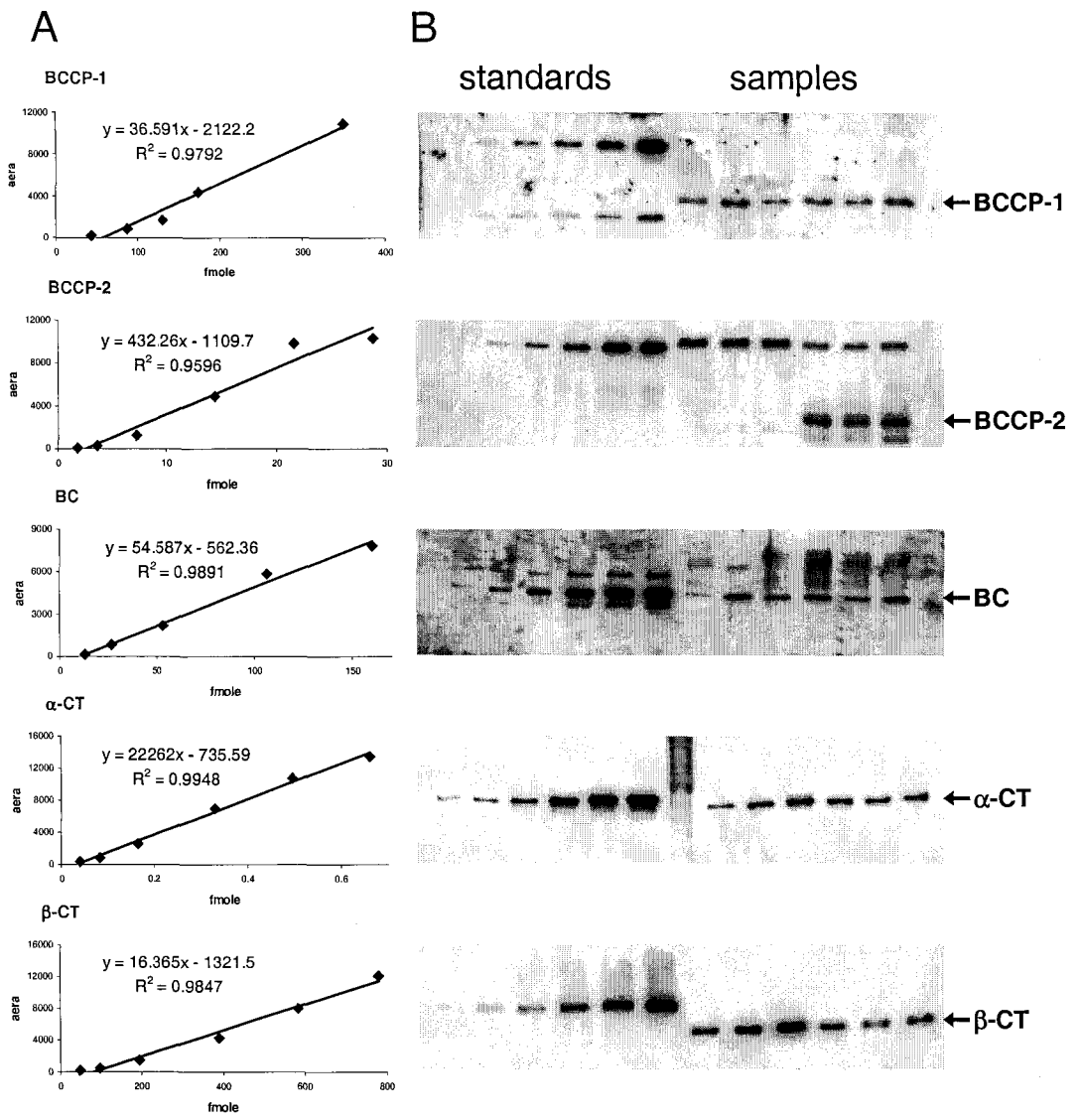

Figure 6. Representative western blots used to quantify each htACCase subunit.

For each subunit, a serial dilution of recombinant protein (left half of the blot) together with samples (right half of the blot) were loaded into the same SDS-PAGE gel and transferred to a nitrocellulose membrane. Standard curves **(A)** were constructed from the blots **(B)** on the right side.

CHAPTER 4. GENERAL CONCLUSIONS

Arabidopsis heteromeric acetyl-CoA carboxylase (htACCase) is constituted of five subunits: BCCP-1, BCCP-2, BC, α-CT, and β-CT. The genes encoding them are *CAC1-A*, *CAC1-B*, *CAC2*, *CAC3*, and *accD*, respectively. To study the possible coordinate expression among these genes, the expression of each individual subunit gene in siliques of different developmental stages and other organs were measured at both the mRNA level and the protein level. Our results showed that at the mRNA levels, *CAC1-A*, *CAC2*, *CAC3*, and *accD* genes are expressed at a constant molar ratio of 0.5:1.0:0.2:2.0 across all the organs examined, but *CAC1-B* has an expression profile different from them. However, at the protein level, none of the five subunits has the same expression pattern. The difference in the expression profiles between mRNA level and protein level suggests the involvement of post-transcriptional regulation of gene expression.

To study the subunit organization of *Arabidopsis* htACCase complex, native PAGE was used to separate plant protein complexes and western blot analysis was performed to detect each individual subunit with specific antibodies. When electrophoresis was conducted at about pH 10, the holoenzyme complex dissociated to the individual subunit complexes. However, at pH 8.5, two subcomplexes were revealed. One contains BCCP-1 and BC subunits, and the other contains α-CT and β-CT subunits. BCCP-2 was never found in a complex with any other subunits under the experimental conditions used. Our analysis indicates that plant htACCase is a very loose complex.

Comparison of the behaviors of each subunit on SDS-PAGE in the presence or absence of DTT revealed that α-CT and β-CT form their own homodimers by disulfide bonds. It is

known that htACCase activity can be increased by illumination. However, the abundance of each subunit in plants under continuous illumination is the same as that of the plants that were maintained in darkness for a period of 24 hours. Moreover, the disulfide linked dimerization of α-CT and β-CT was not affected by illumination.

To understand the individual physiological significance of the two paralogous BCCP subunits, we identified T-DNA knockout mutants for *CAC1-A*, *CAC1-B*, and *CAC3* genes. Characterization of the CAC1-A and CAC1-B knockout mutants revealed an unusual one-way redundancy between BCCP-1 and BCCP-2 subunits. *CAC1-B* knockout mutant has no discernable phenotype, but *CAC1-A* knockout mutant is embryo lethal. *In situ* hybridization analysis showed the accumulation of *CAC1-A* and *CAC1-B* mRNAs in the developing embryos has similar temporal and spatial patterns. The above observations indicate the presence of BCCP-2 cannot compensate the loss of BCCP-1 during embryo development. The data concerning the *CAC1-A* knockdown plants corroborate the important role of BCCP-1 in plant development. *CAC1-A* antisense plants showed a range of phenotypic changes including reduced leaf cell size, altered leaf organelle morphology, and retarded embryo development. The phenotype severity is inversely correlated with the abundance of BCCP-1 protein. These phenotypic changes can be explained by insufficient supply of membrane lipids. Since membrane lipid biosynthesis requires fatty acids, and htACCase catalyzes the first and committed reaction of *de novo* fatty acid biosynthesis, all the phenotypes observed from *CAC1-A* knockout or knockdown plants can be ascribed to abolished or decreased htACCase activity. Consistent with this, fatty acid analysis showed that reduction of BCCP-1 results in reduced amount of fatty acids (on per plant basis) in leaves and seeds, but doesn't affect the fatty acid composition. In contrast, neither the amount nor the composition of seed

fatty acids is changed by loss of BCCP-2. In support of the above explanation, knockout mutant of *CAC3*, the single-copy gene coding for α-CT subunit, showed the embryo lethal phenotype similar to the *CAC1-A* knockout mutant. Thus, although both are expressed in developing embryos, loss of BCCP-1 results in loss of htACCase activity, but loss of BCCP-2 does not.

One model to explain the nonequivalent roles of the two BCCP subunits is that this subunit is not the limiting factor for htACCase activity in normal conditions. Western blot analyses of the *CAC1-A* antisense plants and the *CAC1-B* knockout plants show that reduction of BCCP-1 or BCCP-2 doesn't affect the accumulation of each other or of the other htACCase subunits. Further, in *CAC1-A* antisense plants with moderate phenotype BCCP-1 levels are reduced to about 35% of wild-type level in leaves (where BCCP-2 is not expressed), and plants with a severe phenotype contain about 20% of wild-type level of BCCP-1. In developing siliques the biotinylated BCCP-1 subunit accumulates at about 3 fold higher than the biotinylated BCCP-2. Thus BCCP-2 accounts for only 25% of the total BCCP subunits. One model to explain the embryo lethality of the *cac1-a* mutant is that during the embryogenesis BCCP-1 alone is sufficient for normal htACCase activity, but BCCP-2 alone is not sufficient. However, an alternative model that can explain the embryo lethality of the *cac1-a-1* allele is that BCCP-1 and BCCP-2 are not equivalent for htACCase activity. One simple scenario is that the incorporation of BCCP-2 into the holoenzyme complex is dependent on the presence of BCCP-1, but not *vice versa*. Chapter 3 attempted to find evidence for BCCP-1 and BCCP-2 containing htACCase, however these experiments were inconclusive. The third model is that wherever *CAC1-B* gene is expressed, *CAC1-A* gene is also expressed, but there are a subset of cells that are critical for early embryo development

where *CAC1-A* is expressed, but *CAC1-B* is not. The transgenic lines described in the Appendix can be used to test this hypothesis.

APPENDIX

TRANSGENIC LINES CARRYING PROMOTER-REPORTER TRANSGENES FOR ELUCIDATING EXPRESSION OF HETEROMERIC ACCASE SUBUNIT GENES OF ARABIDOPSIS

To investigate the expression of heteromeric ACCase (htACCase) subunit genes of Arabidopsis at transcription level, promoter-reporter fusion constructs were prepared for each subunit gene (Table 1). These constructs used both the luciferase (LUC) and glucoronidase (GUS) reporter genes. In either case, the promoters of each gene was PCR amplified either from Arabidopsis genomic DNA or from cloned fragments of the htACCase subunit genes, and cloned into the appropriate transformation vector. The PCR primers used to amplify these promoter regions are listed in Table 2.

***CAC1-A* promoter:** Transgenic Arabidopsis plants carrying *CAC1-A::GUS* transgenes were generated with the vector, pCGPH, which was constructed by Jong-kook Choi (Choi, 1999; ISU PhD Thesis). In this construct the *CAC1-A* promoter, as a *Hin*dIII/*Pvu*II fragment, was cloned into *Hin*dIII/*Sma*I sites of pBI101.2 (Clontech, Mountain View, CA).

***CAC1*-B promoter:** The CAC1-*B* promoter was PCR amplified with primers CAC1Bp5 and CAC1Bp3 from Arabidopsis genomic DNA. Using the above PCR product as template, primers CAC1Bp-X and CAC1Bp-B were then used to produce the *CAC1-B* promoter (1.3kb) that contains an *Xba*I site at its 5' end and a *Bam*HI at its 3' end. This fragment was first cloned into T-Vector (Promega, Madison, WI). This construct is named CAC1Bp-T-Vector. Then the *CAC1-B* promoter was cut out of CAC1Bp-T-Vector with *Xba*I and *Bam*HI

and cloned into the same sites of pCAMBIA3300. This construct is named CAC1Bp-CAMBIA3300.

CAC1Bp-luc-CAMBIA3300 was constructed by cutting out the luciferase gene (LUC) from pGEM-luc vector (Promega, Madison, WI) with *Bam*HI and *Sac*I and cloning it into the same sites of CAC1Bp-CAMBIA3300. To make CAC1Bp-CAMBIA3300-GUS construct, *CAC1-B* promoter was cut out from CAC1Bp-CAMBIA3300 with *Hin*dIII and *Bam*HI and cloned into the same sites of pCAMBIA3300GUS (the pCAMBIA3300GUS was made by Wei Huang, a research assistant in the Nikolau lab).

***CAC2* promoter:** The *CAC2* promoter (-1412 to +48) was cloned into pBI101.2 vector, resulting in the BC1 construct (made by Rao, a post-doc in the Wurtele Lab). To fuse the *CAC2* promoter to the LUC reporter, *CAC2* promoter (1.7kb) was amplified with primers CAC2p-5X and CAC2p-B and cloned into T-Vector, making the construct CAC2p-T-Vector. The *CAC2* promoter was then moved into pCAMBIA3300 with *Xba*I and *Bam*HI. The resulting construct is named CAC2p-CAMBIA3300. CAC2p-luc-CAMBIA3300 construct was made by moving LUC gene from pGEM-luc vector into CAC2p-CAMBIA3300 with *Bam*HI and *Sac*I.

***CAC3* promoter:** The *CAC3* promoter (1.2kb) was amplified with primers CAC3p-H and CAC3p-B and cloned into T-Vector, making the construct CAC3p-T-Vector. The luc-CAMBIA3300 construct was made by moving LUC gene from pGEM-luc vector into pCAMBIA3300 with *Bam*HI and *Sac*I. Then the CAC3p-luc-CAMBIA3300 construct was made by moving the *CAC3* promoter from CAC3p-T-Vector into luc-CAMBIA3300 with *Hin*dIII and *Bam*HI. The LUC gene was moved from pGEM-luc vector into pBI101.2 with *Bam*HI and *Sac*I. This construct is named luc-pBI101.2. CAC3p-luc-pBI101.2 construct was

made by moving the *CAC3* promoter from the CAC3p-T-Vector into luc-pBI101.2 with *Hin*dIII and *Bam*HI.

Plant transformations: To compare the expressions among htACCase subunit genes, six transgenic lines were generated by co-transformation of two constructs with different promoters and different reporters into wild-type Arabidopsis plants (Columbia ecotype) (Table 3). T1 plants were screened with kanamycin and glufosinate ammonium, so that only plants carrying both constructs were selected. For each transgenic line, plants homozygous for both constructs were screened at the T2 and/or T3 generations.

Transgenic lines that are homozygous for the GUS reporter construct were stained for GUS activity at different stages of seedling growth (Figure 1). Wild-type Arabidopsis (Columbia ecotype) was used as control.

Table 1. Promoter-reporter constructs for htACCase subunit genes

Construct	Promoter	Reporter	Vector
pCGPH	*CAC1-A*	GUS	pBI101.2
CAC1Bp-luc-CAMBIA3300	*CAC1-B*	LUC	pCAMBIA3300
CAC1Bp-CAMBIA3300-GUS	*CAC1-B*	GUS	pCAMBIA3300
BC1	*CAC2*	GUS	pBI101.2
CAC2p-luc-CAMBIA3300	*CAC2*	LUC	pCAMBIA3300
CAC3p-luc-CAMBIA3300	*CAC3*	LUC	pCAMBIA3300
CAC3p-pBI101.2	*CAC3*	GUS	pBI101.2

Table 2. Primers used to amplify promoter regions of htACCase subunit genes

Primer	Sequence	Promoter
CAC1Bp5	5'-ATGGAGCAAGCTCCTTCAAA-3'	*CAC1-B*
CAC1Bp3	5'-TGTTGAGACAGTGGACGATGA-3'	
CAC1Bp-X	5'-TCTAGACAGGGTCATATGGAGCAAGC-3'	*CAC1-B*
CAC1Bp-B	5'-GGATCCGACGATGAAACCGAGGAAGT-3'	
CAC2p-5X	5'-TCTAGAGCAGCTTTACCCTTCACGTT-3'	*CAC2*
CAC2p-B	5'-GGATCCAAATGCAGGAGGCAAATCCT-3'	
CAC3p-H	5'-TTTGATTCCCCAATCTCAGC-3'	*CAC3*
CAC3p-B	5'-GGATCCGCGTGGATTTTGTGTGGAAG-3'	

Table 3. Tansgenic lines with co-transformed binary vectors

Line name	Binary vector	Promoter-reporter/resistance
A&B	pCGPH + CAC1Bp-luc-CAMBIA3300	CAC1Ap-GUS/kan + CAC1Bp-LUC/Bar
A&2	pCGPH + CAC2p-luc-CAMBIA3300	CAC1Ap-GUS/kan + CAC2p-LUC/Bar
A&3	pCGPH + CAC3p-luc-CAMBIA3300	CAC1Ap-GUS/kan + CAC3p-LUC/Bar
B&2	CAC1Bp-luc-CAMBIA3300 + BC1	CAC1Bp-LUC/Bar + CAC2p-GUS/kan
B&3	CAC1Bp-luc-CAMBIA3300 + CAC3p-pBI101.2	CAC1Bp-LUC/Bar + CAC3p-GUS/kan
2&3	BC1 + CAC3p-luc-CAMBIA3300	CAC2p-GUS/kan + CAC3p-LUC/Bar

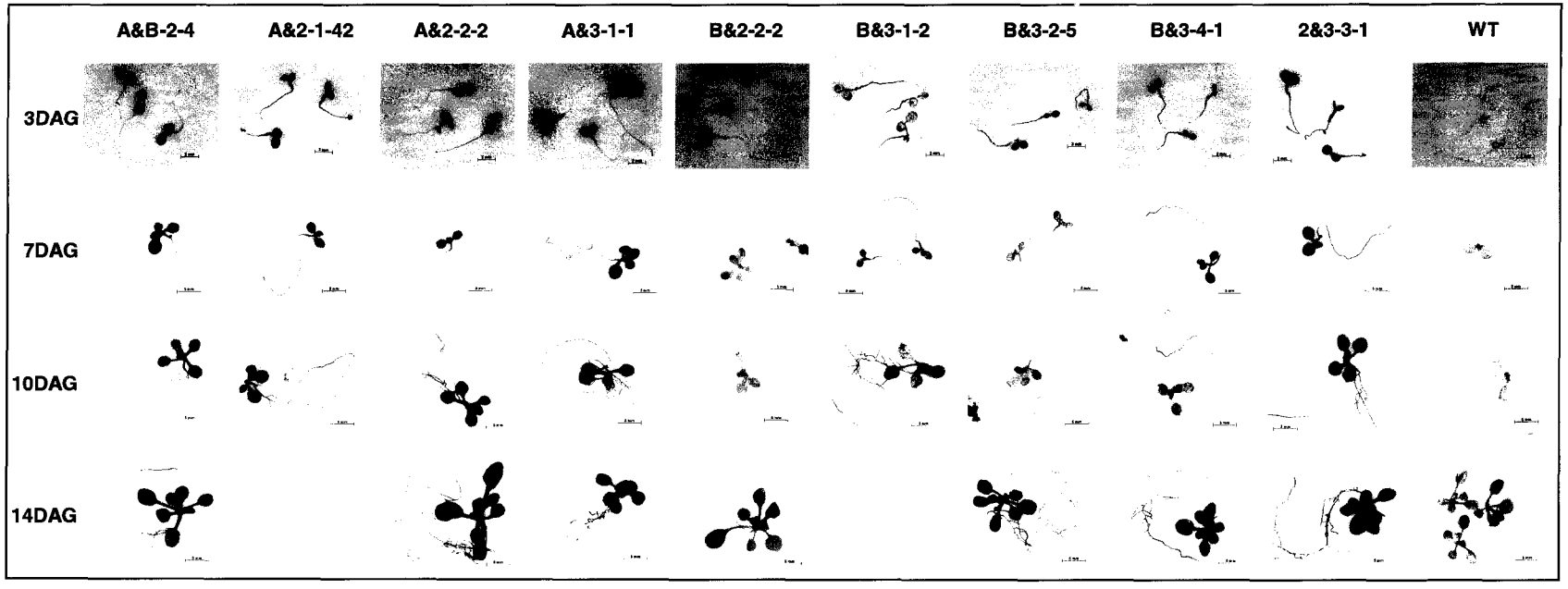

Figure 1. GUS stain of different stage seedlings of transgenic lines homozygous for GUS reporter construct.

DAG, days after germination.

ACKNOWLEDGMENTS

I would like to thank my major professor, Dr. Basil Nikolau, for mentoring me through the course of my Ph.D. research. I also thank him for his help in the preparation of this dissertation.

I would also like to thank Dr. Stephen H. Howell, Dr. Alan M. Myers, Dr. Patrick S. Schnable, and Dr. Eve S. Wurtele for serving on my Program of Study (POS) committee.

I thank Dr. Philip Dixon for his advice and help on statistical analysis of my data.

I thank our lab manager, Libuse Brachova, for her efforts to make the lab an enjoyable place to work in. I also thank all the members of Nikolau lab for their help on my research as well as everyday life.

I am thankful to my parents and sister for their love, support, and sacrifices.